THE PENNSYLVANIA STATE UNIVERSITY
SCHREYER HONORS COLLEGE

DEPARTMENT OF CIVIL AND ENVIRONMENTAL ENGINEERING

AN ANALYSIS OF THE DYNAMIC RESPONSE OF SUSPENSION FOOTBRIDGES MEASURED AGAINST HUMAN COMFORT CRITERIA

JENNIFER KEARNEY
SPRING 2015

A thesis
submitted in partial fulfillment
of the requirements
for a baccalaureate degree
in Civil and Environmental Engineering
with honors in Civil and Environmental Engineering

Reviewed and approved* by the following:

Jeffrey A. Laman
Professor of Civil Engineering
Thesis Supervisor

Eric T. Donnell
Associate Professor of Civil Engineering
Honors Adviser

* Signatures are on file in the Schreyer Honors College.

ABSTRACT

Many rural communities around the world become isolated from their basic needs during the rainy season, so pedestrian suspension bridges are being built to provide hundreds of thousands of people with basic access. However, suspension pedestrian bridges have low stiffness, mass, and damping, causing them to be prone to vibration problems. Pedestrian loading can cause a dynamic effect that creates public alarm to the point where bridge users perceive it to be unsafe. The present study analyzed two scaled, physical models and forty numerical models to determine how changing certain design parameters affects modal frequencies and the dynamic response compared to human comfort limits. The physical models were created to calibrate and validate the numerical models which were used to conduct the parametric study, which included a modal analysis and time-history analysis of a person walking across the bridge. The parametric study analyzed span length, cable sag, vertical stiffening, and lateral stiffening.

The study determined that the modal frequencies of pedestrian suspension bridges do not meet the recommended ranges and the vertical velocities, lateral accelerations, and vertical accelerations of the structure when one pedestrian walks across exceed human comfort limits. Shorter span lengths have higher modal frequencies and dynamic responses. Lower cable sags have higher vertical frequencies and lower vertical dynamic responses. Adding stiffening increases the frequencies and decreases the dynamic response, but the response still exceeds human comfort limits.

TABLE OF CONTENTS

LIST OF FIGURES

LIST OF TABLES

ACKNOWLEDGEMENTS

I would like to express my sincere appreciation to my thesis advisor, Dr. Laman, for his guidance and insight throughout this project. He continually challenged me to step out of my comfort zone and to learn new skills. I would also like to thank Dr. West, Dr. Warn, and Dr. Memari for serving on my committee and for their valuable contributions. I truly appreciate Mr. Matt Hassinger and Mr. Dave Faulds for their support in the lab and assistance with the physical model construction. I could not have built the physical models without them. In addition, I could not have tested the physical models without Dr. Schiano. I would like to thank Dr. Schiano for allowing me to borrow a motor and for helping me with the testing set-up. I am so thankful for my peers and friends who assisted me with testing when I needed an extra set of hands. Last but certainly not least, I am extremely grateful for my parents' support throughout this entire process. Their words of encouragement continue to inspire me to work harder and discover more. They never failed to express interest in my work, and their unwavering support motivated me through the challenging times. While this thesis project might be described as individual, it truly was a team effort.

Chapter 1

Information

1.1 Background

While strength is a very important design consideration, serviceability is also important, especially for suspension footbridges. Pedestrian loading can cause a dynamic effect that creates public alarm to the point where bridge users perceive it to be unsafe. The dynamic response of pedestrian suspension bridges has been an issue for many years and continues to be a problem. The Millennium Bridge in London is an example of a pedestrian suspension bridge that had a serviceability failure as a result of not meeting serviceability limits for pedestrian loading. The bridge was opened on June 10, 2000 and closed two days later due to the continuous lateral sway of the deck that was approximately 70 mm (ARUP, 2014). This is an example of a serviceability problem that can result from the dynamic response of pedestrian bridges. Therefore, pedestrian bridges must be analyzed for the dynamic response, and the structure must be designed to mitigate serviceability failures and to maximize public acceptance of the bridge.

Resonance is caused when a modal frequency of a bridge matches the loading frequency. This is not a new problem. Soldiers were ordered to break step when crossing bridges to reduce the likelihood of impacting the structural integrity. Today, pedestrian loading remains a concern for footbridge design. Pedestrian bridges are slender, meaning they have a low mass, stiffness, and damping. This increases their susceptibility to serviceability failures under normal human walking loads (Shi, 2013). The overall bridge stiffness depends on the bridge mass and damping. The structural damping depends on the elements that make up the bridge and how they are distributed. The stiffness of the bridge determines its modal frequencies and the dynamic response, including the displacements, velocities, and accelerations of the structure. If the modal frequency of the bridge matches the frequency of the pedestrian loading, the bridge will experience resonance that could lead to a serviceability failure. Vibration response is a concern for pedestrian bridges, and this dynamic response must be accounted for in the design.

Many people in third world countries around the globe are in need of pedestrian bridges to access their basic needs. During the rainy season, some rural communities are isolated from healthcare, education, and markets; people must either do without these necessities or risk their lives trying to cross rushing rivers. Bridges to Prosperity (B2P) is a non-profit organization that builds pedestrian suspension bridges in communities in Africa, Asia, Central America, and South America. B2P has created a standard design, which has evolved after several versions of the *Bridge Builder Manual*, so a company can adapt the standard design to a site and construct a bridge for a community in need. Therefore, pedestrian suspension bridges are becoming very common, but there is little research done on the dynamic movement of these slender structures.

1.2 Problem Statement

Serviceability failures are a problem for footbridges where pedestrian loading is often at a frequency near the first modal frequency of the footbridge. The first six modal frequencies for typical pedestrian suspension bridges are about 2 Hz or less, with the first lateral mode having a frequency around 0.3 Hz and the first vertical mode having a frequency around 0.7 Hz. A typical human stride frequency is between 1.6 and 2.4 Hz. Therefore, the fundamental load frequency for vertical excitation is about 2 Hz. The fundamental load frequency for lateral excitation is about 1 Hz; this response is a result from the way people shift their weight from right to left as they walk (Shi, 2013). The American Association of State Highway and Transportation Officials provides limits for fundamental frequencies in the Specification for Pedestrian Bridge Design; the fundamental frequency in the vertical plane of a pedestrian bridge without live load must be greater than 3 Hz, and the fundamental frequency in the lateral direction, which is transverse to the deck, must be greater than 1.3 Hz (Chung, 2014). These fundamental frequency limits are important because if a modal frequency of the bridge matches a fundamental frequency from pedestrian loading, large displacements can occur. Therefore, the dynamic response of footbridges must be determined before they are constructed to create structures without serviceability problems.

Many pedestrian suspension bridges are experiencing large vibrations from normal pedestrian loading. Pedestrian bridges are useless if people feel unsafe to use the structure. Therefore, this serviceability problem warrants research specifically dealing with the dynamics of pedestrian suspension bridges.

1.3 Focus of Research

The purpose of the present study is to determine how certain structural parameters affect the displacements, velocities, accelerations, and modal frequencies of suspension footbridges to mitigate the potential for serviceability concerns. There are many different types of suspension footbridges, but the footbridges used for the present study will be based off the standards from

Bridges to Prosperity because this type of footbridge is being built in countries all around the world and vibration problems are known to be an issue.

1.4 Scope of Research

There are three design quantities evaluated for the present study: 1) cable sag; 2) vertical stiffness; and 3) lateral stiffness. Two values for cable sag are evaluated for the present study – 5 percent of the span and 7.5 percent of the span. Larger cable sag values are unable to be evaluated due to physical constraints. Vertical stiffening is added through cross bracing that connects the main cable to the sides of the deck. The stiffening is located in the middle and at the ends of the footbridges to mitigate the fundamental vertical mode shapes. Lateral bracing is added through cross bracing that connects one corner of the crossbeam to the opposite corner of the adjacent crossbeam underneath the decking boards. Lateral stiffening is also present in the middle and at the ends of the footbridges due to the fundamental lateral mode shapes.

These three design quantities are studied for five different span lengths: 40 m, 50 m, 60 m, 70 m, and 80 m. Numerical models are created to determine the modal frequencies and dynamic response of pedestrian suspension bridges.

SAP2000 is used to complete the parametric study for the numerical models. Each suspension footbridge is modeled in SAP2000, and a modal analysis is conducted to determine the modal frequencies of the structure. Also, the displacements, velocities, and accelerations under pedestrian loading are calculated through the use of a nonlinear direct-integration time-history analysis to determine if the model meets the human tolerance criteria.

Two scaled physical models are constructed to calibrate the numerical models. The physical models' behavior is used to adjust base fixity, material properties, and mass distribution to create numerical models with modal frequencies that match the frequencies of the physical models. The physical models are of a scaled 40 m bridge with 5 percent cable sag and a scaled 80 m bridge with 7.5 percent cable sag because these are the two extremes for the bridges used for the present study; this allows for a comparison of how the bridges behave. The physical models incorporate materials with properties similar to the actual materials used to construct common footbridges; however, the mass and dimensions of the elements are scaled. The physical models are tested by applying an initial pedestrian walking force and recording the vibration on a high speed video camera to determine the modal frequencies.

1.5 Objectives

- Determine how changing span length, cable sag, vertical stiffness, and lateral stiffness changes the dynamic response of footbridges
- Determine ways to mitigate vibration concerns, including displacements, velocities, and accelerations, to meet requirements for human comfort
- Determine ways to adjust the first several modal frequencies to meet the frequency limits for pedestrian bridges

1.6 Organization of Thesis

Chapter 2 presents the literature review conducted for the present study. Chapter 3 presents the physical model design, construction, loading and data collection. Two scaled bridge models were tested to obtain the modal frequencies. These frequencies were used to calibrate the numerical models presented in Chapter 4. Chapter 4 discusses the model design, calibration process, and the parametric study. The parametric study involves forty SAP2000 models used to determine how changing the cable sag or stiffness affects the dynamic response of suspension footbridges. The physical model results are used to validate the numerical models for the parametric study. The results from the parametric study and physical models are presented in Chapter 5; the conclusions and further research are presented in Chapter 6.

Chapter 2

Literature Review

2.1 Suspension Bridge Analysis

The first suspension bridge that had a flat deck connected to a cable through suspended hangers was the Jacob's Creek Bridge build in Pennsylvania in 1801. This was an iron-chain suspension bridge that, unfortunately, collapsed only halfway through its 50-year design life. Several suspension bridges collapsed in the 1800s due to oscillations and vibrations caused by wind and pedestrian loading; this demonstrated the need to develop suspension bridge analysis techniques to design safe structures.

2.1.1 Historical Suspension Bridge Analysis

Suspension bridge analysis theory in the 1800s differs greatly from current suspension bridge theory. Henri Navier was an influential figure in suspension bridge analysis advancement and he considered the cable geometry of suspension bridges as a parabola. He suggested that designers use a flexible deck with sag ratios of 1/12 to 1/15. However, Navier had several misconceptions about suspension bridge behavior. James Finley, who designed Jacob's Creek Bridge, suggested a rigid deck with a 1/7 sag ratio (Kawada, 2010). However, most bridges built in the early 1800s had low stiffness and mass, which resulted in high deflections and oscillations.

The elastic theory was used to design most suspension bridges built in the 1800s. This theory is based on the assumption that cables do not deform under live loads. However, this theory is incorrect, and it was later replaced with the deflection theory. Therefore, many suspension bridges that were designed based on the elastic theory collapsed and the overall suspension bridge analysis techniques did not result in a safe structural design. The Wheeling Bridge in West Virginia collapsed during a storm; the bridge vibrations continued to increase in magnitude, and the structure failed due to the low stiffness of the suspension bridge design (Kawada, 2010).

John Roebling understood the stiffness problems with suspension bridge design of the time. He fabricated wire ropes, which are still in use for suspension bridges. Some suspension bridges were built from chain cable, so when one chain in the cable failed, the entire cable failed; however, the breakage of a single wire in a wire rope cable does not greatly affect the strength of the structure . Roebling bundled wires together to form a cylinder that had the same cross section throughout the cable length. This wire rope was the best solution for economical construction of long span suspension bridges (Kawada, 2010).

Suspension bridge analysis did not turn from the elastic theory to the deflection theory until the 1900s. The deflection theory considers the deflection in the cable caused by loads; this deflection increases the stiffness of the cable as it is loaded due to the geometry of the deflected shape. This method allows for a more efficient structural design because the stiffening effects of the dead load are considered. The deflection theory also allowed for longer span suspension bridges to be built because the vertical stiffness could be increased through the use of the mass of the cables and the suspended structure (Kawada, 2010).

2.1.2 Modern Suspension Bridge Analysis

Stiffness of suspension bridges continues to be a problem today. The Tacoma Narrows Bridge failed under wind loading due to its extreme slenderness. The suspended bridge had a depth-to-span ratio of 1:350 and a width-to-span ratio of 1:72. In addition, the structure had plate girders with no large stiffening trusses that were common for suspension bridges built during that time. To overcome aerodynamic response of suspension bridges, either a stiffening truss with open grating decks was used or the mass of the suspension bridge was increased. Additional mass improves the dynamic properties of the bridge by decreasing the amplitude of the oscillations and increasing the critical wind speed. However, the Severn Bridge attempted to design for stiffness using diagonal hangers. These hangers experienced high stress amplitudes that varied from zero to levels exceeding the allowable design limit, resulting in a fatigue failure of the suspenders after only 10 years of service (Kawada, 2010).

In addition, pedestrian loading can cause concerns regarding lateral stiffness if not properly accounted for in the bridge design. The Millennium Bridge was closed a few days after opening due to large lateral vibrations induced by pedestrian loading. The structure had a first lateral modal frequency of 0.9 Hz, which is very similar to the 1 Hz lateral frequency of pedestrian loading. Therefore, chevron bracing and tuned mass dampers were added beneath the deck to reduce the lateral vibrations. This serviceability problem demonstrates the importance of analyzing suspension bridges for vibrations in the vertical and lateral directions (Kawada, 2010).

Today, suspension footbridges must be designed for both strength and serviceability limit states. Factored design loads are used to size the members for strength limit states. However, to complete a serviceability evaluation, several pieces of information, including the footbridge dynamic properties, a model of the human-induced force, and the human tolerance level for vibrations, must be known (Zivanovic, 2005).

2.2 Dynamic Response

2.2.1 Basic Footbridge Dynamics

Footbridges follow the basic equation of motion, so their dynamics are based on their mass, damping, and stiffness. The stiffness of a slender footbridge is not constant because it experiences large displacements. The stiffness of footbridges is provided by the cable, and it depends on the axial forces in the cable; the axial force depends on the cable geometry, which changes as the structure is loaded and unloaded (Huang, 2007). Therefore, the stiffness changes as the cable deforms or vibrates during loading because cables behave non-linearly. This change must be considered to accurately predict the dynamic response of the structure. The present parametric study was designed based on the dynamics of footbridges and the expected response to certain changes to the structure.

2.2.2 Vibration Modes

Footbridges have several vibration modes that can be in the vertical, lateral, torsional, or longitudinal direction. According to Huang (2007), lateral and torsional modes are coupled together into lateral-torsional modes or torsional-lateral modes. Vertical modes typically appear as pure modes, and longitudinal modes are typically not present in the first 20 frequencies (Huang, 2007). Suspension footbridges are easily excited in the vertical direction due to pedestrian loading; however, lateral vibrations are not excited as easily. People tend to create a larger force in the vertical direction when they walk, which excites the vertical frequencies more easily. In addition, suspension footbridges do not easily develop a torsional response (Brownjohn, 1997). However, some studies, such as the Morca suspension footbridge in northern Italy, exhibit vertical modes in addition to vertical torsion modes that result from the deck moving in the vertical direction while twisting around the centerline of the deck (Gentile, 2008).

2.2.2.1 Singapore Footbridge Response

A 35 m suspension footbridge in Singapore was tested with heel-dropping, walking, and bouncing, and then the bridge was modeled using finite element software. The bridge has a 5.5 m sag with back spans located at a 30 degree angle below the horizontal. The hangers are located at 3 m on center with a 1.2 m wide deck. Two-dimensional models with the deck represented as a beam accurately predicted the dynamic response of the bridge. This accuracy means the lateral and torsional resistance of the deck has little effect on the vertical vibrations, which means the vertical vibration modes are pure (Brownjohn, 1997). This pedestrian bridge was designed with stiff hangers, so the deck and cable vibrated together when the bridge was excited.

Brownjohn (1997) developed 2-D and 3-D numerical models to determine the dynamic response of the footbridge. He developed the 3-D models to confirm the accuracy of the simplified 2-D model. Because the difference between the models was minimal, even for complex mode shapes, the 2-D model was used by Brownjohn to study the critical vertical plane dynamic response of the bridge.

Brownjohn discovered five vibration modes from the 3-D finite element model as presented in Figure 1. The first two vertical modes, which are VS1 and VA1, were excited by jumping followed by free decay. The fundamental lateral mode is LS1 and was heavily damped. The two torsional modes, which are TS1 and TA1, were not easily excited, so they are not a critical concern (Brownjohn, 1997).

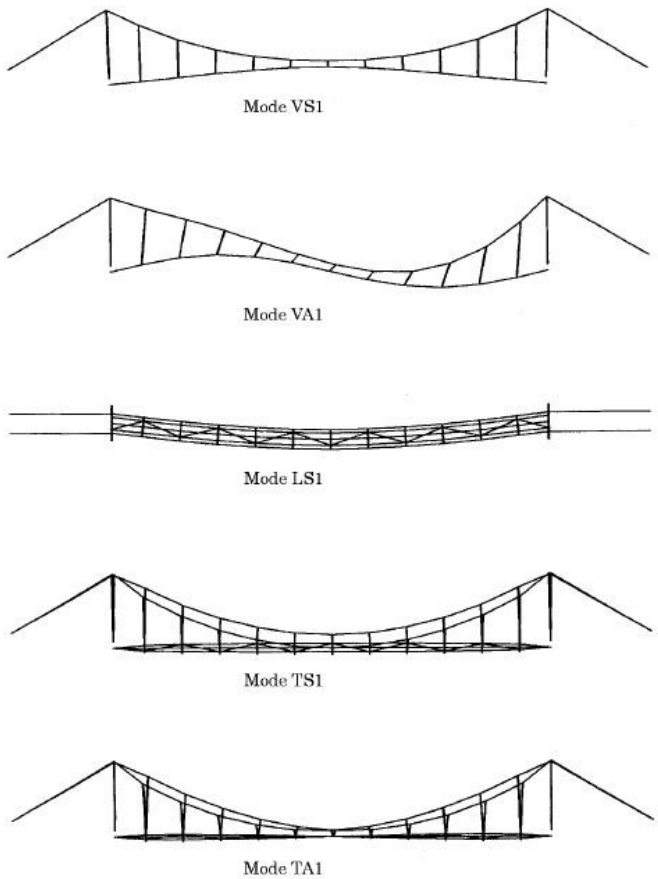

Figure 1: Vibration Modes for Footbridge in Singapore (Brownjohn, 1997)

Because of these results, the present study does not consider longitudinal forces from pedestrians because longitudinal modes are not excited on typical footbridges. However, vertical, lateral, and torsional modes are studied.

2.2.2.2 Morca Footbridge Response

A 91.6 meter suspension bridge in northern Italy was dynamically tested under normal pedestrian and wind loading. This bridge has lateral stiffening trusses along each side of the 2.5 meter wide deck. Five vibration modes were detected within the 0 to 2 Hz frequency range. These modes are vertical bending modes or vertical torsional modes. Figure 2 presents the five vibration modes. Both the first vertical (VA1) and first torsional (TA1) mode involved one complete sine wave (Gentile, 2008). Lateral vibration modes are likely not present due to the lateral stiffening trusses. The first (VA1), second (VS2), and fifth modes (VS3) are bending modes, and the third (TA1) and fourth modes (TS2) are torsional modes.

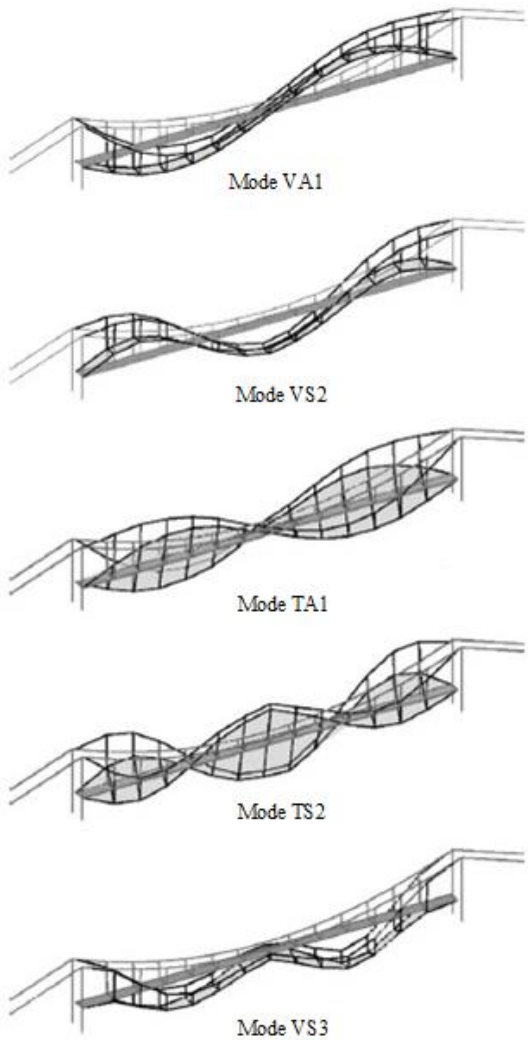

Figure 2: Vibration Modes for Morca Footbridge (Gentile, 2008)

The Morca Footbridge confirms the need to analyze vertical modes for the present study. Because the footbridges considered for the present study do not have a lateral stiffening truss, lateral modes are also analyzed for the present study. However, lateral stiffening is considered for the present study because the Morca Footbridge had no lateral modes due to stiffening in that direction.

2.2.3 Modal Frequency

Each suspension bridge has different modal frequencies; however, the vibration modes are similar. The Singapore frequencies are as follows: the first symmetric mode (VS1) has a frequency of 2.15 Hz, the first asymmetric mode (VA1) has a frequency of 2.11 Hz, the fundamental lateral mode (LS1) has a frequency of 1.25 Hz, and the two torsional modes (TS1 and TA1) have frequencies of 2.52 Hz and 1.84 Hz (Brownjohn, 1997). These frequencies are in the range of walking, which results in large displacements.

The frequency of the bridge in the lateral modes depends heavily on the effectiveness of the diagonal bracing under the deck. The cable axial stiffness affects the frequency of the first symmetric mode in the vertical plane (VS1) the most. The first asymmetric mode in the vertical plane (VA1) behaves similar to a beam with partially fixed ends. This bridge experienced a high dynamic response under typical pedestrian loading due to the match between the frequency for the first modes in the vertical plane (VS1 and VA1) and the typical footfall frequency of 2 Hz. The Singapore footbridge is rigid; however, the modal frequencies match the pedestrian frequency, which results in large vibrations. The frequencies in the vertical modes could be adjusted by changing the girder rigidity or cable stiffness. Also, the length of the backstay could be changed to change the modal frequency of the first vertical mode (VS1) (Brownjohn, 1997).

The modal frequency of the first vertical bending mode (VA1) of the Morca footbridge is 0.443 Hz, the second vertical bending mode (VS2) has a frequency of 0.646 Hz, and the last bending mode (VS3) has a frequency of 1.264 Hz. The first torsional mode (TA1) has a frequency of 0.738 Hz, and the second torsional mode (TS2) has a frequency of 0.965 Hz. The Morca footbridge modal frequencies are lower than those of the Singapore footbridge.

Therefore, the Morca footbridge has a greater chance of reaching resonance for pedestrians walking at a lower frequency.

Overall, many of the structural decisions made during design greatly affect the dynamic response of the bridge and its modal frequencies which could result in serviceability problems under certain types of loading. Based on results of previous studies, it is expected that the footbridges analyzed in the present study will have modal frequencies that fall in the same range as pedestrian walking frequencies. Additional cable stiffening is being considered to adjust the frequencies of the footbridges.

2.2.4 Pedestrian Loading and Structure Interaction

The dynamic response of footbridges changes when pedestrians are present on the structure. Moving pedestrians increase the mass and damping of flexible footbridges with light timber floors. This is due to the fact that the mass of people is significant compared to the mass of the structure. Walking crowds can increase the damping of the structure in the vertical direction; however, there is limited data to quantify this effect, and data for lateral dynamics of footbridges with moving people is very scarce. In addition, jumping and bouncing can change dynamic properties. Jumping forces are about two times less on flexible footbridges than on rigid structures (Zivanovic, 2005). The present study does not model pedestrian and structure interaction.

2.2.5 Dynamic Response Measurement

While calculating the dynamic response of structures from numerical models is helpful, the numerical models must be validated with the actual response of the structures. Therefore, research has been conducted to determine accurate ways to measure the dynamic response of pedestrian suspension bridges; this research includes studying the proper equipment to use and how to place the equipment on the bridge. Modern research includes studying the use of Global Position System (GPS) with accelerometers to gain a full understanding of the dynamic response of the footbridge (Moschas, 2011). After the data is collected, it must be processed properly to obtain the modal frequency of the bridge (Meng, 2007). These results can then be compared to models to validate the model response. However, for small scale models, sensors cannot be attached to the model because the mass of the sensors will greatly affect the dynamic response of the structure. Other tools, such as high speed video cameras, must be used to track the displacements over time intervals. The present study uses a 300 frames-per-second high speed video camera to measure the dynamic response of the physical model footbridges.

2.3 Scaling and Modeling Techniques

The present study includes creating two scaled footbridge models and many numerical models in SAP2000. The present study used the following scaling and modeling techniques.

2.3.1 Scaling

There are several methods that can be used to scale a large object down to a smaller size for experimental testing. However, when gravity loads affect the structure, the scale factor for mass is set at S^3, where S is the scale factor for length that can be calculated by dividing the structure's length by the smaller model's length. The scale factor for force is set at S^2, which results in unity as the scale factor for stress. The scale factor can be determined for additional quantities using dimensional analysis. Table 1 presents the scale factor for pertinent quantities. Smaller models can be built from elements with parameters calculated by dividing the parameters of the actual structure by the scale factor listed in Table 1. The physical footbridge models built for the present study follow the scaling parameters presented in Table 1.

Table 1: Scale Factors for Dynamic Testing (Kumar, 1997)

Quantity	Dimensions	Scale Factor
Length	L	S
Mass	M	S^3
Time	T	S
Stress	$ML^{-1}T^{-2}$	1
Velocity	LT^{-1}	1
Acceleration	LT^{-2}	$1/S$
Force	MLT^{-2}	S^2
Stiffness	MT^{-2}	S
Damping	MT^{-1}	S^2
Natural Frequency	T^{-1}	$1/S$

2.3.2 Numerical Modeling

Most footbridge numerical models are analyzed through the use of a commercially available structural analysis finite element program. Several of the footbridges discussed in this literature review used SAP2000 to determine modes and frequencies of the structures. SAP2000 is used for the present study to determine the mode shapes and the vibration response.

Several types of elements are available in SAP2000 to create the 3D bridge models. Cable elements are used to model the main cables and suspenders because these elements only provide tension forces. Frame elements are used to model the crossbeams, decking, and towers. Frame elements produce internal axial, shear, and moment forces. The end moments between decking boards are released.

Cable elements in SAP2000 use elastic catenary formulation that is ideal for modeling slender cables. A catenary is the curve formed by a free hanging cable, and it is represented by a hyperbolic cosine function. For suspension footbridges, the representation of the main cables is between a catenary curve and a parabolic curve. The catenary action of cable elements results in an increase in stiffness as the cable is loaded. When a cable is initially loaded, it will deflect under small loads; however, as the cable deforms, more load will be required to cause the cable to continue to deflect. The main cables were modeled using the deformed length under self-weight. The curve of the cable can be input by the user in several ways – undeformed length, maximum vertical sag, maximum vertical low-point sag, constant horizontal component of tension, tension at either end, or the minimum tension at either end. The main cables are defined by the maximum vertical sag.

A geometric, nonlinear analysis is required for cable elements. This is due to the changes in the stiffness matrix as the cable deforms. SAP2000 will run 25 or more iterations in each nonlinear load case for models with cable elements to allow for proper convergence. In addition, convergence behavior improves for cable objects with fewer segments.

The mass of a cable element is lumped at the joints in SAP2000, so no inertial effects are considered within the element itself. For the present study, the cable is made up of many elements to connect each of the suspenders at one meter intervals along the bridge, resulting in the mass being lumped at each suspender. Unlike the mass for inertial forces, the self-weight is distributed along the arc length of the cable element (Computers and Structures, Inc., 1995).

2.3.2.1 Numerical Model Updating

Idealized numerical models are based on many assumptions and even very detailed models can have up to 37 percent error (Zivanovic, 2007). Therefore, numerical models are often updated or calibrated to real world experimental data to ensure the model is behaving properly. This experimental data can also provide the modal damping that cannot be obtained analytically (Zivanovic, 2007).

The aerospace and mechanical engineering disciplines use finite element model updating technology “to automatically update numerical models of structures to match their experimentally measured counterparts” (Zivanovic, 2007). However, the numerical models must first be manually adjusted by the user to allow the software to correctly update the model by adjusting a larger number of parameters within defined limits to more accurately match the experimental results. While automatic updating software was not available for the present study, manual model updating was performed.

The goal of manually adjusting the model is to minimize the difference between the measured results and the numerical results by changing uncertain parameters: geometry, boundary conditions, material properties and non-structural elements including decks and handrails, which have a strong relationship to the dynamic response. While these changes are guided by engineering judgment, they are made by systematic trial and error. Models can be updated to more closely match measured response for smaller span bridges; the modal response error increases for larger span bridges, even after the bridges are updated (Zivanovic, 2007). In general, numerical models must be updated, or calibrated, based on measurements to adjust uncertain parameters to create a model that behaves similarly to the physical structure. The present study uses the scaled physical model results to update the numerical models.

2.4 Pedestrian Loading

Pedestrian loading of footbridges is complex to characterize; however, it can often control the dynamic response of the footbridge. Typical pedestrian loading is between 320 kg/m^2 (65 psf) and 415 kg/m^2 (85 psf) (AASHTO, 1997). In extreme cases, the pedestrian loading dynamic response can lead to total structure failure. A bridge in Broughton, England collapsed in 1831 while 60 soldiers were marching across (Zivanovic, 2005). This is the reason soldiers are ordered to break stride while crossing a bridge (Shi, 2013). While most footbridges are controlled by serviceability limits today, total system failure occurs if vibration issues escalate and cause resonance.

2.4.1 Frequency of Pedestrian Loading

Humans typically walk with a frequency up to 2.2 Hz. People can walk quickly with a frequency ranging from 2.2 Hz to over 2.7 Hz (Huang, 2007). “95 percent of pedestrians walk at rates between 1.65 and 2.35 Hz” (Gentile, 2008). Several studies have been conducted to determine frequency ranges for dynamic loading of suspension footbridges. The typical frequency range for walking is 1.6 to 2.4 Hz. Therefore, the mean frequency is 2.0 Hz (Zivanovic, 2005), which is used for the model loading for the present study.

2.4.2 Forces from Pedestrian Loading

As people walk they produce forces in three directions: 1) vertical; 2) lateral; and 3) longitudinal. The forces on a bridge that result from pedestrian loading occur due to the acceleration and deceleration of the person’s mass. The largest force is produced in the vertical direction; it is represented as two peaks with a trough in the middle as presented in Figure 3. The magnitude of the force is presented in the figure, and the direction is downward. The lateral force is initially medial and then reaches an almost constant lateral force level through a normal walking stride as presented in Figure 4. Figure 5 presents the longitudinal force that is anterior at first and then posterior.

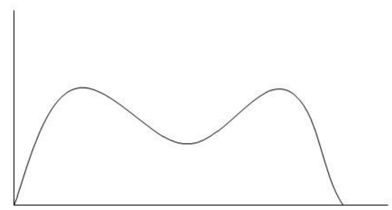

Figure 3: Vertical Pedestrian Walking Force (Zivanovic, 2005)

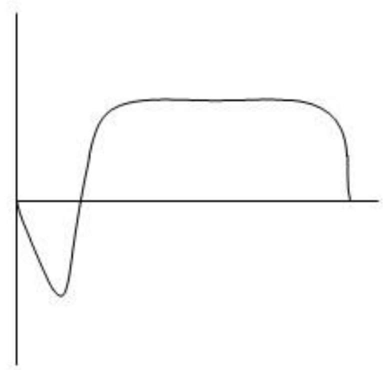

Figure 4: Lateral Pedestrian Walking Force (Zivanovic, 2005)

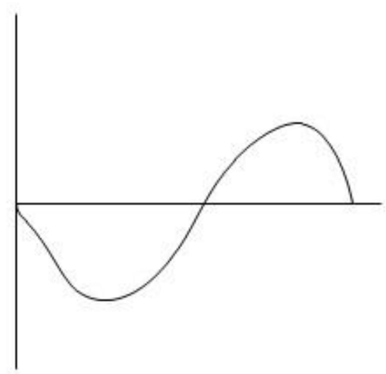

Figure 5: Longitudinal Pedestrian Walking Force (Zivanovic, 2005)

Forces due to pedestrian loading depend on many factors, including pedestrian velocity, stride length, step frequency, mass, and number of pedestrians using the structure. A typical walking speed is slightly greater than 1 m/s. This walking velocity results from pedestrians walking with a stride length of 0.6 m (Zivanovic, 2005). A typical pedestrian's center of gravity is 1 m above the ground. People tend to take two steps per second and they step 10 cm on each side of a centerline, causing their center of gravity to vary by 1 cm from the centerline as presented in Figure 6 (Kawada, 2010). For an average person, this results in a maximum vertical force of 800 N (180 lb) on average with the trough between the peaks reaching about 400 N (90 lb) (Zivanovic, 2005) as presented in Figure 3 and a lateral pedestrian loading of less than 8 percent of a person's weight at a frequency of 1 Hz. The resultant mean lateral force of multiple pedestrians is given in equation (2.1).

$$H = h\sqrt{N} \tag{2.1}$$

where *H* is the mean lateral force of a group of pedestrians, *h* is the lateral force from one pedestrian, and *N* is the number of people on the bridge (Kawada, 2010). Lateral forces for one pedestrian typically start at -45 N (10 lb) in the medial direction and then remain constant at 30 N (6.7 lb) in the lateral direction (Zivanovic, 2005).

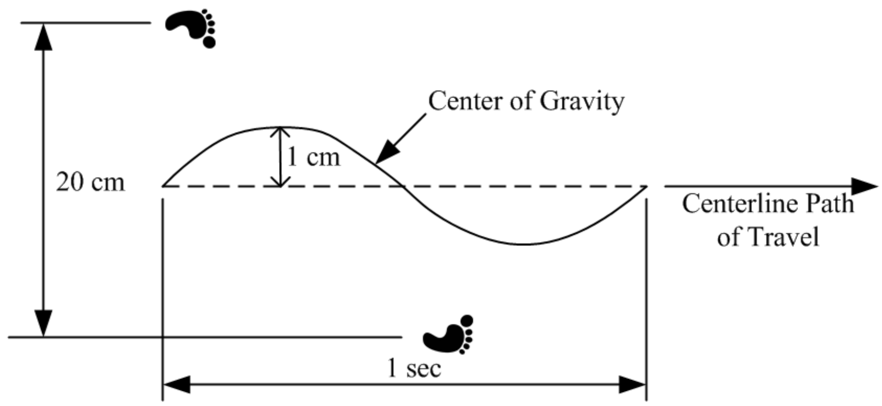

Figure 6: Lateral Pedestrian Movements

The present study models pedestrian forces in the vertical and lateral directions. The longitudinal direction is ignored because the bridge cannot be easily excited in this direction. The vertical pedestrian force used for the present study is 800 N peaks with a 400 N trough and follows the shape in Figure 3. The lateral pedestrian force used for the present study is 30 N with an initial force of -45 N following the shape in Figure 4. The stride length used for the present study is 0.6 m.

2.5 Serviceability Limits

While strength limits are very important for structural design, serviceability limits are as well, especially for modern suspension footbridges. Footbridges are being built with longer spans and greater slenderness due to the reduction in weight of bridge elements. These types of bridges have low stiffness, low mass, and low damping. Suspension footbridges have low modal frequencies and are therefore susceptible to pedestrian loading that occurs at low frequencies. Under typical pedestrian loading, suspension footbridges are at risk of reaching resonance or exceeding human tolerance levels for comfort (Huang, 2007).

2.5.1 Typical Pedestrian Tolerance Levels

While most footbridges are designed to withstand strength criteria, some footbridges have not been designed to satisfy serviceability limits. Pedestrians must use footbridges for the structure to fulfill its purpose; however, in the process of walking across a footbridge, pedestrians create vibrations that cause the structure to move or twist in all directions. If the bridge has excessive movements, the pedestrians become uncomfortable, resulting in a serviceability failure.

Moving pedestrians typically have a higher tolerance level than stationary pedestrians on the bridge. In addition, people have a higher tolerance level when they expect the structure to have certain vibrations (Zivanovic, 2005). Most pedestrians are more sensitive to lateral vibrations than to vertical vibrations. Accepted vertical acceleration amplitudes and deflection amplitudes can be up to five times greater than the lateral accepted amplitudes (Huang, 2007).

2.5.1.1 Pedestrian Vertical Movement Tolerance Levels

Pedestrian sensitivity maximum frequency for typical vertical vibrations is between 1 and 2 Hz with an equivalent harmonic peak acceleration of 0.07 m/s^2 (0.23 ft/s^2). The level of acceptable vertical acceleration, a_{limit}, is defined in equation (2.2) (Zivanovic, 2005).

$$a_{limit}=c\sqrt{f} \tag{2.2}$$

where f is the fundamental frequency in Hertz and c is 0.5 for a_{limit} in m/s^2 or 1.6 for a_{limit} in ft/s^2. Another study observes that outside the frequency range of 1.7 to 2.2 Hz, a more appropriate c value might be 1 for a_{limit} in m/s^2 or 3.28 for a_{limit} in ft/s^2 (Zivanovic, 2005).

According to AISC Design Guide 11 (Murray, 2012), the recommended peak acceleration for outdoor footbridges for human comfort varies from 10 percent of *g* at a frequency of 1 Hz to 5 percent of *g* at a frequency of 4 Hz (Murray, 2012). The peak acceleration is calculated by equation (2.3).

$$\frac{a_p}{g} = \frac{P_0 e^{-0.35 f_n}}{\beta W} \tag{2.3}$$

where a_p is the peak acceleration due to walking excitation, P_0 is a constant force representing the excitation, f_n is the fundamental natural frequency, β is the modal damping ratio, and W is the effective weight of a panel. The criterion states that the peak acceleration, calculated by the equation above, is acceptable if it does not exceed the acceleration limit. For outdoor footbridges, P_0 is 0.41 kN (92 lb), β is 0.01, and the acceleration limit (a_0/g) is 5 percent (Murray, 2012).

Most standards have different vertical acceleration limits. BS 5400 (British Standards Association, 1978) limits the acceleration of footbridges to equation (2.2). Eurocode (European Committee for Standardization, 2002) governs the design for all construction works in the European Union. It limits the vertical acceleration to 0.7 m/s^2 (2.3 ft/s^2). ISO 10137 (International Standardization Organization, 2005) limits the vertical accelerations to 60 times the curve presented in Figure 7. Bro 2004, which is published by the Swedish Road Administration, limits the root mean square acceleration to 0.5 m/s^2 (1.6 ft/s^2) (Hauksson, 2005).

According to the European Design Guide for Footbridge Vibration (Heinemeyer, 2008), pedestrians are comfortable with vertical accelerations up to 0.50 m/s^2 (1.6 ft/s^2). They have a medium comfort level up to 1.00 m/s^2 (3.3 ft/s^2), and the maximum acceleration pedestrians can tolerate is 2.50 m/s^2 (8.2 ft/s^2).

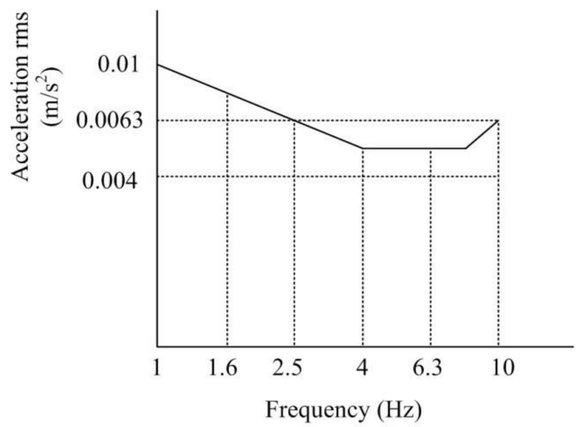

Figure 7: ISO 10137 Vertical Acceleration Vibration Base Curve (International Standardization Organization, 2005)

Obata (1995) found that the maximum velocity of a footbridge that humans can tolerate is 1 cm/s (0.033 ft/s), and typically, pedestrians are comfortable with velocities up to 1.4 cm/s (0.046 ft/s). If these velocity peaks are converted to acceleration peaks for a footbridge with a frequency of 2 Hz, the maximum accelerations for comfort are 0.13 m/s^2 (0.43 ft/s^2) and 0.18 m/s^2 (0.59 ft/s^2) (Zivanovic, 2005). However, these accelerations are much lower than those calculated using equation (2.2). Overall, many studies have concluded different limits for acceptable velocities and accelerations; therefore, no definite serviceability limits for vertical vibrations in footbridges currently exist. The present study will set human tolerance limits at 0.7 m/s^2 (2.3 ft/s^2) for vertical accelerations and at 1 cm/s (0.033 ft/s) for vertical velocities. These limits will be used to evaluate the performance of the footbridges to determine if the models meet human comfort criteria.

2.5.1.2 Pedestrian Lateral Movement Tolerance Levels

Pedestrians on footbridges are much more sensitive to lateral movements than vertical movements; however, lateral movements are typically smaller than vertical movements in suspension footbridges. The Millennium Bridge in London is an example of a bridge that failed due to lateral vibration problems; the deck swayed laterally, and people started to hang onto the sides of the footbridge because they felt unsafe (Huang, 2007). At frequencies over 3 Hz, pedestrians are actually more sensitive to vertical movements than to lateral movements. Based on testing of full-scale footbridges, a reasonable serviceability limit is 45 mm (1.77 inches) for maximum lateral displacements and 1.35 m/s^2 (4.43 ft/s^2) for maximum lateral accelerations. A maximum lateral displacement of 70 mm (2.76 inches) with a 2.1 m/s^2 (6.89 ft/s^2) lateral acceleration caused most people to feel unsafe and avoid using the footbridge (Zivanovic, 2005).

BS 5400 (British Standards Association, 1978) and Bro 2004 (Hauksson, 2005) do not provide requirements for lateral accelerations of footbridges. Eurocode (European Committee for Standardization, 2002) limits the maximum acceleration in the lateral direction to 0.2 m/s^2 (0.66 ft/s^2) for normal use and to 0.4 m/s^2 (1.31 ft/s^2) for crowded conditions. ISO 10137 (International Standardization Organization, 2005) limits the lateral acceleration to 60 times the base curve presented in Figure 8. The highest sensitivity of 3.1 percent g is for bridges up to 2 Hz (Hauksson, 2005). All pedestrians are comfortable with lateral accelerations up to 0.10 m/s^2 (0.33 ft/s^2) according to the European Design Guide for Footbridge Vibration (Heinemeyer, 2008). Pedestrians have a medium comfort for lateral accelerations up to 0.30 m/s^2 (0.98 ft/s^2), and the maximum lateral acceleration a person can tolerate is 0.80 m/s^2 (2.62 ft/s^2). The present study will set human tolerance limits at 0.3 m/s^2 (0.98 ft/s^2) for lateral accelerations and at 45 mm (1.77 inches) for lateral displacements. These limits will be used to evaluate the performance of the footbridges to determine if the models meet human comfort criteria.

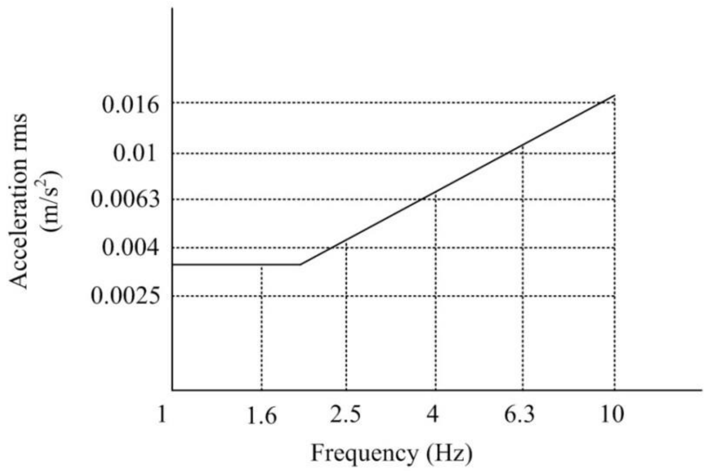

Figure 8: ISO 10137 Lateral Acceleration Vibration Base Curve (International Standardization Organization, 2005)

2.5.2 Synchronization of Pedestrians with Bridge Vibrations

While pedestrians have certain tolerance levels, they also can subconsciously add to the dynamic response of the bridge through synchronization. High densities of people can add to synchronous excitation when they walk together with a frequency that matches the low frequency of the footbridge. When the footbridge starts to resonate, pedestrians have a tendency to change their walking frequency to match the vibration of the bridge. This escalates the vibration and adds to the discomfort of the users (Huang, 2007).

Sometimes pedestrians are limited in their movement on footbridges. When people walk in small groups, they tend to all walk at the same velocity. Therefore, each person walks with a different frequency because their step length varies. However, when footbridges are exposed to a crowd of people with a density between 0.6 and 1.0 pedestrians/m^2, free walking is limited, and pedestrians are forced to adjust their step length and velocity to the group. This is typically when synchronization occurs, which can lead to structure serviceability problems (Zivanovic, 2005).

2.5.2.1 Vertical Synchronization

Vertical synchronization of pedestrians with footbridge vibrations is less common than lateral synchronization and more difficult to measure. Therefore, there are several ranges of predictions for the probability of pedestrians synchronizing to vertical vibrations. One study suggested a probability of synchronization of 22.5 percent for a bridge with a frequency of 2 Hz. However, other studies predicted higher percentages. While there are many equations that attempt to characterize pedestrian synchronization, more research is needed to determine the relationship between the number of pedestrians, walking speed, walking frequency, and probability of synchronization (Zivanovic, 2005). Vertical synchronization will not be modeled for the present study.

2.5.2.2 Lateral Synchronization

Synchronization in the lateral direction is much more probable than in the vertical direction due to the way humans maintain their body balance on a laterally moving structure. The only known way to reduce the change of the vibration escalating to the point where it exceeds serviceability limits is to reduce the number of people on the bridge or disrupt the pedestrian movement. However, not all people will move in a way to escalate lateral vibrations, and excessive swaying only occurs when the lateral modal frequency of the footbridge is 1 Hz, which matches the first harmonic of the pedestrian lateral force. According to tests of a single walking person on a platform, there is a 40 percent chance people will change their step to match the bridge movement when the structure is moving at 1 Hz with a 5 mm (0.2 inch) amplitude. However, people tend to change their steps more often when they are in a large crowd of people (Zivanovic, 2005). While lateral synchronization is dependent on many variables, people do tend to match their step to the structure, which results in increased vibrations and lateral movement of the footbridge. Lateral synchronization will not be modeled for the present study.

2.5.3 Serviceability Design Procedures

Most design procedures for serviceability limit states determine the peak or root mean squares response of the pedestrian bridge. There are two domains for design procedures – time or frequency. The time domain is based on the assumption that human-induced forces are perfectly periodic, so they can be broken into harmonics through Fourier decomposition. Therefore, a single force harmonic is considered that could cause a single degree of freedom footbridge to resonate through one of the first three or four excitation harmonics. This type of time domain modeling is only applicable for vertical forces. Frequency domain modeling has not specifically been studied for footbridges; however, the auto spectral density can be determined by applying the theory of stationary random processes to obtain the peak acceleration (Zivanovic, 2005).

Currently, design guidelines have different approaches to evaluating footbridge performance against serviceability limits. Some codes, such as the British Standard 5400 recommend avoiding the first or second force harmonic to avoid the resonant frequency range. There are no universal limits for frequencies; however, requiring the minimum bridge frequency in the vertical direction to be 4 Hz and the minimum bridge frequency in the lateral direction to be the smaller of 1.5 times the vertical frequency or 1.5 Hz typically results in a pedestrian bridge with no vibration problems (Zivanovic, 2005). Eurocode 5 allows all frequency ranges but requires a complex design procedure to determine the acceptability of the bridge response. However, for footbridges with a lateral fundamental frequency of less than 2.5 Hz or a vertical fundamental frequency less than 5 Hz, a detailed dynamic analysis is required. This method is not described, but procedures for checking vertical vibrations for footbridges with frequencies up to 5 Hz are available.

The Ontario Highway Bridge Design Code requires footbridge dynamics to be studied due to footfall force represented by a moving sinusoidal force with an amplitude of 180 N (40.5 lbs) and a frequency equal to the fundamental frequency of the structure or 4 Hz, whichever is lower (Zivanovic, 2005). The European Design Guide for Footbridge Vibration specifies a lively bridge as having a vertical fundamental frequency between 1.3 and 2.3 Hz and a lateral fundamental frequency between 0.5 and 1.2 Hz (Heinemeyer, 2008). The American Association of State Highway and Transportation Officials (1997) provides limits for fundamental frequencies in the *Specification for Pedestrian Bridge Design*; The fundamental frequency in the vertical plane of a pedestrian bridge without live load must be greater than 3 Hz, and the fundamental frequency in the lateral direction must be greater than 1.3 Hz (Chung, 2014).

Therefore, codes have limits on frequencies that fall within a typical range but do not exactly agree on the frequency range; also, the codes propose design procedures to evaluate the footbridge performance against serviceability limits, but finite element modeling is still the standard procedure used to evaluate the serviceability limit state of the footbridge. The present study uses SAP2000 to evaluate the vibration response of the bridge based on the tolerance limits described in this section.

2.6 Summary

Suspension bridge analysis has changed over the years, but serviceability analysis of suspension bridges continues to be a problem. Suspension footbridges can have a large dynamic response to pedestrian loading because of their low modal frequencies. Modal frequencies for suspension footbridges can be determined through properly scaling models. In addition, numerical models can be used to study footbridge dynamics. Pedestrian loading must be applied to determine the response of the footbridge, and this response must be compared to serviceability limits to determine if the footbridge meets human comfort criteria.

Chapter 3

Physical Model

3.1 Overview

Two physical models were constructed to calibrate the numerical models and validate the parametric study. Physical, scaled models were built of a 40 m span bridge with 5 percent cable sag and an 80 m span bridge with 7.5 percent cable sag. The overall model geometry is presented in Figure 9 and the model elements are presented in Figure 10. These span and sag limits are the two extremes for the bridges used for the present study, which allow for a comparison of bridge behaviors.

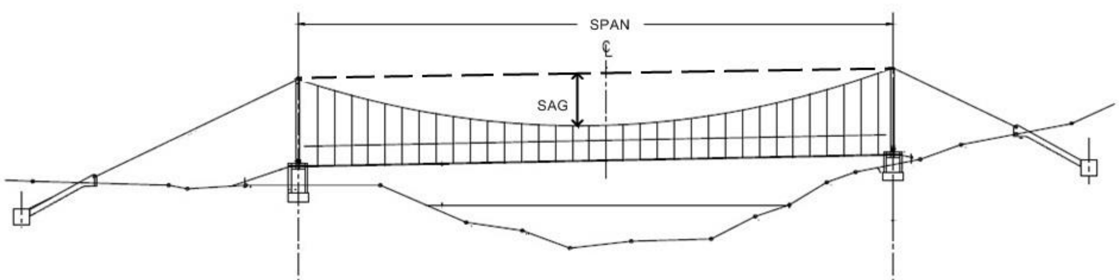

Figure 9: Suspension Bridge Model (Bridges to Prosperity, 2013)

Figure 10: Suspension Bridge Model Elements

The models were designed based on a calculated scale factor. The materials were chosen to most closely match the full scale bridge material stiffness and scaled mass. The models were created based on the scaled geometry of suspension footbridges. Both models were loaded with a scaled pedestrian model and the vibration response was recorded with a high speed video camera. The response data was processed to determine the modal frequencies of the bridge models. The response data were then used to calibrate the numerical simulations.

3.2 Physical Model Design

The physical model design included setting the scale factor for the models relative to the full scale suspension footbridges and determining materials for the models. The materials were selected based on mass, which is the controlling parameter.

3.2.1 Model Scale

The models were designed at a 1:18 scale of the 40 and 80 m suspension footbridges. Scale factors depend on the parameter being scaled; therefore, scale factors were determined as presented in Table 1. The controlling parameter for the present study is mass. Mass is scaled by S^3; where S = model length/actual length (Kumar 1997). The smallest steel cable available for the physical model is $\frac{1}{16}$ inch diameter galvanized cable. The mass of the $\frac{1}{16}$ inch diameter cable is 10.7 g/m (0.0072 lb/ft). The mass of 1⅛ inch diameter cable is 3480 g/m (2.34 lb/ft). The mass of the cables and the scale factor was determined based on the following:

$$m_{real\ cable} = 3480 \text{ g/m} \times 130 \text{ m} = 452{,}400 \text{ g} \tag{3.1}$$

$$m_{model\ cable} = 10.7 \text{ g/m} \times (130 \text{ m} / S) = 452{,}400 \text{ g} / S^3 \tag{3.2}$$

Solving equation (3.2) for S resulted in a scale factor of 18 that was used for the present study. S also scales the cable diameter, which is scaled from 1⅛ inch to $^1/_{16}$ inch. However, the effective area of 1⅛ inch diameter cable is 382 mm^2 or 1.18 mm^2 scaled (0.59 $inch^2$ or 0.0018 $inch^2$ scaled) and the effective area of $^1/_{16}$ inch diameter cable is 1.15 mm^2 (0.00178 $inch^2$), a 2.5 percent scaling error in the effective cable areas. The effective cable area was calculated based on equation (3.3).

$$A = F \times d^2 \tag{3.3}$$

where A is the effective cable area in mm^2, F is the compactness factor, and d is the nominal diameter of the cable in mm. The $^1/_{16}$ inch diameter cable used for the physical models is 6×7 around a strand core. The compactness factor for 6×7 wire cable is 0.38. In addition, for six strand cable with strand core, 20 percent must be added to the cross sectional area (A. Noble and Son Ltd., 2013). Therefore, the resulting cross sectional area of 1.59 mm ($^1/_{16}$ inch) diameter wire cable is 1.15 mm^2 (0.00178 $inch^2$) as presented in equation (3.4).

$$A = 1.2 \times \left(0.38 \times 1.59^2\right) = 1.15 \text{ mm}^2 \tag{3.4}$$

3.2.2 Model Materials

The model materials were chosen to most closely match the full scale bridge materials. Some model materials, such as decking and cables, have the same properties as the full scale bridges. The decking is constructed of wood for the full scale structure and model structure. While the properties of wood vary greatly, the properties of the physical model deck are in the same range as a full scale footbridge deck. In addition, the cables are made of wire rope for both structures.

The model materials used to represent the crossbeams, suspenders, and fence do not perfectly match the full scale bridge materials because of modeling constraints and masses. The crossbeams are made of aluminum instead of steel. Aluminum is a metal, but its mechanical properties differ from steel. Steel has a higher elastic modulus, strength, and hardness. However, aluminum has a lower density, which is needed to achieve the proper mass for the model. Because mass is the controlling scaling parameter, aluminum elements are used for the crossbeams instead of steel elements. The suspenders are made out of copper wire that represents rebar. Rebar is heavier and less ductile than copper. However, the proper weight of steel wire was not available, which is why copper wire is used for the suspenders. Steel wire is used to represent the chain link fence, hand cable, and cable clamps on the full scale footbridge.

The tower model materials do not need to closely match the full scale bridge towers because the tower material properties do not significantly affect the dynamic response. The towers are considerably stiffer than all other elements and do not participate so the material properties are not required to closely match the full scale bridge materials.

Materials were identified based on a scale factor of 18 to closely represent the bridge elements. Table 2 presents the materials used for the physical scaled model corresponding to the full scale bridge materials (Bridges to Prosperity, 2013). The 40 m scaled model towers are made of ⅜ inch hollow, square aluminum tubing and the 80 m scaled model towers are made of ½ inch hollow, square aluminum tubing.

Table 2: Model Materials

Element	Actual Bridge	Model Structure
Cable	1⅛" diameter cable	1/16" diameter cable
Suspenders	9 mm diameter rebar	24 gage copper wire
Crossbeam	2-L 1¾" × 1¾" × ¼" bolted back-to-back	0.032" thick aluminum plate (7/16" × 2⅜")
Towers	Hollow steel pipe with angle bracing	⅜" or ½" hollow, square aluminum tube with ¼" aluminum angles
Nailers	2"×8" wood board	3/32" thick basswood pieces (1/16" × 2⅜")
Decking	2"×8" wood board	3/32" thick basswood pieces (1/16" × 2⅜")
Fence	Fence, hand cable, and cable clamps	4 pieces of 24 gage steel wire

3.2.3 Model Element Masses

Aside from the towers, the mass of all other elements is within 10 percent of the ideal scale mass determined from the full scale bridge elements. The mass of the towers does not exactly match the scaled mass; however, Gentile (2008) demonstrated that the towers need not be modeled in his dynamic analysis of the Morca suspension footbridge because the towers are considerably stiffer than all of the other structural elements. For the present study, the numerical model was used to verify that the mass of the towers does not greatly affect the dynamic response of the footbridge.

3.2.3.1 40 m Span Model Mass

Table 3 presents the mass of each element for the 40 m span model. The actual scaled mass was determined by weighing the member or calculating the weight from the material specifications. The weight of the copper wire is based on 1.233 lb/1000 ft or 1.82 kg/km. The aluminum tower weight and aluminum plate weight is established on the specified density of 0.097 lbs/in^3 (2.7 g/cm^3) for 6061 alloy aluminum. The weight of the basswood is based on a wood density of 29 pcf. The weight of the fence is constructed off a standard 2" mesh, 11 gage, 3.5' high fence weight of 1.63 lb/ft (0.00243 kg/mm) (Builders Fence Company, 2014). The weight of the hand cable is established on 6 mm (¼") 6×19 IPS-IWRC diameter wire cable weight of 0.11 lb/ft (Armstrong – Alar Chain Corporation, 2014). The weight of the clamps for the hand cable is based off 0.48 lbs (0.218 kg) per clamp (The Crosby Group, 2012). This results in a total weight for the fence and fence components of 2.84 kg (6.26 lbs) per suspender.

Table 3: 40 m Span Model Masses

Element	Actual Member	Constructed Model Member	Ideal Scaled Mass g	Actual Mass g	Mass Error %
Cable	29 mm diameter 6×19 IPS-IWRC (A = 382 mm² / cable)	(1⁄16" diameter galvanized cable	45.9	45.7	0.5
Suspenders	9 mm diameter rebar (#3 rebar)	24 gage copper wire	0.485	0.510	5.1
Towers	128 mm inner diameter steel pipe with 13 mm thick walls	⅜" hollow aluminum tube	18.7	20.7	10.8
Crossbeams	2-L 1¾" × 1¾" × ¼" (Metric: L44x44x6)	Aluminum plate (0.032" thick)	1.64	1.63	1.0
Nailers	2"×8" (Metric: 40×200); actual size = 1½"× 7¼" (Metric: 38.1×184.2)	Basswood (3⁄32" thick)	0.79	0.74	6.2
Decking	2"×8" (Metric: 40×200); actual size = 1½"× 7¼" (Metric: 38.1×184.2)	Basswood (3⁄32" thick)	1.44	1.37	4.9
Diagonal Tower Members	L3" × 3" × ¼" (Metric: L76×76×6)	Aluminum angle (1⁄16" thick × ¼")	4.1	8.6	110
Horizontal Tower Members	2L3" × 3" × ¼" (Metric: 2L76×76×6)	Aluminum angle (1⁄16" thick × ¼")	3.1	6.6	110
Fence	Fence, hand cable, and cable clamp	4 pieces of 24 gage steel wire	0.479 g /suspender	0.487 g /suspender	1.6

3.2.3.2 80 m Span Model Mass

Table 4 presents the mass of each element for the 80 m span model. The actual scaled mass was determined by weighing the member or calculating the weight from the material specifications. The weight of the copper wire is based on 1.233 lb/1000 ft or 1.82 kg/km. The aluminum tower weight and aluminum plate weight is established on the specified density of

0.097 lbs/in^3 (2.7 g/cm^3) for 6061 alloy aluminum. The weight of the basswood is based on a wood density of 29 pcf. The weight of the fence is constructed off a standard 2” mesh, 11 gage, 3.5’ high fence weight of 1.63 lb/ft (0.00243 kg/mm) (Builders Fence Company, 2014). The weight of the hand cable is established on 6 mm (¼") 6×19 IPS-IWRC diameter wire cable weight of 0.11 lb/ft (Armstrong – Alar Chain Corporation, 2014). The weight of the clamps for the hand cable is based off 0.48 lbs (0.218 kg) per clamp (The Crosby Group, 2012). This results in a total weight for the fence and fence components of 2.84 kg (6.26 lbs) per suspender.

Table 4: 80 m Span Model Masses

Element	Actual Member	Constructed Model Member	Ideal Scaled Mass g	Actual Scaled Mass g	Mass Error %
Cable	29 mm diameter 6x19 IPS-IWRC (A = 382 mm² / cable)	1/16" diameter galvanized cable	79.4	78.9	0.5
Suspenders	9 mm diameter rebar (#3 rebar)	24 gage copper wire	0.82	0.87	5.1
Towers	178 mm inner diameter steel pipe with 16 mm thick walls	½" hollow aluminum tube	51.1	47.9	6.2
Crossbeams	2-L 1¾" × 1¾" × ¼" (Metric: L44x44x6)	Aluminum plate (0.032" thick)	1.64	1.63	1.0
Nailers	2"×8" (Metric: 40×200); actual size = 1½"× 7¼" (Metric: 38.1×184.2)	Basswood (3/32" thick)	0.79	0.74	6.2
Decking	2"×8" (Metric: 40×200); actual size = 1½"× 7¼" (Metric: 38.1×184.2)	Basswood (3/32" thick)	1.44	1.37	4.9
Diagonal Tower Members	L3" × 3" × ¼" (Metric: L76×76×6)	Aluminum angle (1/16" thick × ¼")	4.7	10.0	110
Horizontal Tower Members	2L3" × 3" × ¼" (Metric: 2L76×76×6)	Aluminum angle (1/16" thick × ¼")	4.3	8.9	110
Fence	Fence, hand cable, and cable clamp	4 pieces of 24 gage steel wire	0.479 g /suspender	0.487 g /suspender	1.6

3.3 Model Geometry

Each element's dimensions and the overall dimensions of the model bridges are scaled to represent the full scale suspension footbridge as closely as possible.

3.3.1 Model Element Geometry

The scaled dimensions of some elements do not closely match the full scale dimensions because the ideal scaled mass is the controlling parameter. Tradeoffs were considered to most closely match the full scale bridge response. In addition, physical constraints, such as having a nailer that is long enough to support all decking pieces, had to be considered for constructability. The lengths of most members were chosen to match the ideal model. However, the nailer was cut slightly shorter so a hole could be drilled in the crossbeam to attach the suspender.

3.3.1.1 40 m Span Model Element Geometry

Table 5 presents the dimensions of each element for the 40 m span model. The width and height or the diameter of some elements varies from the ideal model to most closely match the mass of the ideal model.

Table 5: 40 m Span Model Element Dimensions

Element	Ideal Model				Constructed Model			
	Diameter (mm)	Width (mm)	Height (mm)	Length (mm)	Diameter (mm)	Width (mm)	Height (mm)	Length (mm)
Cable	1.61			4278	1.56			4278
Suspenders	0.50			Varies	0.51			Varies
Towers	7.83			278		9.53	9.53	278
Crossbeams		7.06	2.83	66.7		11.11	0.81	66.7
Nailers		10.23	2.12	61.1		11.11	2.38	60.3
Decking		10.23	2.12	111		11.11	2.38	111
Diagonal Tower Members		4.22	4.22	181		19.05	19.05	181
Horizontal Tower Members		8.44	4.22	139		19.05	19.05	139

3.3.1.2 80 m Span Model Element Dimensions

The dimensions of each element for the 80 m span model were calculated in a way similar to the 40 m span model. Because the decking is the same for all span lengths, the dimensions for the crossbeams, nailers, and decking did not change. Table 6 presents the dimensions of each element for the 80 m span model.

Table 6: 80 m Span Model Element Dimensions

Element	Ideal Model				Constructed Model			
	Diameter (mm)	Width (mm)	Height (mm)	Length (mm)	Diameter (mm)	Width (mm)	Height (mm)	Length (mm)
Cable	1.61			7389	1.56			7389
Suspenders	0.50			Varies	0.51			Varies
Towers	10.78			472		19.05	19.05	472
Crossbeams		7.06	2.83	66.7		11.11	0.81	66.7
Nailers		10.23	2.12	61.1		11.11	2.38	60.3
Decking		10.23	2.12	111		11.11	2.38	111
Diagonal Tower Members		4.22	4.22	211		19.05	19.05	211
Horizontal Tower Members		8.44	4.22	189		19.05	19.05	189

3.3.2 Overall Model Geometry

The standard tower height, tower width, and deck camber are used based on the *Bridge Builder Manual* (2013). In addition, the cable back span length is a 1:2 slope – one vertical to two horizontal – to the anchor that is at the same elevation as the tower base. The cable sag is one of the variables being studied. According to the *Bridge Builder Manual* (2013), the standard cable sag is 7.3 percent. A 1 m deck width (2 3⁄16 inch scaled) with 2 m staggered decking boards is used with the nailers and crossbeams extending past the deck for connection details. The spacing of suspenders along the length is 1 m (2 3⁄16 inch scaled). The width between suspenders increases along the bridge height as presented in Figure 11. This gives the bridge more stiffness because the two sides of the bridge are not in parallel planes. Also, due to the weight of the structure, the main cables are pulled closer to the deck width in the center of the bridge, which provides lateral stability.

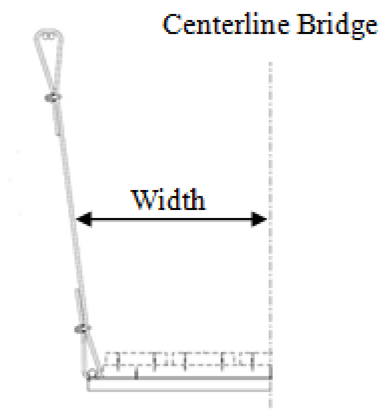

Figure 11: Suspender Geometry

<u>3.3.2.1 40 m Span Model Geometry</u>

The complete 40 m span model is slightly less than 11 feet long. It is built on a 13 foot by 1 foot wide OSB plywood board. The length from tower to tower is 7' 3½". The length from tower to anchor connection is 1' 9⅞". This model has a deck camber of $2\frac{11}{16}$" and cable sag of 4⅜" that results in an initial cable sag height above the ground of $6\frac{9}{16}$". The tower design was based on the full scale towers for 40 m span bridges specified in the *Bridge Builder Manual* (2013). Figure 12 presents the tower layout on the plywood foundation. Figure 13 presents the final bridge model with the span length, back span length, deck camber, and cable sag dimensions labeled.

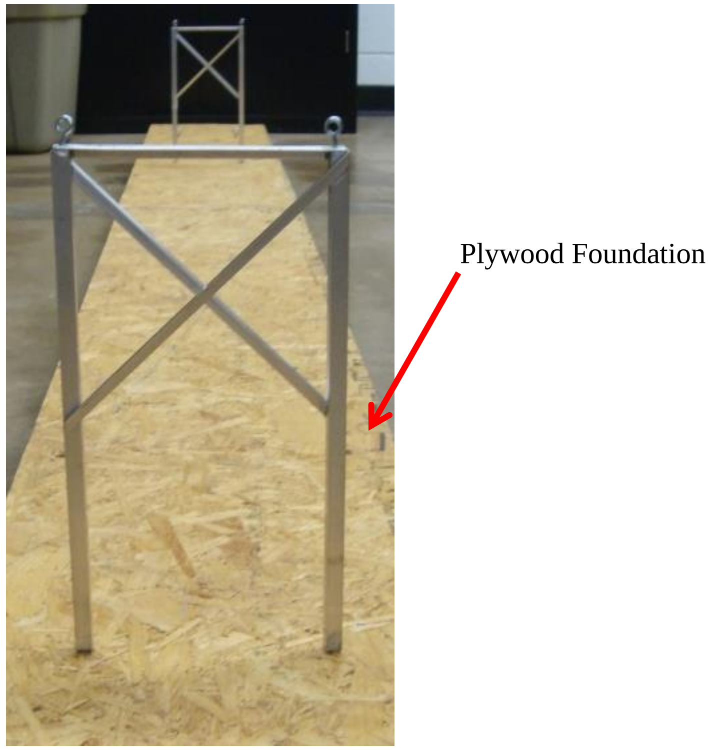

Figure 12: Towers for 40 m Span Model

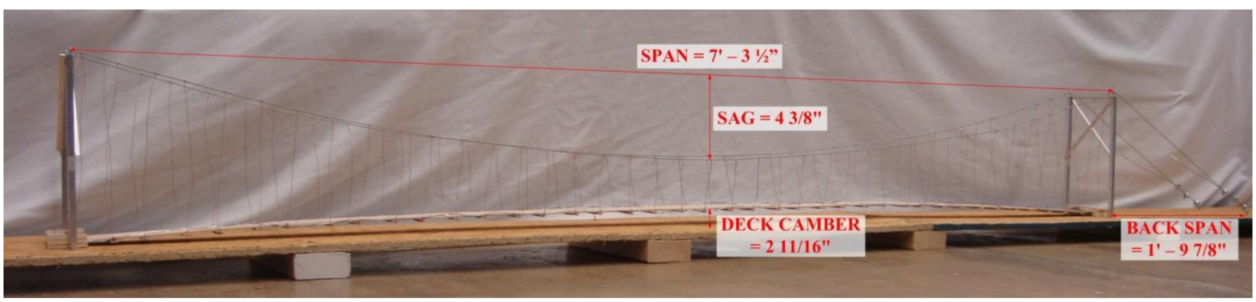

Figure 13: 40 m Span Bridge Model with Dimensions

<u>3.3.2.2 80 m Span Model Geometry</u>

The complete 80 m span model is slightly less than 21 feet long. It is built on a 22 foot by 2 foot wide OSB board. The length from tower to tower is 14' 7". The length from tower to anchor connection is 3' $1\frac{3}{16}$". This model has a deck camber of $3\frac{15}{16}$" and cable sag of $13\frac{1}{8}$" that results in an initial cable sag height above the ground of $5\frac{7}{16}$". The tower design was based on the full scale towers for 80 m span bridges specified in the *Bridge Builder Manual* (2013).

Figure 14 presents the tower design. Figure 15 presents the final bridge model with the span length, back span length, deck camber, and cable sag dimensions labeled.

Figure 14: Towers for 80 m Span Model

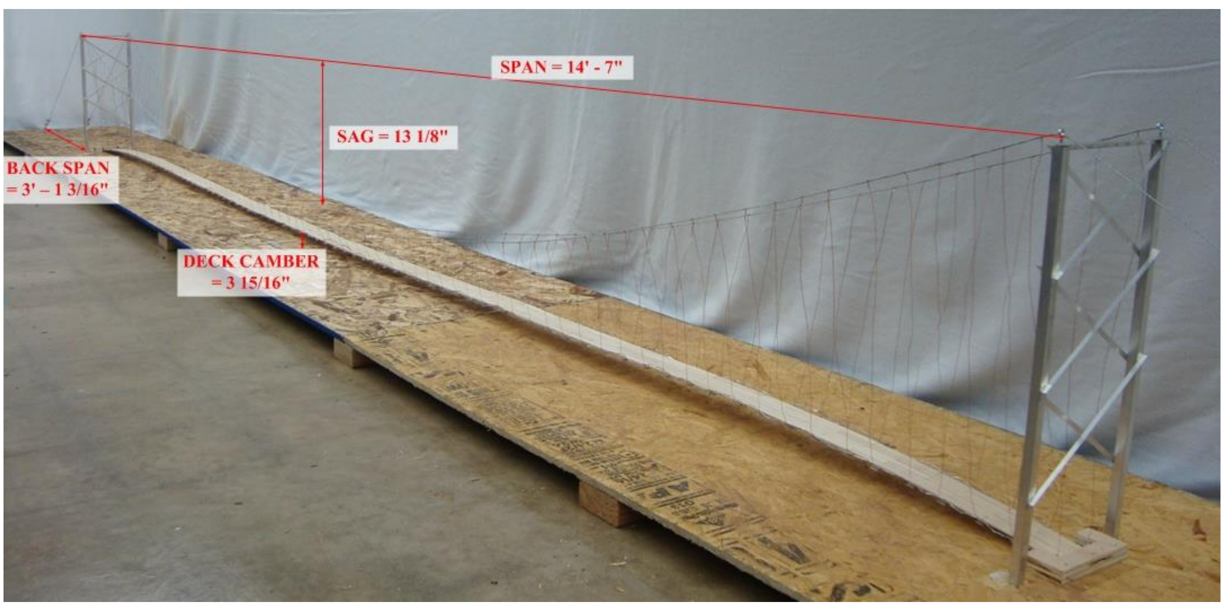

Figure 15: 80 m Span Bridge Model with Dimensions

3.4 Model Construction

The bridge construction method for the two models was very similar, except the 80 m span model involved more elements. The materials were purchased and cut to size. Table 7 presents all quantities for the 40 m span model, and Table 8 presents all quantities for the 80 m span model.

Table 7: Quantities for 40 m Span Model

Element	Material	Width	Length	Quantity	Notes
Cable	1/16" steel cable	1/16" diameter	14 feet	2	Attached to #208 screw eye with 3 clamps at anchor location
Crossbeams	0.032" thick aluminum plate	7/16"	2⅝"	41	1 hole drilled on each end for 24 gage copper wire
Nailers	3/32" thick Basswood	7/16"	2⅜"	41	Glued with epoxy to center of crossbeams
Decking	3/32" thick Basswood	7/16"	4⅜"	100	Glued with wood glue to nailers; 5 wide along deck; staggered
Tower Pipe	⅜" diameter hollow aluminum tube	⅜"	10 15/16"	4	#212 screw eye in top of tube
Horizontal Tower Angles	(2) 1/16" × ¼" aluminum angle	¼"	5 13/16"	4	Notched out ends to sit on top of tube; drilled hole for #212 screw eye
Diagonal Tower Angles	1/16" × ¼" aluminum angle	¼"	8¼"	4	Glue with epoxy to tube
Suspenders	24 gage copper wire	0.511 mm diameter	Varies	82	Looped around the cable and crossbeam; superglued to hold to cable
Fence	24 gage steel wire	0.511 mm diameter	7' 3½"	4	Wires twisted together and attached at ends of crossbeams

Table 8: Quantities for 80 m Span Model

Element	Material	Width	Length	Quantity	Notes
Cable	1/16" steel cable	1/16" diameter	24.2 feet	2	Attached to #208 screw eye with 3 clamps at anchor location
Crossbeams	0.032" thick aluminum plate	7/16"	2 5/8"	81	1 hole drilled on each end for 24 gage copper wire
Nailers	3/32" thick Basswood	7/16"	2 3/8"	81	Glued with epoxy to center of crossbeams
Decking	3/32" thick Basswood	7/16"	4 3/8"	200	Glued with wood glue to nailers; 5 wide along deck; staggered
Tower Pipe	½" diameter hollow aluminum tube	½"	18 9/16"	4	#212 screw eye in top of tube
Horizontal Tower Angles	(2) 1/16" × ¼" aluminum angle	¼"	7 15/16"	4	Notched out ends to sit on top of tube; drilled hole for #212 screw eye
Diagonal Tower Angles	1/16" × ¼" aluminum angle	¼"	9 7/16"	12	Glued with epoxy to tube
Suspenders	24 gage copper wire	0.511 mm diameter	Varies	162	Looped around the cable and crossbeam; superglued to hold to cable
Fence	24 gage steel wire	0.511 mm diameter	14' 7"	4	Wires twisted together and attached at ends of crossbeams

The anchor and tower base connections are simplified compared to real pedestrian suspension bridges. The physical models are built on OSB plywood boards elevated off the ground with 2"×4" wood supports to allow for all connections to be made to the foundation. The tower base connection is modeled as a pin connection, and it was constructed by drilling a hole in the plywood board and inserting a bolt. The bolt diameter is slightly smaller than the inner diameter of the tube, so the tower can rotate but not slide on the surface. Figure 16 presents the tower connection. The bolt is glued in place from beneath the plywood board.

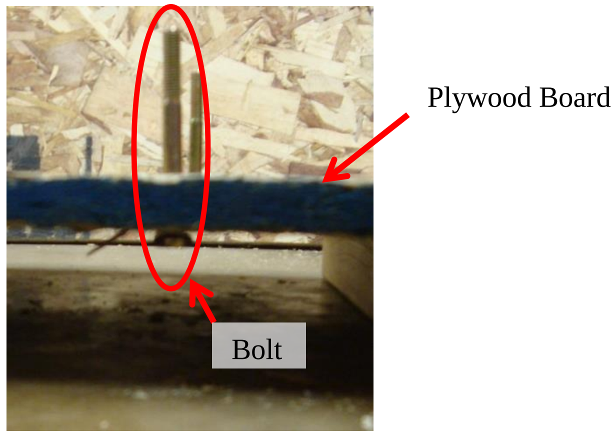

Figure 16: Tower Connection

The anchor connection is modeled as a pin connection, and it was constructed by running the cable through a #208 screw eye that is attached to the plywood board and securing the cable with three $\frac{1}{16}$" diameter drop forged cable clamps. Three clamps is the standard for this size cable. The clamps are spaced at 2" on center. The clamps are attached to saddle the live cable, which is the part of the cable that comes from the bridge, and compress the dead end of the cable. Figure 17 presents the anchor connection. Figure 18 presents the tower and anchor connections before the bridge was attached.

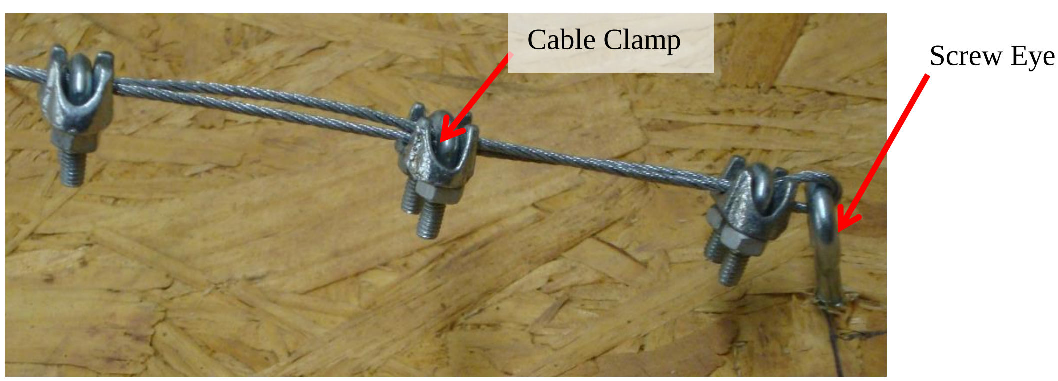

Figure 17: Anchor Connection

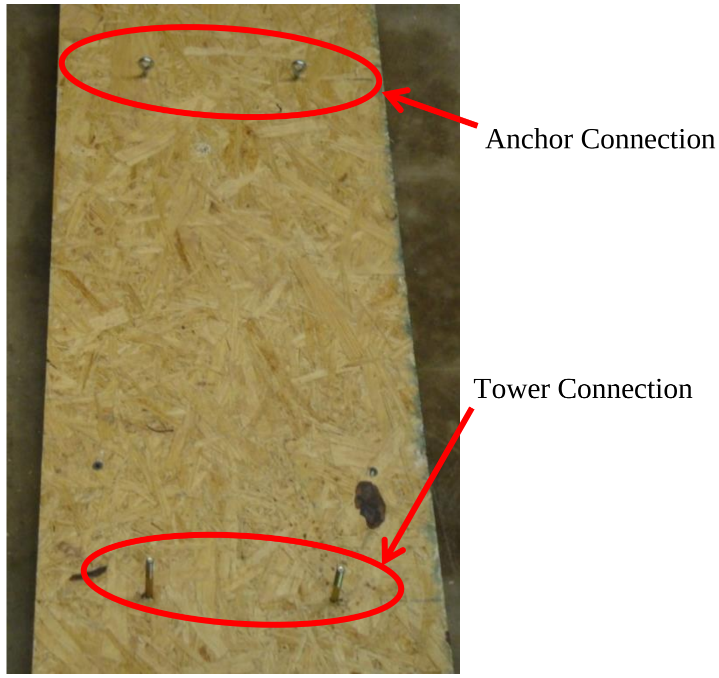

Figure 18: Tower and Anchor Connections

The tower elements are glued together with epoxy and screw eyes are inserted through the horizontal double angle at the top of the tower into the tower tubes to allow the cable to run over the tower as presented in Figure 19. The crossbeams were cut to size and holes were drilled in each end to allow the suspenders to connect to the crossbeam. In addition, epoxy was used to attach the nailers to the crossbeams as presented in Figure 20. Then, loops were created at both ends of the suspenders around the crossbeam and cable. Figure 21 presents the crossbeam/nailer connection to the cable through the suspender. After all suspenders were attached, the decking was glued to the nailer using wood glue. Figure 22 presents the staggered pattern of the decking. The decking boards are continuous over one crossbeam. Next, the model fence was attached as presented in Figure 23.

Figure 19: Cable to Tower Connection

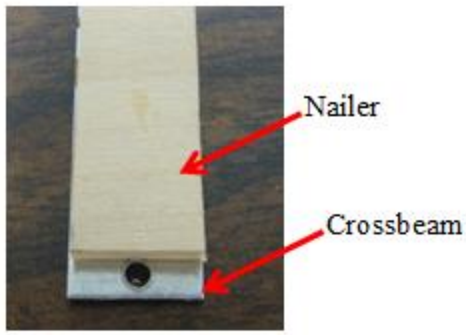

Figure 20: Nailer and Crossbeam

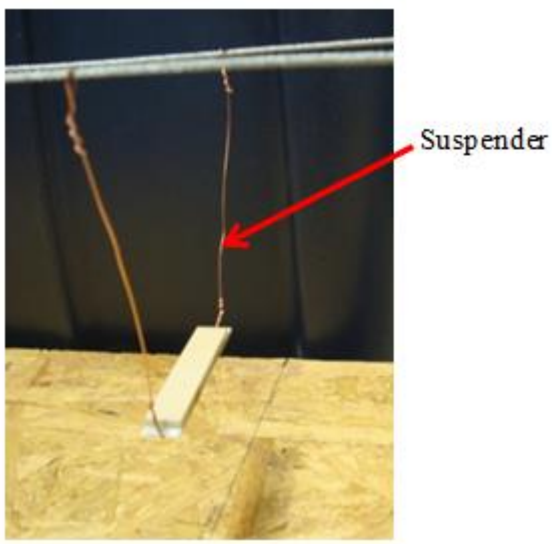

Figure 21: Suspender Connection

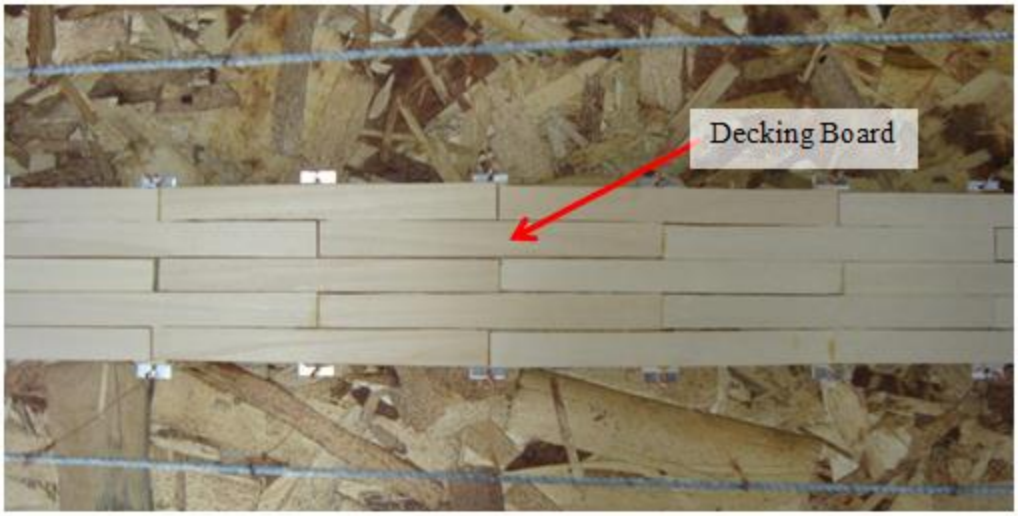

Figure 22: Bridge Deck

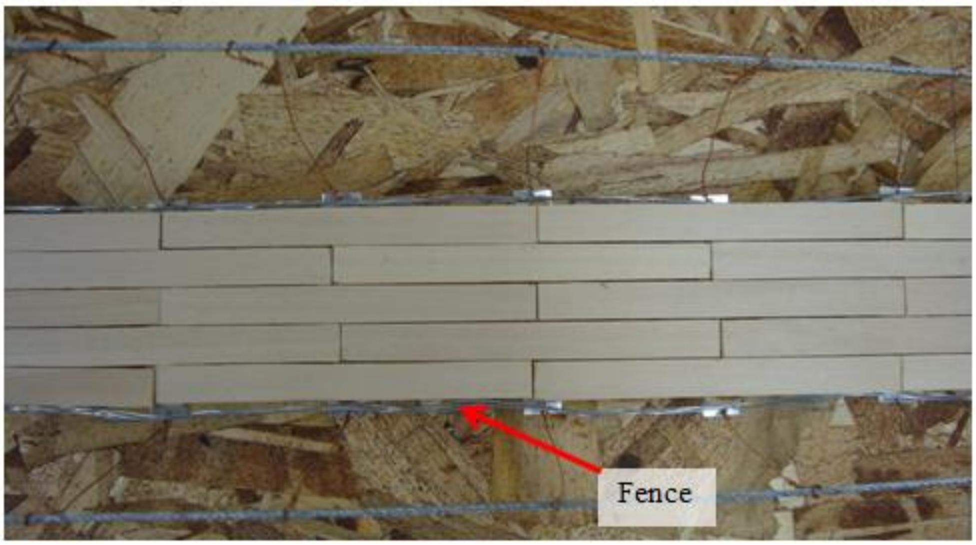

Figure 23: Model Fence

Lastly, the connection at the end of the deck was completed. Full scale suspension bridges are built with a masonry ramp up to the bridge, but there is a 20 mm (0.79") gap on all sides of the bridge to allow the structure to expand or contract and move slightly when in service. Figure 24 presents a plan view of the end of the deck connection for full scale footbridges. For the present study, the deck connection is modeled by a wood block around the end of the deck with a small gap of 1.11 mm (0.044"), which is the scaled distance from the full scale deck connection. Figure 25 presents the model deck connection.

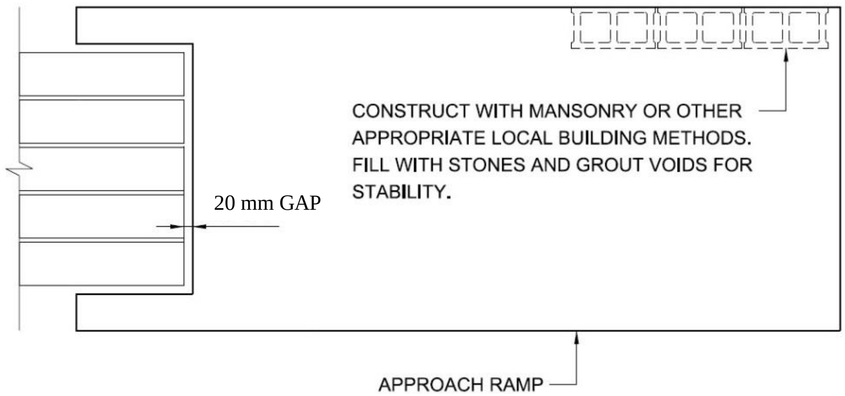

Figure 24: Deck Connection (Bridges to Prosperity, 2013)

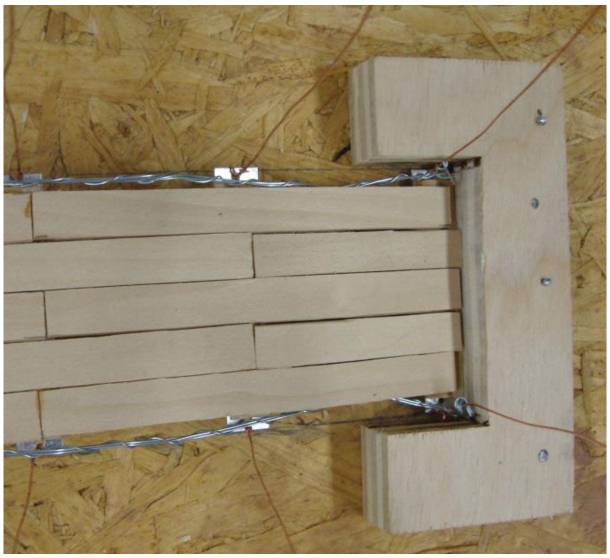

Figure 25: Model Deck Connection

3.5 Loading

The bridges were loaded with a symbolic pedestrian. The symbolic person is made of a plastic cylinder with eight small feet spaced evenly around the circumference. A typical walking speed is approximately 1 m/s (3.3 ft/s), and because velocity is scaled by unity, the symbolic person's walking speed is 1 m/s (3.3 ft/s). This walking velocity results from pedestrians walking with a stride length of 0.6 m (Zivanovic, 2004). The scaled stride length for the symbolic person is 1.31 inches. An average foot is slightly over 10 inches long, so the symbolic person has 0.5 inch long feet. Figure 26 presents the symbolic person. A marble was added inside the person to keep it vertical during testing. Also, a hole was drilled through the cylinder and a straw was placed through the hole to make an axle. Washers were placed on either side of the cylinder and they were taped in place to keep the cylinder from wobbling back and forth. Fishing line was used to pull the symbolic person.

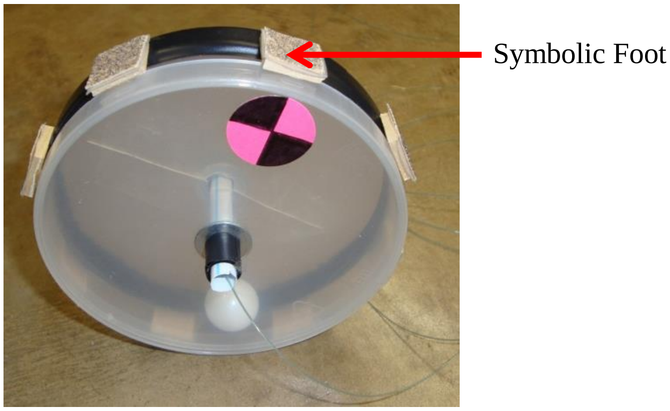

Figure 26: Symbolic Person

The symbolic person was powered with a dc motor. The motor was attached to a power supply, amplifier, and attenuator to adjust the speed. Figure 27 presents the motor. The fishing line was attached to the axle on the motor to pull the symbolic person. The speed was properly calibrated by counting the number of frames in the high speed video per revolution of the symbolic person.

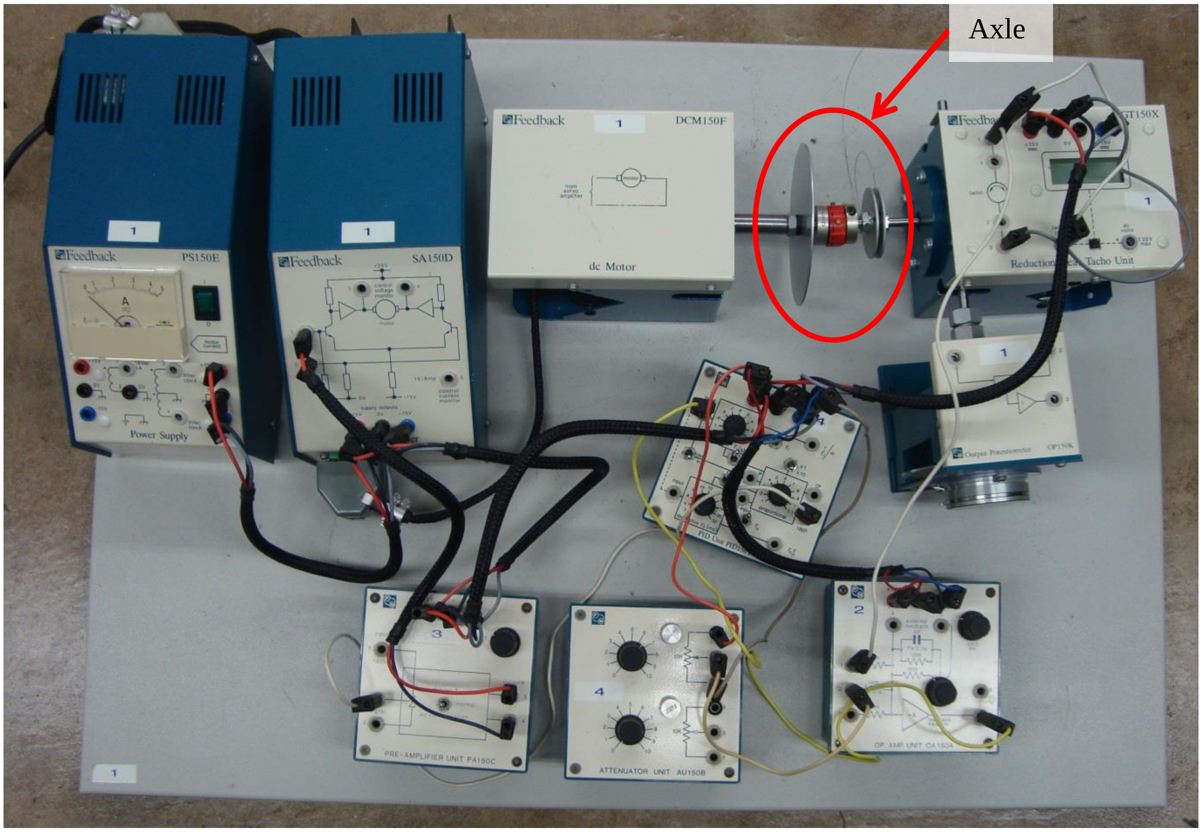

Figure 27: DC Motor

3.6 Data Collection

The response data from the model bridge test was collected through the use of a Casio EX-F1 high speed video camera. The camera is set to a rate of 300 frames per second. Certain points on the bridge are marked with a crosshair target located at points of interest based on the fundamental mode shapes from the numerical models. These points are easily identified in the video during analysis. Figure 28 presents one of the model bridges with seven targets and the symbolic person set up for testing. The video was started before the motor was turned on and continued while the symbolic person traversed half of the bridge length. This test was conducted at least three times for each bridge so the results could be compared to ensure accuracy. For any test that produced results that were outliers, the results were discarded, and the test was conducted again.

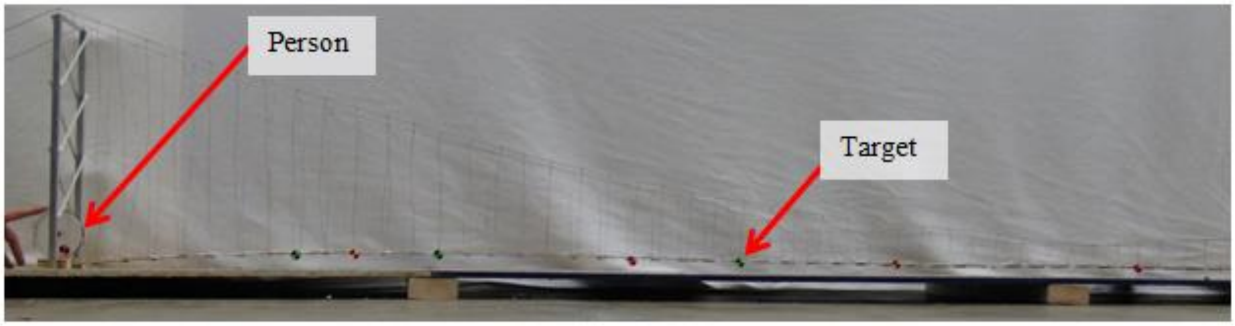

Figure 28: Bridge Model Testing Set-up

3.7 Data Processing and Results

The videos collected with the high speed digital camera were imported into Tracker, which is a video analysis program. Each test was analyzed to determine the displacement of each crosshair for every frame during the bridge testing. The video was calibrated by measuring the known distance of an object placed in the field of the video. The origin for the video analysis was placed at the base of the tower, and the frame rate was adjusted to 300 frames per second. Points labeled A through G (starting with A closest to the tower) were placed on each crosshair in each frame of the video to determine the exact displacement the point experienced in that time frame. Figure 29 presents the Tracker program used to analyze the videos. The displacement versus time graphs were overlaid and zeroed to each other. Then, any trails that did not agree with the others were retested and reanalyzed to ensure the average for all trials is accurate. Figure 30 presents a sample of the displacement vs. time data for one point on the 40 m span model. Seven points were analyzed for each span length, and the graphs for the other points are similar.

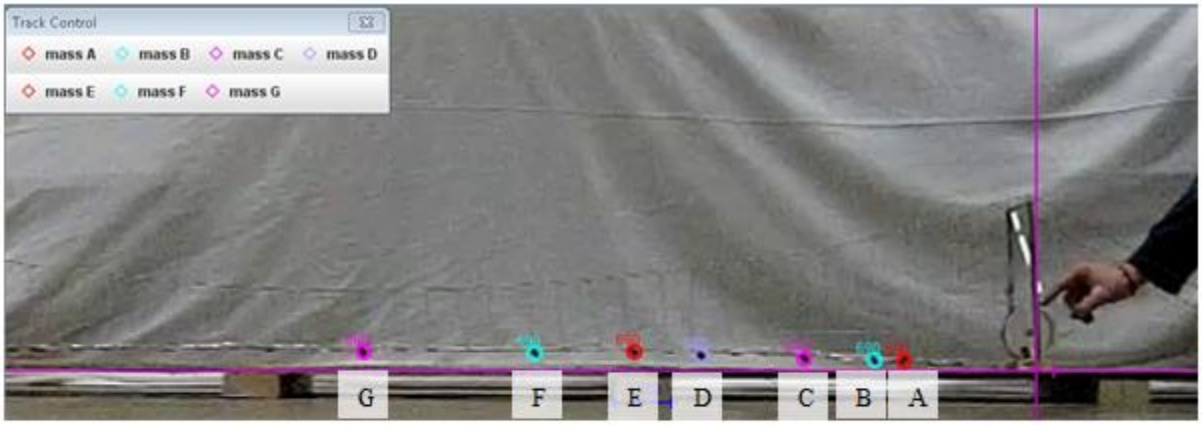

Figure 29: Tracker Video Analysis

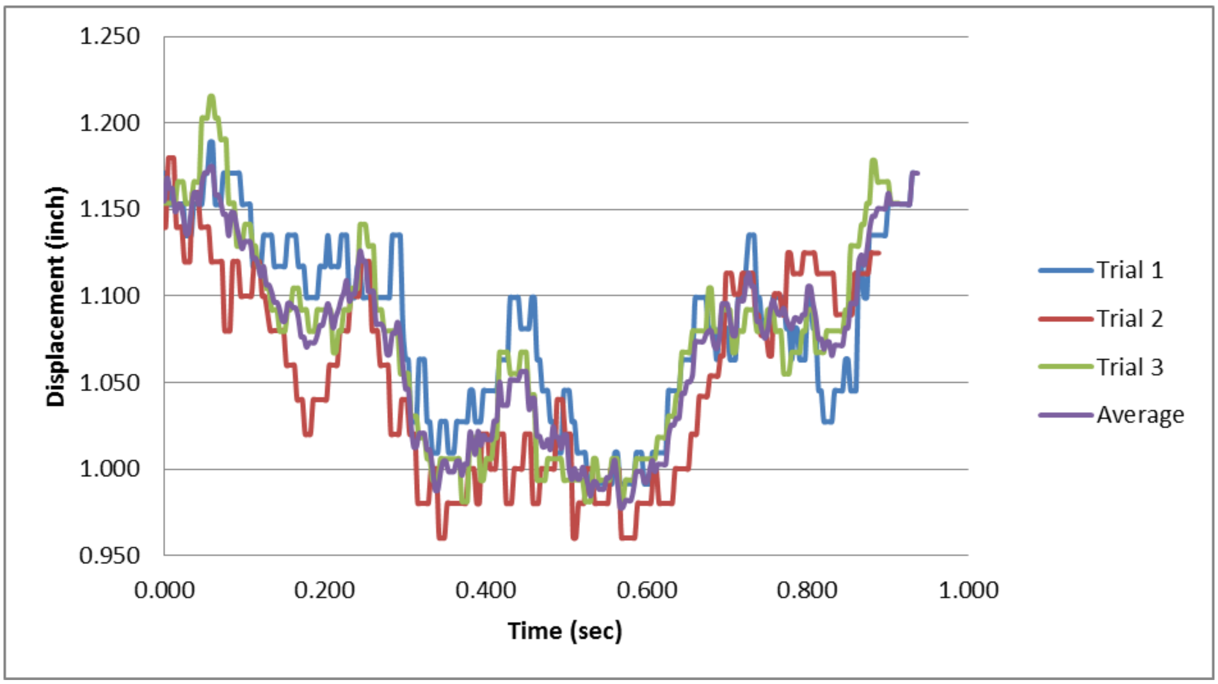

Figure 30: Displacement vs. Time Data for Point E on 40 m Model

Next, a power spectral density (PSD) program was written in Matlab to determine the modal frequencies of the bridge models. The PSD is calculated through the use of a Fast Fourier Transform (FFT). A FFT is a computer algorithm that is based off Fourier's theory that any signal can be represented by a superposition of several sine wave functions at varying frequencies and amplitudes. The PSD is calculated by determining the frequencies that make up a signal through the use of a FFT. The modal frequencies are represented by the highest peaks on the power versus frequency graph. The static portion of the signal is represented by the lowest frequency peak. Figure 31 presents a PSD graph of Point B on the 40 m Model. Seven points were analyzed for each span length, and the graphs for the other points are similar.

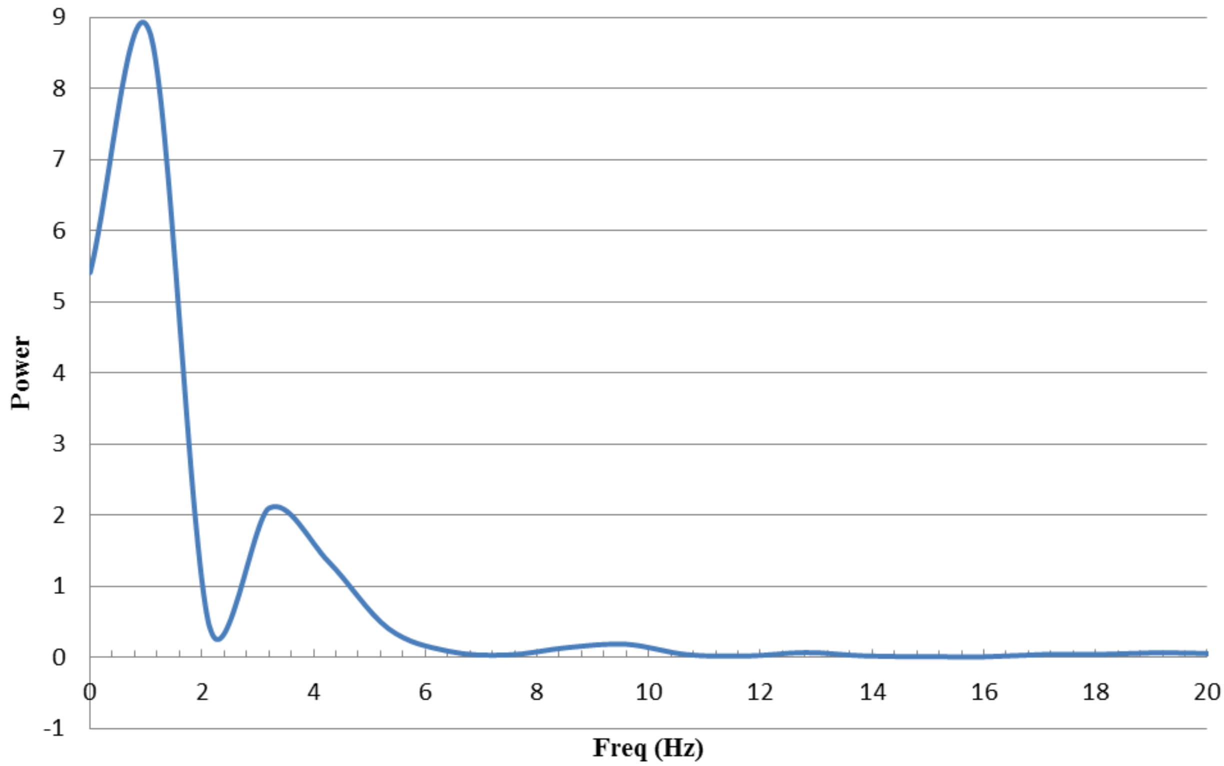

Figure 31: Power Spectral Density for Point B on 40 m Model

The modal frequencies of the models were determined by averaging the PSD results from the analysis points along each bridge. Table 9 presents the frequency at each peak for each point on the 40 m span model, and Table 10 presents the frequency at each peak for the 80 m span model. The frequencies for each peak from the graph in Figure 31 are located in the B column of Table 9. The mode shapes are determined based on the numerical models. The results are averaged for the three calibration modes: 1) vertical mode with 1 wave; 2) vertical mode with 1.5 waves; and 3) vertical mode with 2 waves. The average is calculated by only considering the points on the physical model where the mode shape of interest is represented. For example, point G, which is located at the center of the bridge, does not displace for the vertical mode with 1 wave; therefore, it was not considered when determining the frequency of this mode shape. The scaled modal frequency is found by taking the average from all participating locations and dividing it by the scale factor of 18. The scaled frequencies for the 40 m model footbridge are 0.45 Hz, 0.87 Hz, and 1.09 Hz for the first three vertical modes present in SAP. The scaled modal frequencies for the 80 m model footbridge are 0.41 Hz, 0.53 Hz, and 0.63 Hz. These scaled modal frequencies were used to calibrate the numerical models.

Table 9: Results from PSD for Each Point on 40 m Model

Peak #	Mode Shape	Frequency for Each Target on Physical Model (Hz)						
		A	B	C	D	E	F	G
1	Static	1.1	1.1	1.1	1.1	1.1	1.1	1.1
2	Vert - 0.5 wave	5.3	3.2	4.3	4.3	4.3	6.4	4.3
3	Vert - 1 wave	7.4	9.6	8.5	7.4	7.4	8.5	6.4
4	Torsion - 0.5 wave	11.7	12.8	12.8	10.6	9.6	10.6	12.8
5	Vert - 1.5 wave	16.0	17.1	14.9	13.8	13.8	14.9	14.9
6	Vert - 2 wave	23.4	19.2	19.1	20.2	19.1	17.0	17.0

Table 10: Results from PSD for Each Point on 80 m Model

Peak #	Mode Shape	Frequency for Each Target on Physical Model (Hz)						
		A	B	C	D	E	F	G
1	Static	0.48	0.48	0.48	0.48	0.48	0.48	0.49
2	Vert - 0.5 wave	3.8	3.8	4.3	3.8	3.8	2.9	3.9
3	Vert - 1 wave	7.6	7.2	7.6	7.2	7.7	7.2	7.8
4	Vert - 1.5 wave	10.0	9.1	9.5	9.1	10.5	8.6	9.8
5	Vert - 2 wave	12.4	10.5	11.5	11.5	12.4	11.0	12.2

3.8 Summary

Two physical models of a 40 m bridge with 5 percent cable sag and an 80 m bridge with 7.5 percent cable sag were tested to calibrate the numerical simulations. These span lengths and cable sag values are the two extremes of the numerical study; therefore, calibrating these models allows for the modeling techniques to be accepted for all of the numerical simulations. The models were designed based on a scale factor of 18. The geometry and mass of the models was scaled from full scale pedestrian suspension bridges.

Chapter 4

Numerical Model and Parametric Study

4.1 Introduction

Numerical models were constructed in SAP2000 to determine how certain selected design parameters affect the dynamic response of suspension footbridges. Each suspension footbridge is modeled in SAP2000 to conduct a modal analysis to determine frequencies of the footbridge. In addition, the maximum displacements, velocities, and accelerations under pedestrian loading were calculated through a nonlinear, direct-integration, time-history analysis to determine if the numerical models meet human comfort criteria. The physical models were used to calibrate the numerical models and validate the modeling technique. Numerical simulations were evaluated in a parametric study to determine how cable sag, vertical stiffness, and lateral stiffness affect 40 m, 50 m, 60 m, 70 m, and 80 m footbridges. The two cable sag values considered are 5 percent and 7.5 percent. The two types of vertical stiffening considered are no additional bracing and cable cross-bracing between suspenders from the deck to the main cables. The two types of lateral bracing considered are no additional lateral bracing and cable cross-bracing under the deck. The bracing schemes evaluated were determined to have the greatest effect based on the mode shapes.

4.2 Model Design

The model design was determined based on standard full scale pedestrian suspension bridges. This design was used to model the footbridges in SAP2000 for calibration and to conduct the parametric study. The following sections describe the model materials, model element geometry, and overall model geometry.

4.2.1 Model Materials

Material properties are based on estimated material properties available in regions where pedestrian suspension bridges are common. Table 11 presents each element and the defined properties. Specific material properties were input for the cable based on A. Noble & Son Ltd. *Wire Rope and Strand Catalog* (2013) and Armstrong-Alan Chain Corporation *Wire Rope* (2014). Material properties were also input for the wood decking based on research of available hardwoods in Central and South America, firsthand experience of hardwood in Central America, and testing of wood from Nicaragua.

Table 11: Material Definitions for Each Element

Element	Material	Modulus of Elasticity kgf/mm^2 (psi)	Density kgf/mm^3 (pcf)
Tower Pipe	A53 Gr. B Steel	20,000 (2.8e7)	7.85e-6 (490)
Tower Angles	A36 Steel	20,000 (2.8e7)	7.85e-6 (490)
Crossbeams	A36 Steel	20,000 (2.8e7)	7.85e-6 (490)
Suspenders	A615 Gr. 60	20,000 (2.8e7)	9.42e-6 (590)
Wood	Native Hardwood	1,200 (1.7e6)	1.19e-6 (74.3)
Cable	(2) 1-$^1/_8$" Diameter Steel Wire Cable	11,200 (1.6e7)	9.11e-6 (570)
Stiffening Cable	6.4 mm (¼") Diameter Steel Wire Cable	11,200 (1.6e7)	9.11e-6 (570)

4.2.2 Model Element Geometry

All element sizes are the same for all span lengths, except the towers. Table 12 presents the dimensions for the bridge model elements. The 29 mm (1⅛") diameter cable is Improved Plowed Steel (IPS) 6×19 class of wire cable with six outer strands of 19 wires and an independent wire rope core (IWRC). The effective cable area is calculated based on equation (3.3) with a compactness factor of 0.395 and 15 percent added to the cross sectional area for six strand cable with IWRC (*Wire Rope and Strand Catalog*, 2013). Therefore, the resulting cross sectional area of one 29 mm (1⅛") diameter wire cable is 382 mm^2 (0.59 in^2), so the effective area used for the parametric study is 764 mm^2 (1.18 in^2).

Table 12: Model Element Dimensions

Element	Dimension
Tower Pipe	Varies
Tower Diagonal Angles	L76×76×6 (L3"×3"×¼")
Tower Horizontal Angles	2L76×76×6 (2L3"×3"×¼")
Crossbeams	2L44×44×6 (2L1¾"×1¾"×¼") Bolted Back to Back
Suspenders	9 mm (0.35") Diameter
Decking and Nailers	38.1 mm × 184.2 mm (1½"×7¼")
Cable	(2) 29 mm ((2) 1⅛") Diameter Cables; Effective Area = 764 mm^2 (1.18 $inch^2$)
Stiffening Cable	6.4 mm (¼") Diameter Cable; Effective Area = 18.3 mm^2 (0.028 $inch^2$)

The tower geometry and steel pipe size differ depending on the span length. The type of angle bracing is constant for all span lengths, but the steel pipe dimensions vary. Table 13 presents the dimensions for the hollow steel pipe that is used for the vertical members of the towers. Figure 32 presents the overall tower dimensions and the locations of angle bracing. All horizontal members in the towers are double angles and all diagonal members are single angles.

Table 13: Tower Pipe Dimensions

Span m (ft)	Pipe Outside Diameter mm	Pipe Inner Diameter mm
40 (130)	141	128
50 (160)	168	155
60 (200)	168	155
70 (230)	194	178

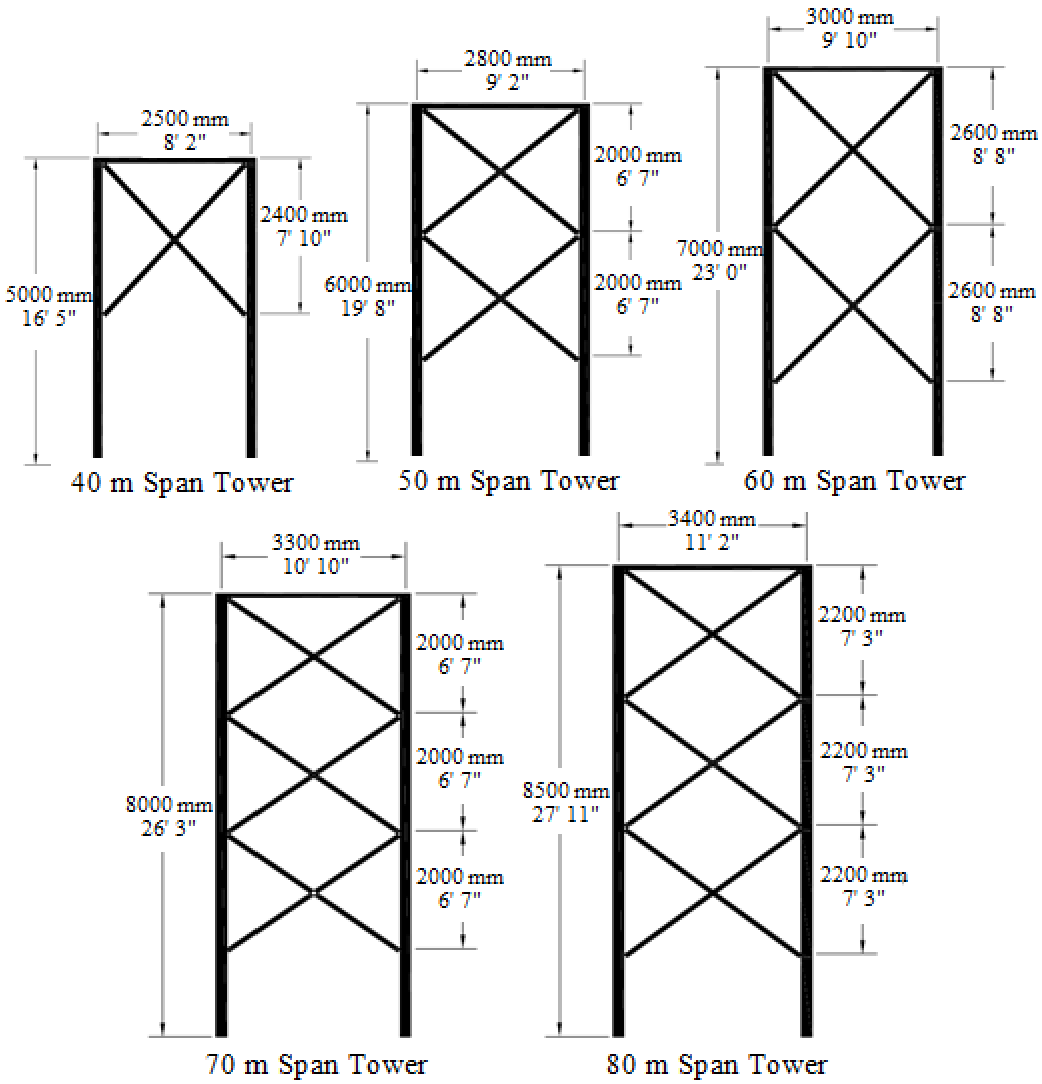

Figure 32: Tower Elevation Geometry

4.2.3 Overall Model Geometry

Geometry for the models differs depending on the span length. The height of the towers, the width of the towers, and the deck camber depends on the span length. Table 14 presents the parameters as a function of the bridge span (*Bridge Builder Manual*, 2013). The deck camber is approximated as a sine wave following equation (4.1).

$$z = camber \times \sin\left(\frac{\pi}{span} \times x\right) \tag{4.1}$$

where *z* is the vertical coordinate, *camber* is the deck camber specified in Table 14, *span* is the span length of the model, and *x* is the horizontal distance coordinate measured from the tower.

Table 14: Geometric Parameters for Models

Span m	h_{tower} m	w_{tower} m	Deck Camber m
40	5	2.5	1.23
50	6	2.8	1.5
60	7	3	1.77
70	8	3.3	2.04
80	8.5	3.4	1.81

4.3 Numerical Model Design

The SAP2000 numerical models are designed to simulate full scale suspension footbridges. The SAP elements were chosen to correctly represent the behavior of the full scale footbridge elements. The boundary conditions and connectivity are defined to cause the model to behave in the same way as the full scale structure. The numerical model elements, boundary conditions, and connectivity are described below.

The numerical model consists of cable and frame elements. The main cables, suspenders, and stiffening braces are cable elements because these members only carry tension forces. The suspenders are modeled as undeformed cable elements that connect the main cable to the crossbeam. The main cables are modeled based on the maximum vertical sag in the deformed shape. The stiffening braces are modeled as cables with an initial pretension force of 120 kgf (270 lb). The towers, crossbeams, and decking panels are modeled as 3D frame elements.

The nailers, which are wood boards attached to the double angle crossbeams for ease of nailing the decking boards, are not modeled in SAP explicitly. Instead, the nailers are represented as a distributed dead load centered on the crossbeams that acts along the length of the standard nailer. In addition, the fence and hand rail cable are represented in SAP as 2.84 kg (6.3 lbs) joint masses on the ends of every crossbeam.

The boundary conditions at the anchors, the ends of the deck, and the base of the towers consist of pin or roller connections. All base connections are modeled on the same plane. The tower columns are pin connected. The cables are pin connected at the anchor locations. The deck has roller connections at both ends with 200 kgf/mm (11.2 ksi) longitudinal and lateral springs that were calibrated to the physical models. Figure 33 presents a plan view of the deck boundary conditions, including the rollers and springs. In addition, the end moments between decking boards are released.

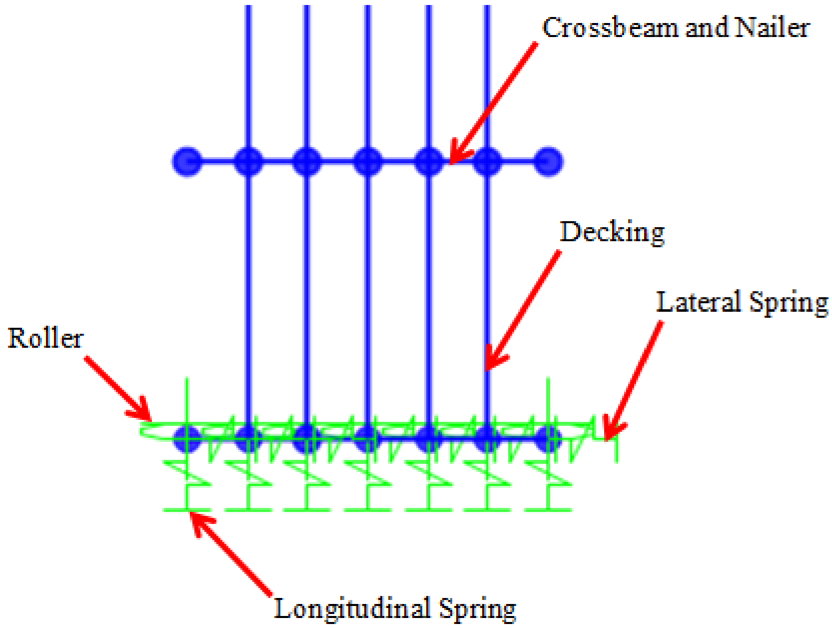

Figure 33: View of Deck Boundary Conditions

4.4 Loading

Footbridges are subject to many types of loading. The present study is limited to static dead load for the self-weight of the structure and dynamic pedestrian loads. A dynamic, moving, live load is modeled through a time-history analysis to determine the model response to a pedestrian traversing the bridge. A typical stride length for a person is 0.6 m (1.97 ft); therefore, a gravity load of 81.6 kgf (180 lb) and a lateral load of 3.06 kgf (6.7 lb) applied in the direction away from a person's center of mass are placed at 0.6 m (1.97 ft) intervals along half of the length of the bridge. Table 15 presents the number of steps from the right foot and left foot for each span length. The loads are placed 20 cm (7.9 inches) apart because people typically step 10 cm (3.9 inches) out from a centerline when they walk.

Table 15: Number of Steps for Each Bridge

Model Span Length (m)	# Steps - Right Foot	# Steps - Left Foot
40	17	16
50	21	20
60	25	25
70	29	29
80	33	33

The time functions used to define the dynamic loading are based on existing pedestrian forces data discussed in Chapter 2. Figure 34 and Figure 35 present the force vs. time function for the vertical pedestrian force and the lateral pedestrian force respectively. The vertical and lateral time functions act simultaneously, and the time function for the next step begins 0.5 seconds after the previous step began, which means the steps overlap slightly. The steps overlap because walking requires both feet on the ground between steps. Table 16 presents the time an average person requires to traverse half of the bridge for each span length.

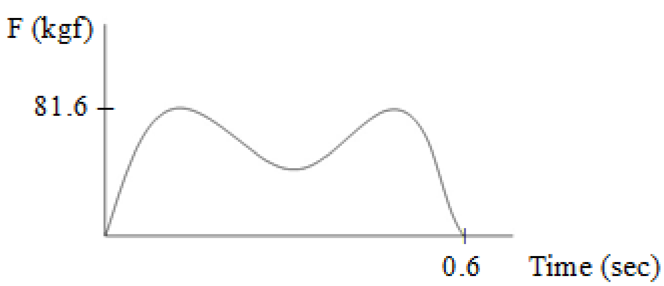

Figure 34: Vertical Pedestrian Force Time Function

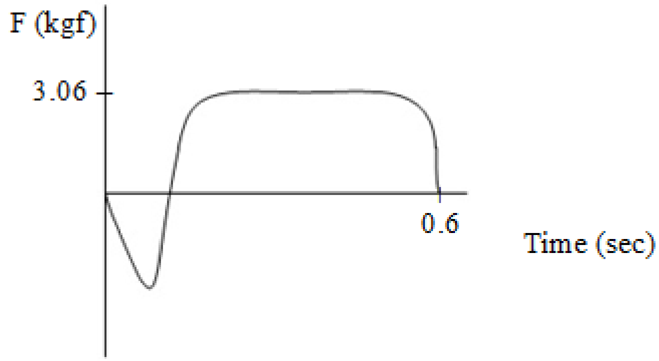

Figure 35: Lateral Pedestrian Force Time Function

Table 16: Analysis Time for Each Bridge

Model Span Length (m)	Length of Analysis (sec)
40	16.6
50	20.6
60	25.1
70	29.1
80	33.1

4.5 Analysis

Several SAP2000 analyses were conducted to determine the total response of the structure. First, a dead load analysis was run because all pedestrian loading occurs after the self-weight is applied to the structure. Then a modal analysis and a nonlinear, direct-integration, time-history analysis were run to determine the dynamic response.

The dead load case is defined as nonlinear static to account for the nonlinearity of the cable elements. The case considers self-weight of the members, distributed loads from the nailers, and the lumped mass of the fence.

A modal analysis was conducted of each model to determine the mode shapes and corresponding frequencies. The modal analysis was set as an Eigen vectors analysis. The modal analysis starts from the end of the nonlinear dead load analysis to evaluate the mode shapes of the structure under self-weight.

To determine the displacements, velocities, and accelerations of the footbridge under pedestrian loading, a load case is defined to represent a pedestrian moving halfway across the bridge. The modal damping ratio is defined as 0.01 or 1 percent, which is recommended for outdoor footbridges in AISC Design Guide 11 (Murray, 2012). A damping of 0.005 or 0.5 percent was also evaluated and the results were not significantly different. The Rayleigh damping frequencies are defined as the first and tenth modal frequencies for each model. However, the first and twentieth frequencies were also set as the Rayleigh damping frequencies to ensure the results are properly captured by analyzing the models based on the first and tenth frequencies, and the results were not significantly different. Therefore, the present study uses 1 percent damping with the first and tenth modal frequencies defined for Rayleigh damping.

4.6 Calibration

The physical model results for three vertical mode shapes (1 wave, 1.5 waves, and 2 waves) for two different footbridges were used to adjust connection rigidity, material stiffness, and mass distribution to create numerical models that mimic the behavior of the physical models. The physical models were studied and used to calibrate the SAP analysis to improve the numerical modeling methodology. The parameters studied for calibration are based on differences between the physical and numerical models. Each parameter was studied and realistic changes were made to the numerical model, so the results are more similar to the physical models' results.

Table 17 presents all of the changes made to the numerical model based on the physical model construction. These changes were not incorporated into the parametric study. The physical models were built based on one 29 mm (1⅛") diameter cable on each side of the deck, so the effective cable area in the numerical calibration models is 382 mm^2 (0.59 $inch^2$). Two cables on each side of the deck are used for the parametric study because the new standard for suspension bridge design calls for two cables for redundancy.

Table 17: Calibration Parameters

Physical Model Construction Difference	Adjustment to Numerical Calibration Model
(1) 29 mm (1⅛") diameter cable	Effective Area = 382 mm^2 (0.59 $inch^2$)
Deck is made of basswood	Wood Density = 5.6e-07 kgf/mm^3 (35 pcf); Wood Modulus of Elasticity = 1,030 kgf/mm^2 (1,500,000 psi)
Suspender weight difference; Additional suspender wire used for looped connections around main cable and crossbeams	Suspender Density = 8.24e-06 kgf/mm^3 (510 pcf); Lumped mass located every fifth bay
Epoxy used to connect nailers to crossbeam and fence, nailer, and crossbeam weight difference	Crossbeam Density = 8.2e-06 kgf/mm^3 (510 pcf)

After the calibration parameters listed above were adjusted and based on a comparison between the physical model results and numerical model results, the longitudinal and lateral spring stiffness at the ends of the deck was calibrated to 200 kgf/mm (11.2 kips/inch). Table 18 presents the calibration results for the 40 m model, and Table 19 presents the calibration results for the 80 m model.

Table 18: 40 m Model Calibration Results

Vertical Mode	Physical Model Freq (Hz)	SAP Model Freq (Hz)	Percent Difference
1 wave	0.45	0.545	21.1
1.5 waves	0.87	0.993	14.1
2 waves	1.09	1.082	0.73

Table 19: 80 m Model Calibration Results

Vertical Mode	Physical Model Freq (Hz)	SAP Model Freq (Hz)	Percent Difference
1 wave	0.41	0.332	19.0
1.5 waves	0.53	0.551	3.96
2 waves	0.63	0.644	2.22

The SAP model modal frequencies are not the same as the physical model modal frequencies. This is a result of construction imperfections in the physical model that are not present in the numerical model. In addition, wire is used for the suspenders in the physical models; some of the suspenders are not perfectly straight, so the load vs. deflection graph for each suspender varies. This uneven response could be greatly affecting the modal frequencies of the physical models. Even though there is error between the physical models and the SAP models, the modeling techniques are accepted for the parametric study. Through constructing the physical models, the numerical modeling methodology, including boundary condition behavior and member connectivity, was improved and the numerical models were determined to accurately represent the full scale structures.

4.7 Parametric Study

The parametric study was conducted through analyzing the forty numerical models presented in Table 21. The models are named according to their span length, cable sag percentage, presence of vertical bracing, and presence of lateral bracing. Table 21 presents each model that is studied, and Table 20 presents a key for each character in the bridge model names. The vertical and lateral stiffening braces are 6.4 mm (¼") diameter cables with a pretension force of 120 kgf (270 lbs). The purpose of the bracing is to stiffen the structure to increase the modal frequencies and decrease the displacements, velocities, and accelerations of the structure resulting from a pedestrian walking across the bridge.

Table 20: Key for Bridge Model Names

Character	Parameter	Character Options
1	Span Length	40, 50, 60, 70, or 80 m
2	Cable Sag	5 or 7.5 percent
3	Vertical Stiffening	N = none or V = vertical at center and ends
4	Lateral Stiffening	N = none or L = lateral at center and ends

Table 21: Bridge Models for Parametric Study

Span (m)	Cable Sag (%)	Vertical Stiffening	Lateral Stiffening	Name
40	5	None (N)	None (N)	40-5-N-N
			Center and Ends (L)	40-5-N-L
		Center and Ends (V)	None (N)	40-5-V-N
			Center and Ends (L)	40-5-V-L
	7.5	None (N)	None (N)	40-7.5-N-N
			Center and Ends (L)	40-7.5-N-L
		Center and Ends (V)	None (N)	40-7.5-V-N
			Center and Ends (L)	40-7.5-V-L
50	5	None (N)	None (N)	50-5-N-N
			Center and Ends (L)	50-5-N-L
		Center and Ends (V)	None (N)	50-5-V-N
			Center and Ends (L)	50-5-V-L
	7.5	None (N)	None (N)	50-7.5-N-N
			Center and Ends (L)	50-7.5-N-L
		Center and Ends (V)	None (N)	50-7.5-V-N
			Center and Ends (L)	50-7.5-V-L
60	5	None (N)	None (N)	60-5-N-N
			Center and Ends (L)	60-5-N-L
		Center and Ends (V)	None (N)	60-5-V-N
			Center and Ends (L)	60-5-V-L
	7.5	None (N)	None (N)	60-7.5-N-N
			Center and Ends (L)	60-7.5-N-L
		Center and Ends (V)	None (N)	60-7.5-V-N
			Center and Ends (L)	60-7.5-V-L
70	5	None (N)	None (N)	70-5-N-N
			Center and Ends (L)	70-5-N-L
		Center and Ends (V)	None (N)	70-5-V-N
			Center and Ends (L)	70-5-V-L
	7.5	None (N)	None (N)	70-7.5-N-N
			Center and Ends (L)	70-7.5-N-L
		Center and Ends (V)	None (N)	70-7.5-V-N
			Center and Ends (L)	70-7.5-V-L
80	5	None (N)	None (N)	80-5-N-N
			Center and Ends (L)	80-5-N-L
		Center and Ends (V)	None (N)	80-5-V-N
			Center and Ends (L)	80-5-V-L
	7.5	None (N)	None (N)	80-7.5-N-N
			Center and Ends (L)	80-7.5-N-L
		Center and Ends (V)	None (N)	80-7.5-V-N
			Center and Ends (L)	80-7.5-V-L

The mode shapes were studied to determine the best locations for lateral and vertical bracing. The first vertical mode shape, VA1, is presented in Figure 36. Vertical bracing was evaluated at the ends of the structure and near the middle because these areas see the largest distortions to rectangular geometry. It was determined that more bracing is needed for the ends than in the middle.

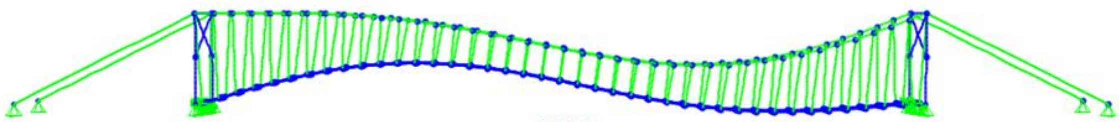

Figure 36: First Vertical Mode Shape

Vertical bracing is present over 60 percent of the structure: 20 percent on each end and 20 percent centered in the middle of the bridge. Vertical bracing connects the ends of the crossbeams to the main cable. The dimensions of the bracing depend on the span length of the bridge. Each brace pattern incorporates approximately 5 percent of the total number of suspenders in the bridge. The brace pattern at the ends of the models is presented in Figure 37 through Figure 41 for all span lengths, and the brace pattern at the center of the models is presented in Figure 42 to Figure 46; the bracing is highlighted in red. The braces do not connect at the center of the "X"; the center of one "X" is indicated by a circle on Figure 37.

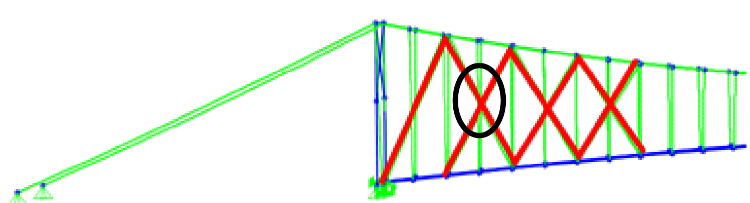

Figure 37: Vertical Bracing Pattern at Ends of 40 m Span Footbridge

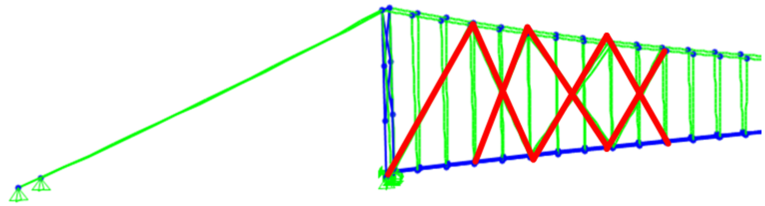

Figure 38: Vertical Bracing Pattern at Ends of 50 m Span Footbridge

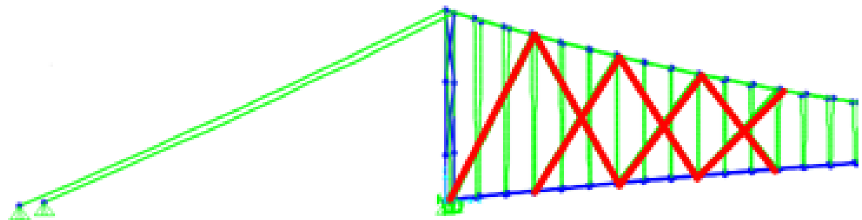

Figure 39: Vertical Bracing Pattern at Ends of 60 m Span Footbridge

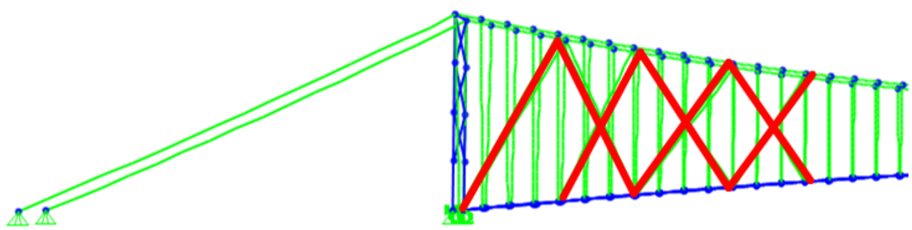

Figure 40: Vertical Bracing Pattern at Ends of 70 m Span Footbridge

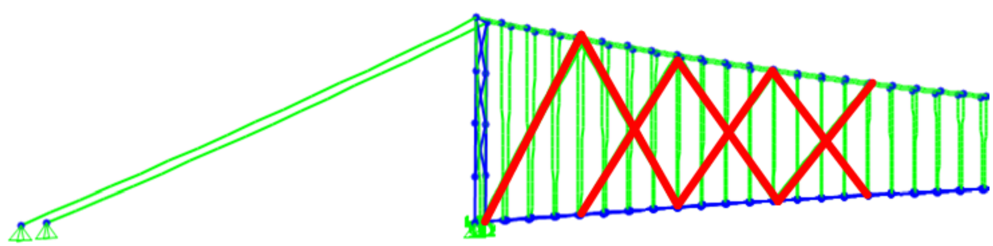

Figure 41: Vertical Bracing Pattern at Ends of 80 m Span Footbridge

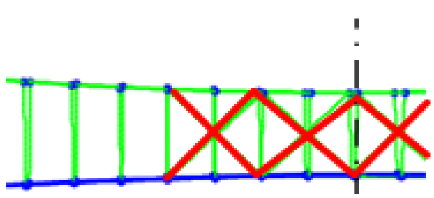

Figure 42: Vertical Bracing Pattern at Center of 40 m Span Footbridge

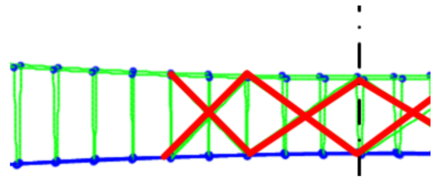

Figure 43: Vertical Bracing Pattern at Center of 50 m Span Footbridge

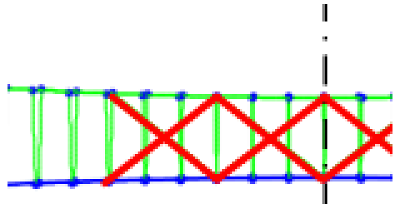

Figure 44: Vertical Bracing Pattern at Center of 60 m Span Footbridge

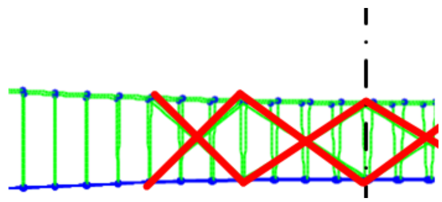

Figure 45: Vertical Bracing Pattern at Center of 70 m Span Footbridge

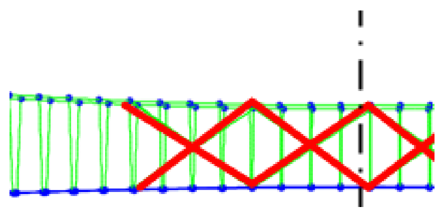

Figure 46: Vertical Bracing Pattern at Center of 80 m Span Footbridge

Figure 47 presents the first two lateral modes. Bracing was also studied at the ends and middle of the span, and it was determined that more bracing is needed at the center because this is the area with the largest distortions of rectangular geometry for the first lateral mode. Therefore, the bracing is located at the ends and middle of the footbridges because the rectangular geometry in these areas has the greatest deformations for the first two mode shapes.

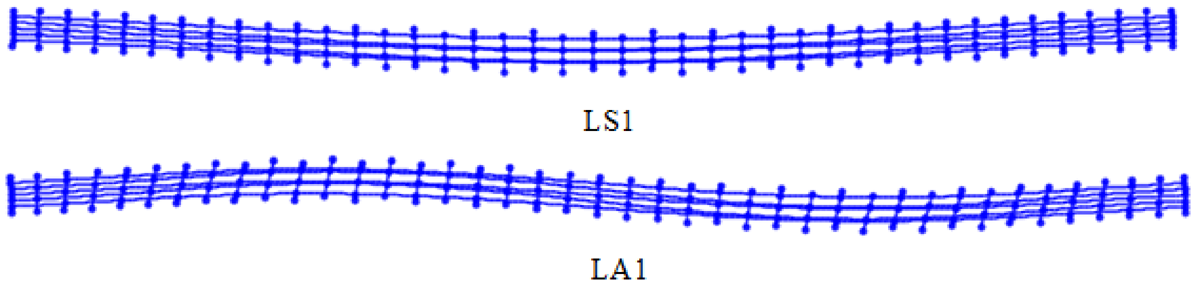

Figure 47: First Two Lateral Mode Shape

Lateral bracing is between 40 percent of the crossbeams: 10 percent on each end and 20 percent centered at the middle of the bridge. Lateral bracing is located under the deck and it connects adjacent crossbeams. Figure 48 presents the lateral bracing pattern under the deck for a 60 m span footbridge; the bracing is highlighted in red. The braces do not connect at the center of the “X,” which is located halfway between crossbeams where the cables cross each other.

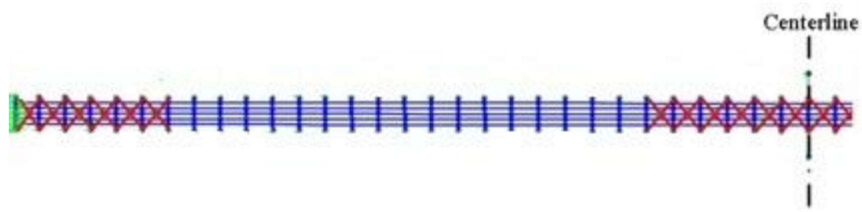

Figure 48: Lateral Bracing Pattern for 60 m Span Footbridge

The parametric study was conducted by running a dead load case, modal analysis, and nonlinear, direct-integration, time-history analysis for all forty models. The modal analysis calculated the mode shapes and modal frequencies for each model. These frequencies are compared to the suggested limits for footbridges presented in Chapter 2. Footbridges with vertical modal frequencies of 1.3 to 2.3 Hz and lateral modal frequencies of 0.5 to 1.2 Hz are known to have serviceability problems. The time history analysis calculated the displacements, velocities, and accelerations for each model. These movements are compared to human comfort criteria presented in Chapter 2. The vertical velocity limit is 1 cm/s (0.033 ft/s), and the vertical acceleration limit is 0.7 m/s^2 (2.3 ft/s^2). The lateral displacement limit is 45 mm, and the lateral acceleration limit is 0.3 m/s^2 (1.0 ft/s^2).

4.8 Summary

SAP2000 was used for the numerical models. The physical models were used to calibrate and validate the numerical models. A parametric study was then conducted in SAP by studying forty numerical simulations to determine how cable sag, vertical stiffness, and lateral stiffness affect suspension footbridges with span lengths ranging from 40 m to 80 m. These analyses calculated the frequencies of each mode shape in addition to the displacements, velocities, and accelerations of the bridge under pedestrian loading. These results are useful in determining the best ways to mitigate vibration problems for pedestrian suspension bridges.

Chapter 5

Parametric Study Results

5.1 Overview

The parametric study was conducted in SAP2000, and it includes studying five span lengths, two cable sag values, the presence of vertical stiffening, and the presence of lateral stiffening. A total of forty models were studied to evaluate all combinations of these parameters. A modal analysis was conducted to determine the mode shapes and modal frequencies for each footbridge. Also, a nonlinear, direct-integration, time-history analysis was conducted to determine the displacements, velocities, and accelerations that result from a person traversing the structure. The results are compared to determine if the modal frequencies fall within the recommended range to avoid the frequency at which pedestrians walk and if the displacements, velocities, and accelerations meet the human comfort criteria.

5.2 Results

The parametric study results include modal frequencies and time history response data. The modal frequencies are presented for five mode shapes for all forty models. The time history response data, including vertical velocities, lateral accelerations, and vertical accelerations are presented for all forty models in the Appendix.

5.2.1 Modal Frequency Results

A modal analysis was conducted for all forty models in the parametric study and the results are presented in Table 22 through Table 28. Five mode shapes, including two vertical, two lateral, and one torsional, are presented because these were determined to be the critical mode shapes; as discussed in Chapter 2, these five mode shapes are known to be problematic for pedestrian suspension bridges, and they are the vertical, lateral, and torsional modes with the lowest frequencies. Figure 49 visually presents the five mode shapes listed in the tables. The cables are removed from the lateral mode diagrams for clarity.

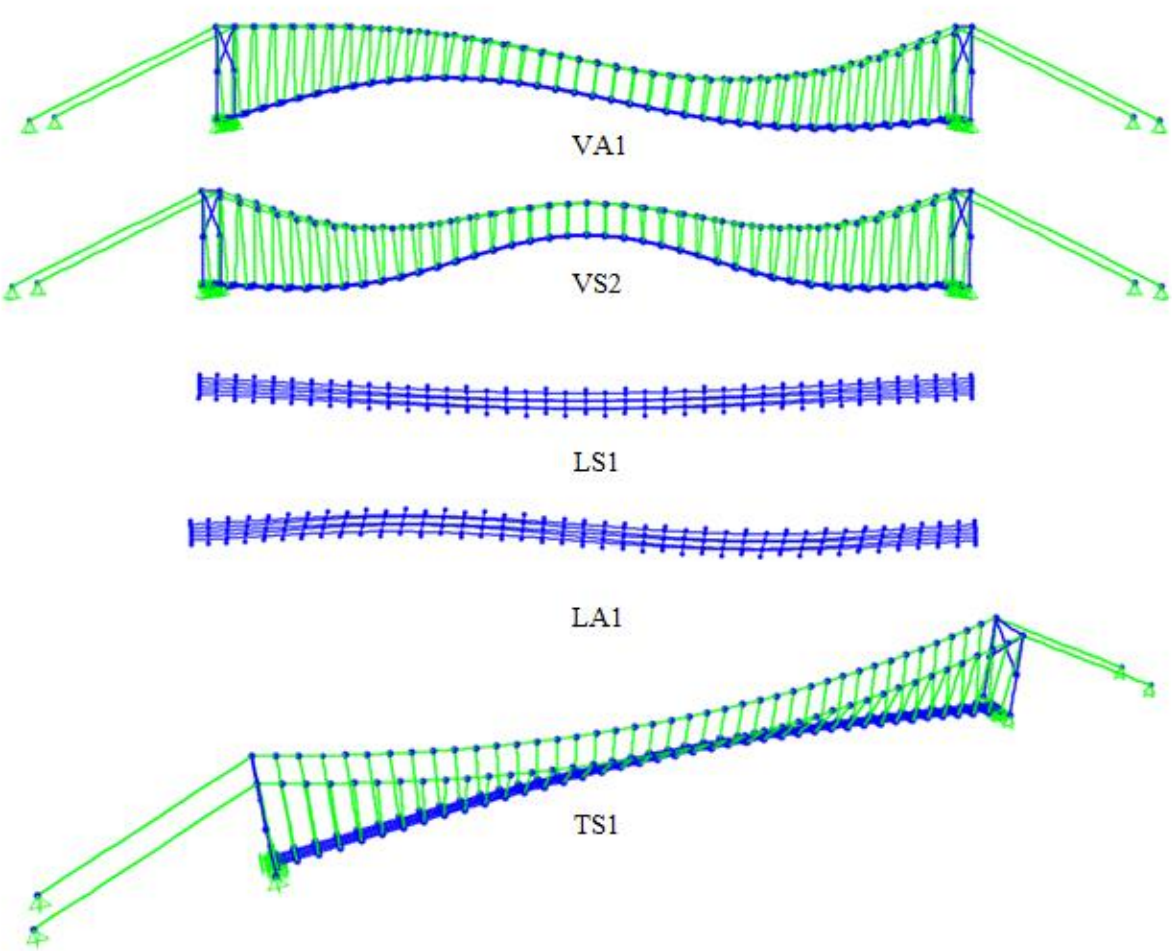

Figure 49: Mode Shapes

Table 22: Modal Frequencies for Models with 5 Percent Cable Sag and No Stiffening

Mode Shape	40 m Model	50 m Model	60 m Model	70 m Model	80 m Model
VA1	0.60	0.53	0.49	0.45	0.45
VS2	0.99	0.86	0.78	0.71	0.66
LS1	0.73	0.53	0.39	0.31	0.28
LA1	1.39	1.22	1.08	0.87	0.75
TS1	0.84	0.74	0.69	0.63	0.64

Table 23: Modal Frequencies for Models with 7.5 Percent Cable Sag and No Stiffening

Mode Shape	40 m Model	50 m Model	60 m Model	70 m Model	80 m Model
VA1	0.47	0.41	0.38	0.35	0.37
VS2	0.87	0.77	0.68	0.62	0.55
LS1	0.70	0.51	0.38	0.30	0.27
LA1	1.13	0.99	0.91	0.81	0.74
TS1	0.83	0.73	0.67	0.62	0.71

Table 24: Modal Frequencies for Models with 5 Percent Cable Sag and Lateral Stiffening

Mode Shape	40 m Model	50 m Model	60 m Model	70 m Model	80 m Model
VA1	0.61	0.54	0.49	0.45	0.45
VS2	0.99	0.86	0.78	0.71	0.66
LS1	0.77	0.58	0.44	0.35	0.31
LA1	1.39	1.22	1.11	0.92	0.79
TS1	0.87	0.75	0.70	0.64	0.65

Table 25: Modal Frequencies for Models with 7.5 Percent Cable Sag and Lateral Stiffening

Mode Shape	40 m Model	50 m Model	60 m Model	70 m Model	80 m Model
VA1	0.48	0.42	0.39	0.36	0.37
VS2	0.87	0.76	0.68	0.62	0.55
LS1	0.72	0.55	0.42	0.34	0.30
LA1	1.13	0.99	0.91	0.83	0.77
TS1	0.88	0.75	0.69	0.64	0.71

Table 26: Modal Frequencies for Models with 5 Percent Cable Sag and Vertical Stiffening

Mode Shape	40 m Model	50 m Model	60 m Model	70 m Model	80 m Model
VA1	0.73	0.61	0.56	0.54	0.55
VS2	1.07	0.94	0.84	0.77	0.71
LS1	0.73	0.53	0.39	0.31	0.28
LA1	1.34	1.19	1.08	0.90	0.77
TS1	0.82	0.73	0.68	0.61	0.64

Table 27: Modal Frequencies for Models with 7.5 Percent Cable Sag and Vertical Stiffening

Mode Shape	40 m Model	50 m Model	60 m Model	70 m Model	80 m Model
VA1	0.56	0.50	0.48	0.44	0.52
VS2	0.93	0.81	0.72	0.65	0.61
LS1	0.68	0.51	0.38	0.30	0.27
LA1	1.08	0.96	0.88	0.80	0.78
TS1	0.79	0.68	0.65	0.60	0.69

Table 28: Modal Frequencies for Models with 5 Percent Cable Sag and Vertical and Lateral Stiffening

Mode Shape	40 m Model	50 m Model	60 m Model	70 m Model	80 m Model
VA1	0.74	0.62	0.56	0.54	0.56
VS2	1.08	0.94	0.84	0.77	0.71
LS1	0.76	0.57	0.44	0.35	0.31
LA1	1.35	1.19	1.09	0.93	0.79
TS1	0.87	0.74	0.69	0.62	0.64

Table 29: Modal Frequencies for Models with 7.5 Percent Cable Sag and Vertical and Lateral Stiffening

Mode Shape	40 m Model	50 m Model	60 m Model	70 m Model	80 m Model
VA1	0.57	0.51	0.49	0.46	0.54
VS2	0.92	0.81	0.72	0.66	0.62
LS1	0.69	0.54	0.42	0.34	0.30
LA1	1.08	0.96	0.89	0.81	0.80
TS1	0.86	0.72	0.68	0.64	0.68

5.2.2 Time History Results

The time history results evaluated include lateral displacement, vertical velocity, lateral acceleration, and vertical acceleration. The center of the deck was evaluated based on six meter sections; it takes a person five second to walk six meters. These six meter sections are numbered for a 40 m span bridge in Figure 50. The response data for all numerical models are included in the Appendix. The tables are named in accordance with the model naming described in Chapter 4. The response data is based on one person walking to mid-span from the 0 m location starting at time 0 seconds. The walking pedestrian feels the responses listed on the diagonal line in each table; for example, the walking or moving person experiences the response in region 1 when he (meaning the moving person) is in region 1. A bystander, or stationary person, feels a given response based on the region they are located in (column in the table) and based on the region the walker is in (row in the table). The lateral displacement data are not included for any of the models because the lateral displacement of all models subject to one pedestrian loading does not exceed the lateral displacement limit.

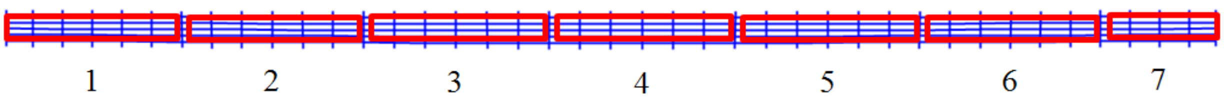

Figure 50: Regions of 40 m Models for Time History Results

5.3 Discussion of Results

The results are studied to determine the changes in modal frequencies and dynamic response data due to span length, cable sag, vertical stiffening, lateral stiffening, and both vertical and lateral stiffening. The dynamic response data are measured against human comfort criteria as described in Chapter 2. The trends and insights in the data are discussed in the following sections for each parameter of interest. A full bracing scheme for the 40 m model with 5 percent cable sag was also investigated to determine how close the current bracing patterns are to the best achievable result.

5.3.1 Span Length

The modal frequencies of footbridges are dependent on the span length of the structure. All five modal frequencies are higher for shorter spans as observed from Figure 51. The exception is VA1 and TS1 for longer spans. The modal frequencies for these two modes begin to plateau or remain constant as the span length increases, so the slight increase in modal frequencies for the longer spans is expected. The modal frequencies decrease by 11 to 33 percent when the span length is increased from 40 m to 50 m. However, this percent change decreases as the span length increases, demonstrating that the span length has a greater effect on the modal frequencies for shorter span lengths.

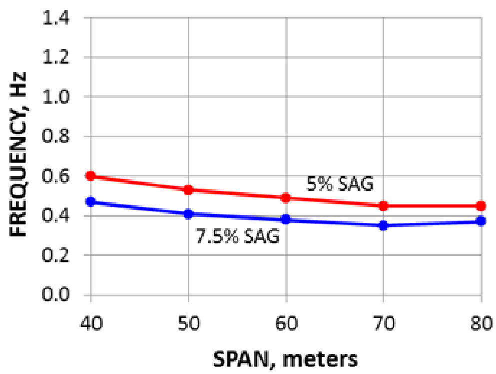

a) VA1 Frequency vs. Span

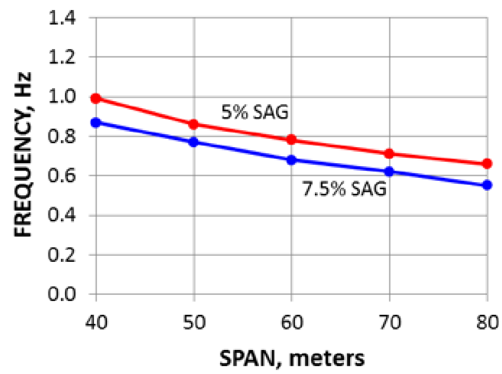

b) VS2 Frequency vs. Span

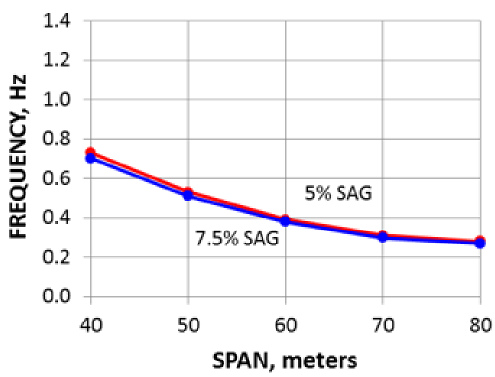

c) LS1 Frequency vs. Span

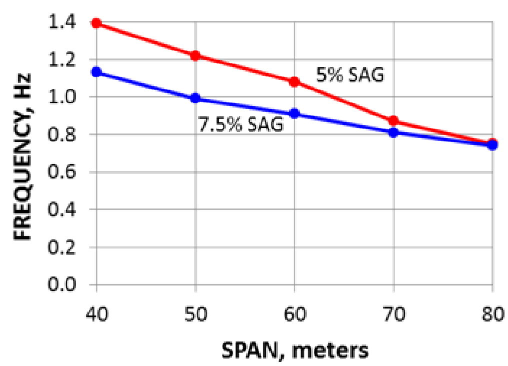

d) LA1 Frequency vs. Span

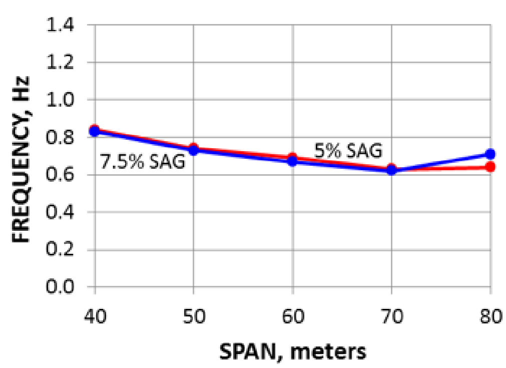

e) TS1 Frequency vs. Span

Figure 51: Modal Frequencies

The dynamic response, including the displacements, velocities, and accelerations, tend to decrease as the span length increases as observed from Figure 52. The average vertical velocities experienced by the walking pedestrian and by the bystander, who is defined to be a stationary person located away from the walker, typically decrease as the span length increases for models with 5 percent cable sag; however, for models with 7.5 percent cable sag, the average vertical velocities are the greatest for 60 m span models. The 60 m span model with 7.5 percent cable sag has a higher vertical mode with a frequency of 2 Hz, which is the frequency of the walker. Therefore, it is expected that the vertical velocities are larger since the forcing frequency matches a modal frequency of the structure causing resonance to occur. For 40 m span bridges, the average vertical velocities experienced by the walking pedestrian are 20 to 26 times greater than the comfort limit, and the average vertical velocities experienced by the bystander are 15 to 18 times great than the 10 mm/sec (0.39 inch/sec) limit. For 80 m span bridges, the average vertical velocities experienced by the walking pedestrian are 12 to 15 times greater than the comfort limit, and the average vertical velocities experienced by the bystander are 11 times greater than the limit. It was anticipated that the velocities would be larger for the walker than the bystander, since the walker is the forcing function on the structure.

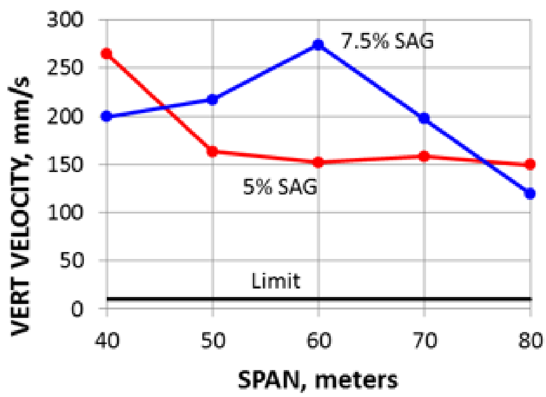

a) Walker Vert Velocity vs. Span

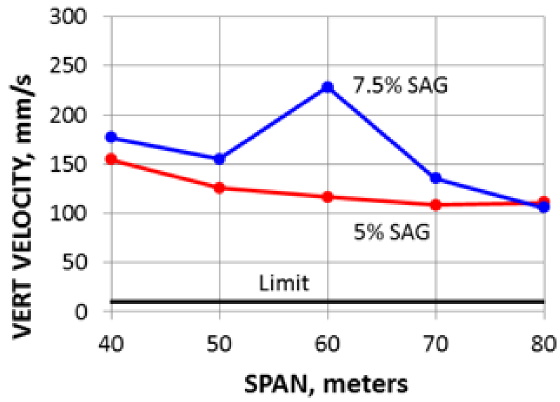

b) Bystander Vert Velocity vs. Span

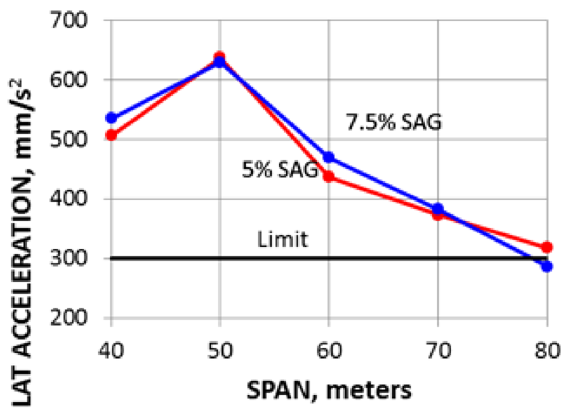

c) Walker Lat Acceleration vs. Span

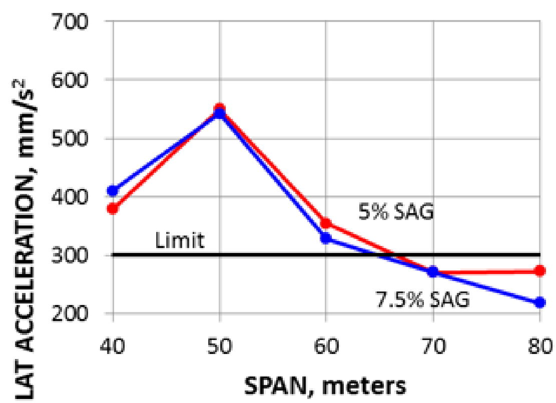

d) Bystander Lat Acceleration vs. Span

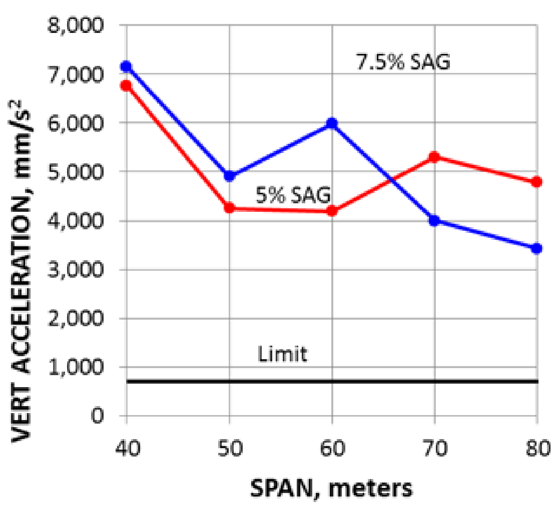

e) Walker Vert Acceleration vs. Span

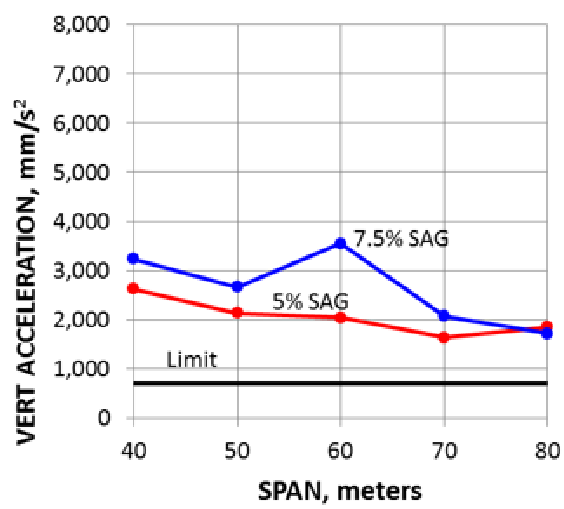

f) Bystander Vert Acceleration vs. Span

Figure 52: Dynamic Response

The average lateral accelerations also tend to decrease as the span length increases as observed from Figure 52, but 50 m span bridges have the greatest lateral accelerations for both cable sag values for both a walker and bystander. The modal frequency of LA1 for a 50 m span model with 7.5 percent cable sag is 0.99 Hz, which is very similar to the 1 Hz lateral frequency of the walker, so the lateral accelerations should be higher for this model. The average lateral accelerations experienced by the walking pedestrian and by the bystander are up to 2 times greater than the comfort limit of 300 mm/s^2 (0.98 ft/s^2); however, the bystander accelerations are lower as expected.

The vertical accelerations tend to decrease as the span length increases. Models with a span length of 40 m have the greatest vertical accelerations for both cable sag types. The average vertical accelerations experienced by the walker are 5 to 10 times the limit of 700 mm/s^2 (2.3 ft/s^2), and the average vertical accelerations experienced by the bystander are up to 5 times the limit. The vertical accelerations experienced by the walker are typically double the vertical accelerations experience by the bystander. The model with a 60 m span length and 7.5 percent cable sag has high vertical accelerations because of resonance.

5.3.2 Cable Sag

The vertical modal frequencies are dependent on the cable sag. The frequencies are typically lower for the 7.5 percent cable sag models as observed from Figure 51. The modal frequencies differ for 5 percent cable sag as compared to 7.5 percent cable sag by 20 percent for the VA1 mode. The modal frequencies differ by 14 percent for the VS2 mode. The vertical modes are anticipated to depend on the cable sag because the sag is in the vertical direction. The cable sag has less of an effect on LS1, and the percent difference in lateral modes between the two cable sag types decreases greatly as the span length increases. TS1 is the only mode that occasionally has a higher frequency for 7.5 percent cable sag as compared to 5 percent cable sag. The stiffest component of pedestrian suspension bridges is the deck, and the lateral modes are dependent on the deck so they are not affected by the cable sag.

The time history responses are not greatly affected by the cable sag, but the vertical responses tend to be slightly higher for models with 7.5 percent cable sag as observed from Figure 52. The average vertical velocities and vertical accelerations experienced by the walker and bystander are the greatest for 60 m span models with 7.5 percent sag because a higher vertical modal frequency for this model matches the walker vertical frequency. The lateral accelerations are similar for 5 percent and 7.5 percent cable sag models. This is because the vertical cable sag does not affect the deck lateral stiffness and the lateral time history response.

5.3.3 Vertical Stiffening

Adding vertical stiffening causes the vertical modal frequencies to increase by 5 to 42 percent. Figure 53 presents the difference in modal frequencies when vertical stiffening is added for models with 5 percent cable sag. The graphs are similar for models with 7.5 percent cable sag. The first vertical mode, VA1, increases by 14 to 42 percent. The second vertical mode, VS2, increases by 5 to 10 percent. The increase is similar for all span length and cable sag types. The first vertical mode was anticipated to increase more when stiffening was added because the vertical stiffening is strategically located to improve this mode. However, the stiffening is also located in some of the areas where it can best mitigate VS2. Adding vertical stiffening causes the lateral modes to change by 5 percent or less. Vertical stiffening causes the frequency of the torsional mode, TS1, to decrease by up to 2 percent for models with 5 percent cable sag and up to 7 percent for models with 7.5 percent cable sag. Vertical stiffening does not affect the lateral modes because they are dependent on the deck stiffness, and adding vertical bracing does not increase the deck stiffness. Overall, vertical stiffening increases the frequencies of the vertical modes.

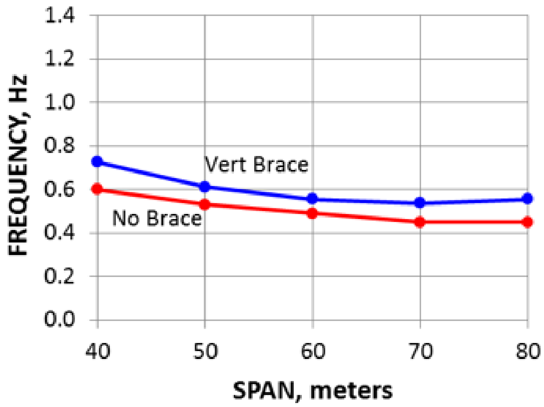

a) VA1 Frequency vs. Span

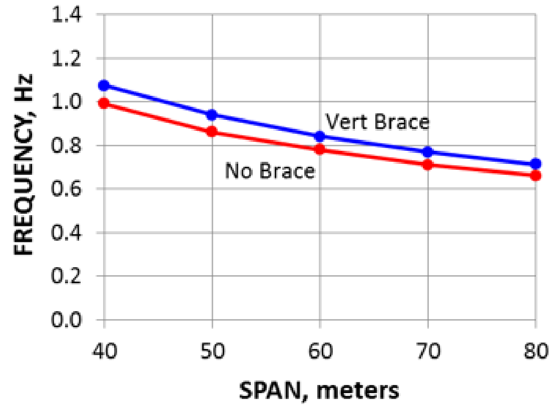

b) VS2 Frequency vs. Span

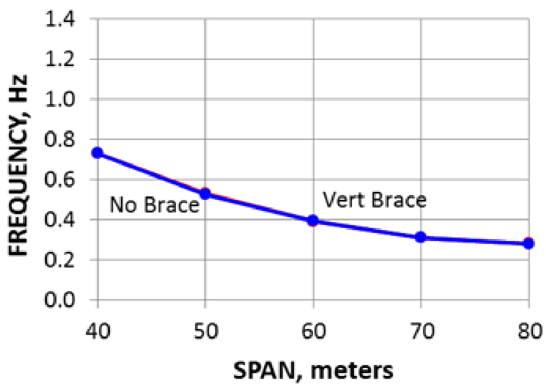

c) LS1 Frequency vs. Span

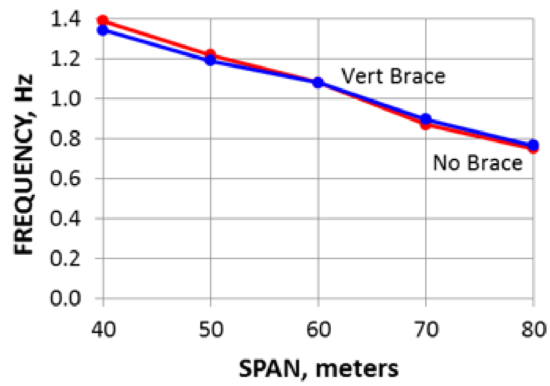

d) LA1 Frequency vs. Span

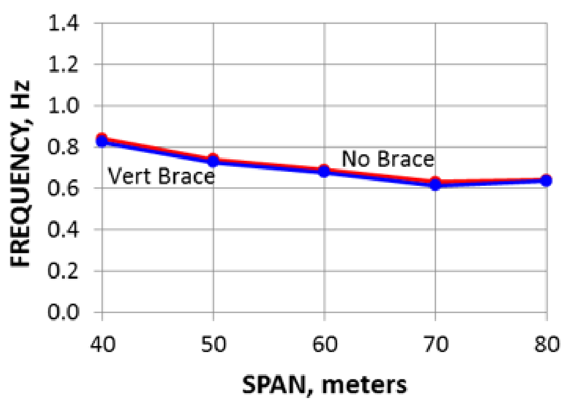

e) TS1 Frequency vs. Span

Figure 53: Modal Frequencies with Vertical Bracing

Adding vertical stiffening causes the vertical velocities and vertical accelerations to decrease for most span lengths. Figure 54 presents the average vertical velocities, lateral accelerations, and vertical accelerations felt by a walker or a bystander for models with 5 percent cable sag. The graphs are similar for models with 7.5 percent cable sag. For 40 m span bridges with vertical stiffening, the average vertical velocity for a walking pedestrian is 15 times the comfort limit, and the vertical velocity for a bystander is 4 times the limit. For 80 m span bridges with vertical stiffening, the average vertical velocity experienced by the walking pedestrian is 10 times greater than the comfort limit, and the average vertical velocity experienced by the bystander are 3 times greater than the limit. The average vertical accelerations for a walking person are typically up to 6 times greater than the limit, and the average vertical accelerations for a bystander are less than the comfort limit for models with vertical stiffening. The dynamic response felt by the bystander decreases to a greater degree than the response felt by the walker because the stiffening decreases the overall bridge movement, but the walker is still creating the force on the bridge, so the localized movement is not as greatly affected. The lateral accelerations decrease slightly when vertical stiffening is added; the lateral accelerations were not anticipated to change because the deck stiffness is not affected by the presence of vertical bracing.

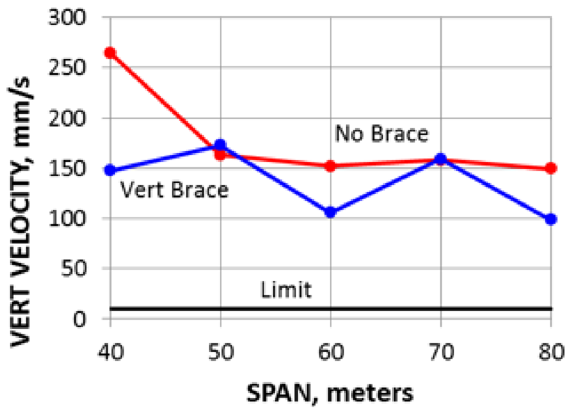

a) Walker Vert Velocity vs. Span

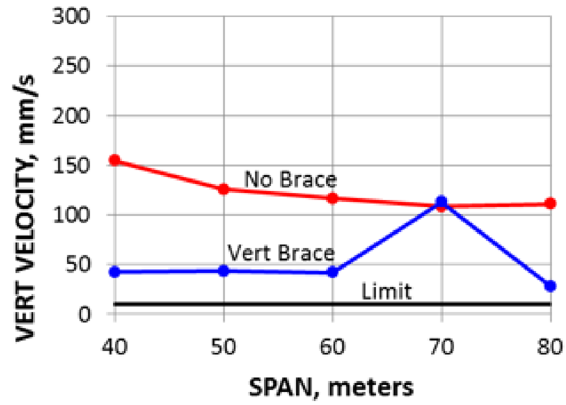

b) Bystander Vert Velocity vs. Span

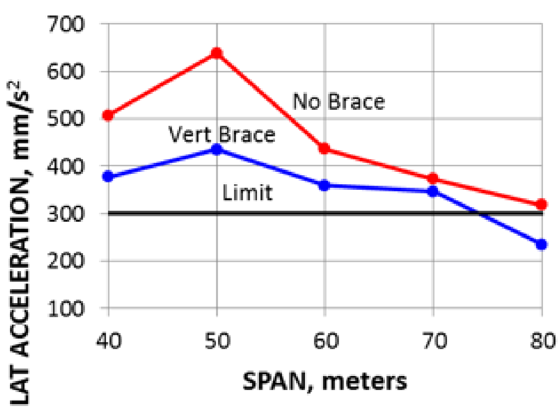

c) Walker Lat Acceleration vs. Span

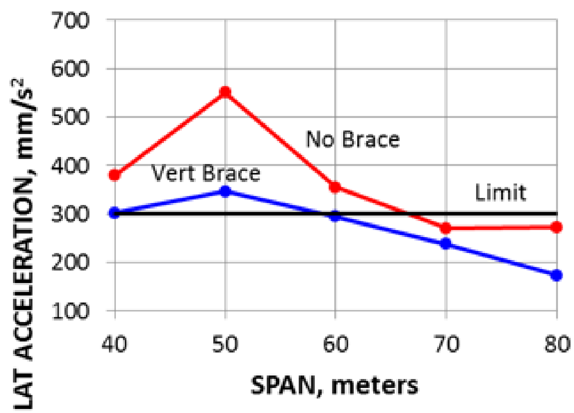

d) Bystander Lat Acceleration vs. Span

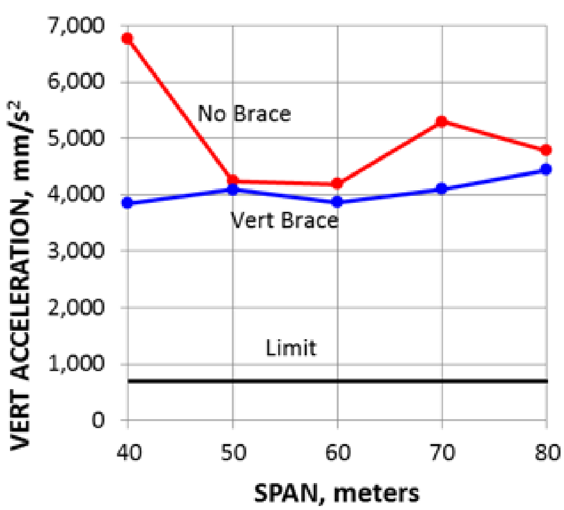

e) Walker Vert Acceleration vs. Span

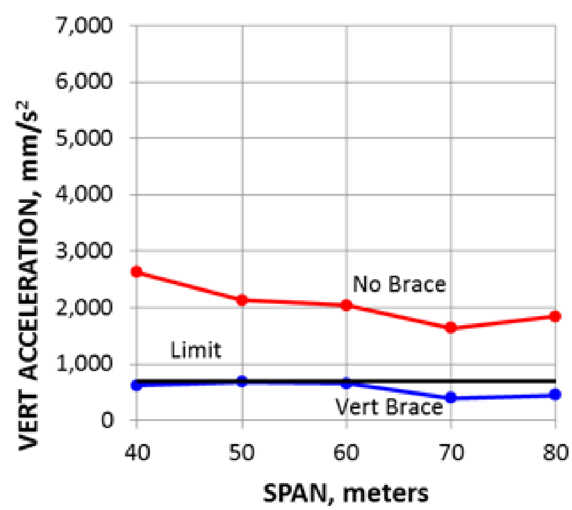

f) Bystander Vert Acceleration vs. Span

Figure 54: Dynamic Response of Models with Vertical Stiffening

5.3.4 Lateral Stiffening

Adding lateral stiffening causes the lateral modal frequencies to increase by up to 13 percent. Figure 55 presents the difference in modal frequencies when lateral stiffening is added for models with 5 percent cable sag. The graphs are similar for models with 7.5 percent cable sag. The first lateral mode, LS1, increases by 3 to 13 percent. The second lateral mode, LA1, increases by 0 to 5 percent. The first lateral mode was anticipated to increase the most because the lateral stiffening is located to strategically limit the displacements for this mode. The longer spans see a higher percent increase than the shorter spans, but the results are similar for both cable sag types. The longer spans have more lateral bracing because the amount of bracing is based on the span, so the longer spans should have a slightly higher percent increase. The lateral modes are not dependent on the cable sag, so the results should be the same for both sag types. Adding lateral stiffening causes the vertical modes to change by 2 percent or less and the torsional mode to increase by up to 6 percent. The vertical modes are not dependent on the lateral stiffness of the deck, so these modes were not anticipated to change. The torsional mode is affected by the deck stiffness, so it was anticipated to increase slightly.

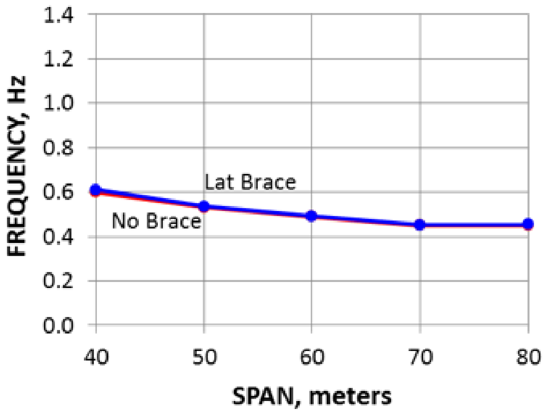

a) VA1 Frequency vs. Span

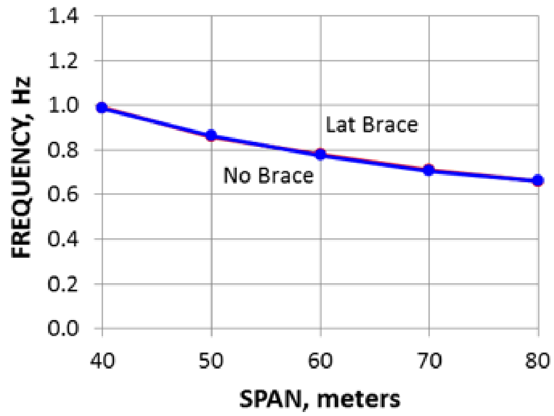

b) VS2 Frequency vs. Span

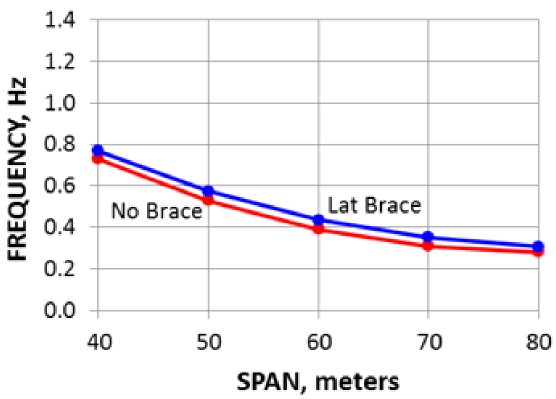

c) LS1 Frequency vs. Span

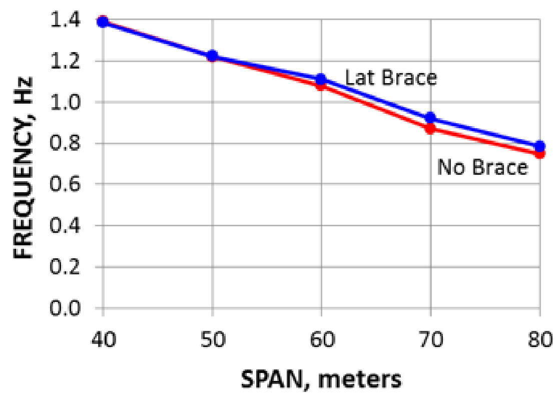

d) LA1 Frequency vs. Span

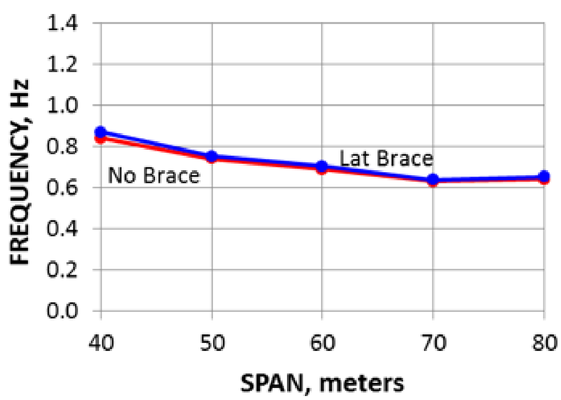

e) TS1 Frequency vs. Span

Figure 55: Modal Frequencies with Lateral Bracing

The presence of lateral stiffening has a different response on the lateral accelerations depending on the span length of the footbridge. For most span lengths, the lateral accelerations decrease when lateral stiffening is present as observed from Figure 56 for models with 5 percent cable sag; the results are similar for models with 7.5 percent cable sag. However, for 70 m span bridges, the lateral accelerations actually increase for the walker and bystander. The modal frequency of LA1 for 70 m models with 5 percent cable sag is close to the walker lateral frequency, so the lateral response is greater for this model. The vertical velocities and vertical accelerations are not greatly affected by lateral stiffening because the vertical response does not depend on the lateral stiffness of the deck.

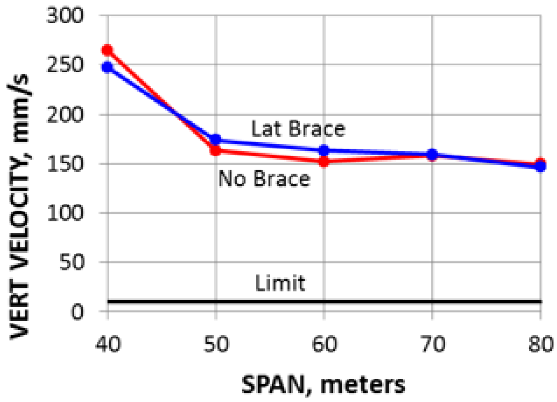

a) Walker Vert Velocity vs. Span

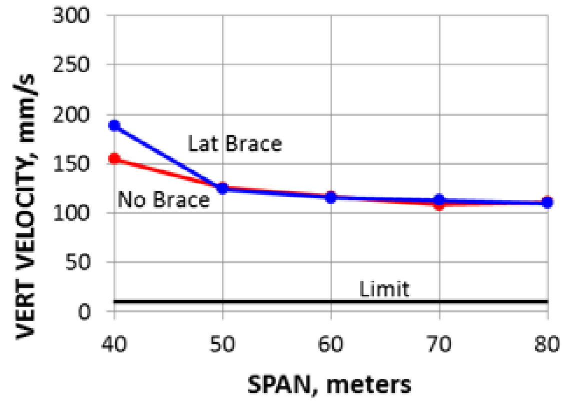

b) Bystander Vert Velocity vs. Span

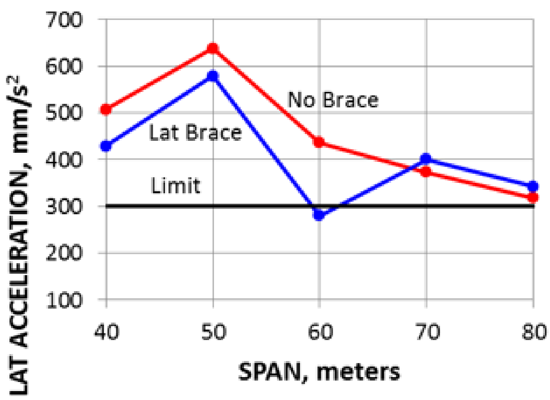

c) Walker Lat Acceleration vs. Span

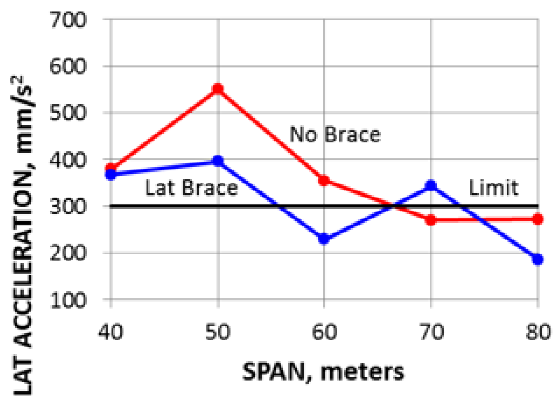

d) Bystander Lat Acceleration vs. Span

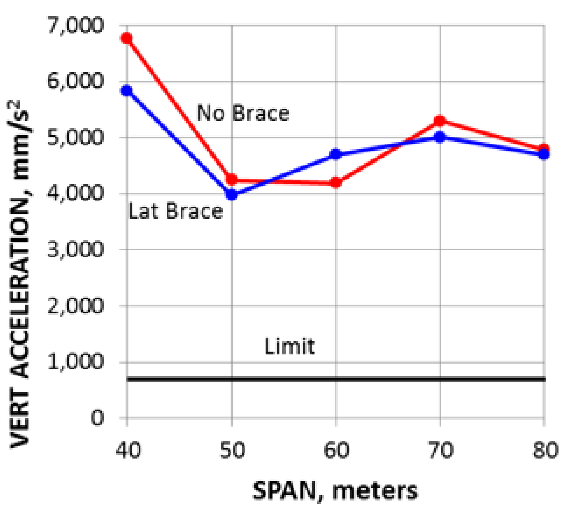

e) Walker Vert Acceleration vs. Span

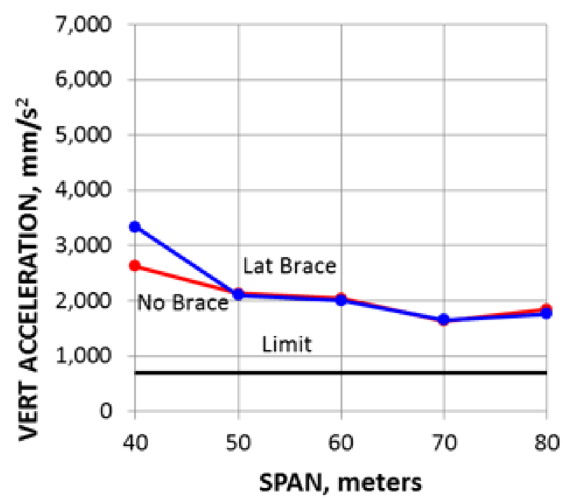

f) Bystander Vert Acceleration vs. Span

Figure 56: Dynamic Response of Models with Lateral Stiffening

5.3.5 Vertical and Lateral Stiffening

When vertical and lateral stiffening are provided, the modal frequency that increases the most is the first vertical mode, VA1, as observed from Figure 57 for models with 5 percent cable sag; the graphs are similar for models with 7.5 percent cable sag. VA1 increases by 15 to 46 percent. The second vertical mode, VS2, increases by 6 to 11 percent. As observed previously vertical bracing has a greater effect on the vertical frequencies than lateral bracing has on the lateral frequencies; therefore, VA1 and VS2 were expected to have the greatest increase. For the 40 m span bridge with 5 percent cable sag, VA1 increases by 22 percent and VS2 increases by 9 percent. For the same model with a full bracing scheme, VA1 increases by 40 percent and VS2 increases by 72 percent. The vertical bracing scheme evaluated for the parametric study is based on mitigating VA1, so the percent increase when all bays are braced should be less for VA1 than VS2. However, both modes greatly increase when full bracing is provided, so the results could be greatly improved if additional bracing is provided. The first lateral mode, LS1, increases by up to 13 percent. For spans less than 70 m, the second lateral modal frequency decreases by up to -5 percent; for 70 and 80 m spans, the LA1 frequency increases by up to 8 percent. The greatest increase in LA1 for models with only lateral stiffening occurred at longer spans, so a higher percent increase was anticipated for longer spans. For the 40 m 5 percent sag model, LS1 increased by 4 percent, and a fully braced version of this model increases by 5 percent. Therefore, the maximum lateral frequencies are almost reached with the current bracing scheme. The torsional modal frequency varies by up to 4 percent. The torsional mode is not directly dependent on vertical or lateral stiffness, so adding these bracing schemes does not greatly affect the torsional mode. Vertical and lateral stiffening increase the vertical and lateral modes, but little changes are seen in the torsional mode.

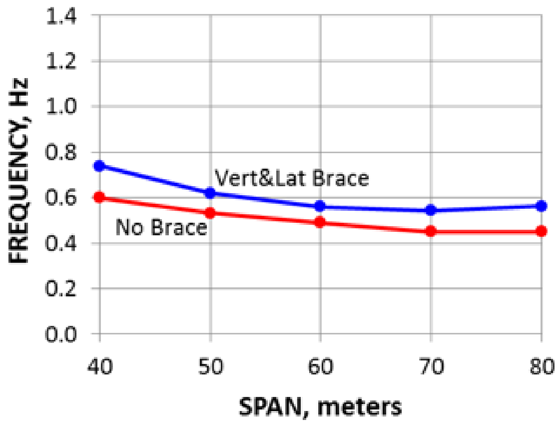

a) VA1 Frequency vs. Span

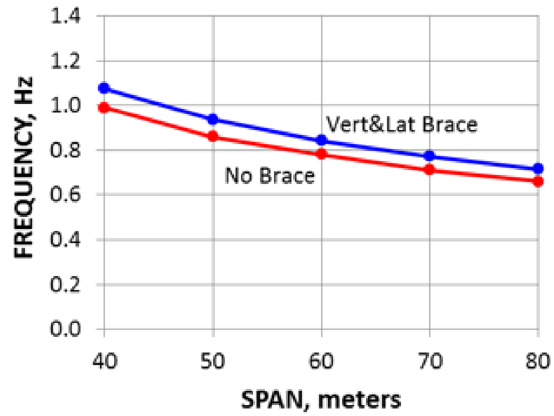

b) VS2 Frequency vs. Span

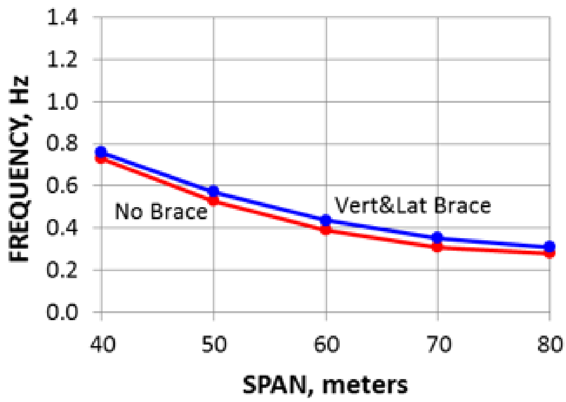

c) LS1 Frequency vs. Span

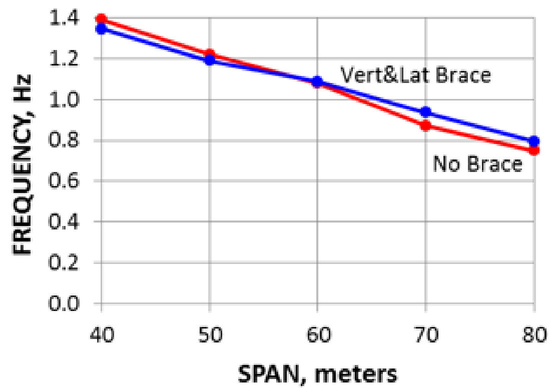

d) LA1 Frequency vs. Span

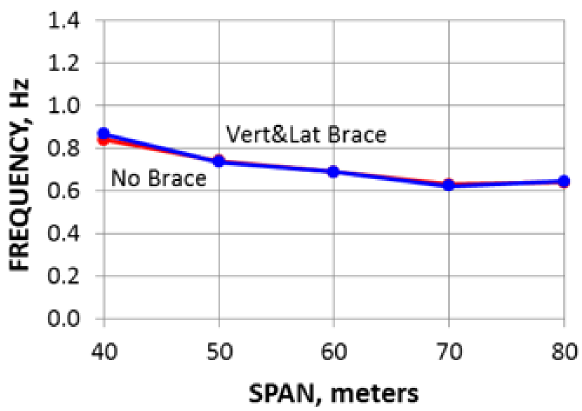

e) TS1 Frequency vs. Span

Figure 57: Modal Frequencies with Vertical and Lateral Bracing

Vertical and lateral stiffening typically decreases all of the time history responses. The vertical velocities, lateral accelerations, and vertical accelerations for a walker and bystander are greatly improved for almost all models as observed from Figure 58 for models with 5 percent cable sag. The graphs are similar for models with 7.5 percent cable sag. The average lateral accelerations for 70 m span bridges increase when stiffening is present, but all other response data decrease. The lateral accelerations increase for this span length because the second lateral modal frequency for this model is very close to the walker lateral frequency, so resonance occurs. In general, the response data for a bystander improves the most because the stiffening is very effective on a global scale rather than in the localized area where the walker is positioned. The bystander average vertical velocities are only up to 5 times the limit for 40 m span bridges and 3 times the limit for 80 m span bridges when vertical and lateral stiffening are provided. The bystander average lateral accelerations are only up to 1.2 times the comfort limit. The bystander average vertical accelerations are only up to 1.1 times the limit. The walker vertical velocities, lateral accelerations, and vertical accelerations are not as greatly affected as the bystander, but all of these quantities typically decrease when vertical and lateral stiffening are provided.

The vertical velocities and vertical accelerations of the 40 m span bridge with 5 percent cable sag and both vertical and lateral stiffening are very similar to a fully braced bridge of the same size; however, the lateral accelerations decrease by an additional 34 percent for the walker and 40 percent for the bystander when the model is fully braced. Therefore, the vertical responses for the models in the parametric study cannot be decreased by adding additional vertical stiffening past the vertical stiffening scheme evaluated, but the lateral accelerations can be decreased by at least 30 percent to the point where they meet lateral acceleration comfort limits when the model is fully braced.

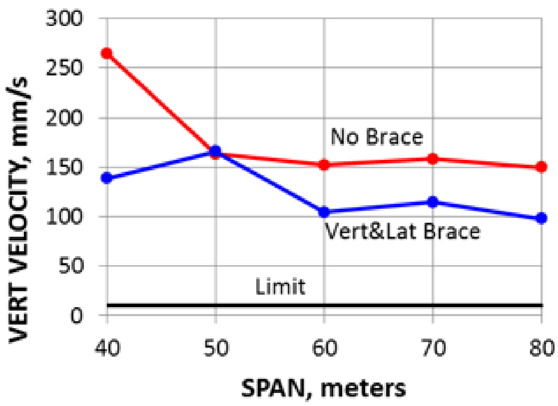

a) Walker Vert Velocity vs. Span

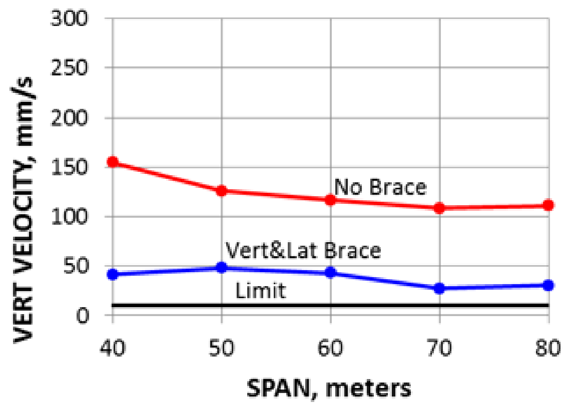

b) Bystander Vert Velocity vs. Span

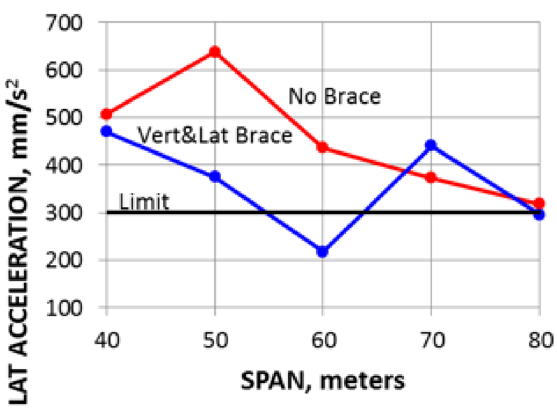

c) Walker Lat Acceleration vs. Span

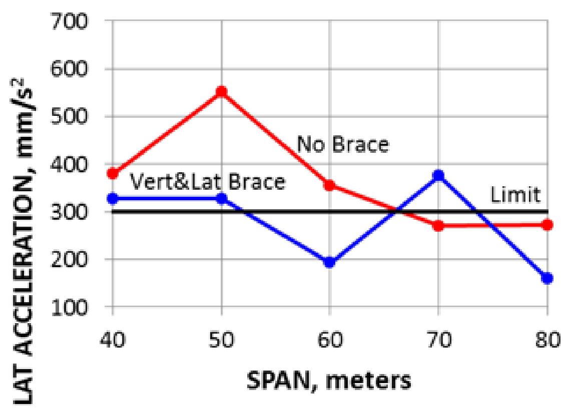

d) Bystander Lat Acceleration vs. Span

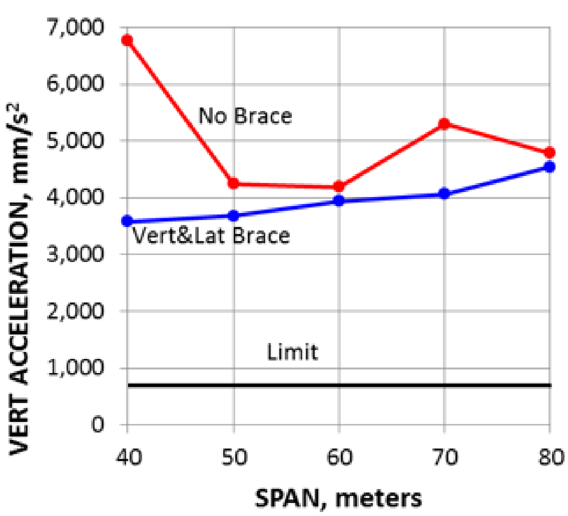

e) Walker Vert Acceleration vs. Span

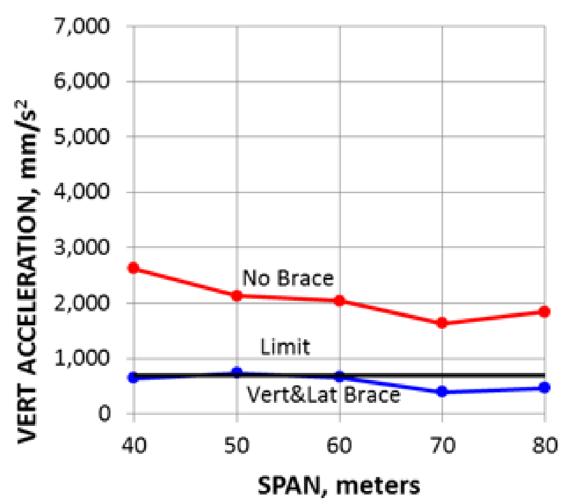

f) Bystander Vert Acceleration vs. Span

Figure 58: Dynamic Response of Models with Vertical and Lateral Stiffening

5.4 Summary

A total of forty models were evaluated in a parametric study to determine the effect of span length, cable sag, vertical stiffening, lateral stiffening, and both vertical and lateral stiffening on footbridge modal frequencies and dynamic response data, including lateral displacements, vertical velocities, lateral accelerations, and vertical accelerations. The results were compared to determine if the modal frequencies fall in the same range as the pedestrian walking frequency and if the dynamic response data are within the human comfort limits. Most modal frequencies and response data do not meet the required criteria, except all lateral displacements are within the human comfort limit. In addition, the dynamic responses are larger for the walking pedestrian versus the bystander.

The modal frequencies decrease as the span length increases. The vertical modal frequencies decrease as the cable sag increases, and the lateral and torsional modal frequencies are not dependent on the cable sag. Typically, dynamic responses decrease as the span length increases, except when a vertical or lateral modal frequency is close to the walker vertical or lateral frequency. The lateral accelerations are similar for both 5 and 7.5 percent cable sag models, and the vertical velocities and vertical accelerations are typically greater for 7.5 percent cable sag models.

Stiffening typically increases the modal frequencies and decreases the response data, especially for a bystander. Vertical stiffening greatly increases the vertical modes and does not greatly affect the lateral and torsional modes. Vertical stiffening also decreases the vertical velocities and vertical accelerations. The vertical accelerations experienced by a bystander are within the comfort limits when vertical stiffening is present. Also, the lateral accelerations decrease slightly when vertical stiffening is provided. Lateral stiffening increases the lateral modes, slightly increases the torsional mode, and has little effect on the vertical modes. Lateral stiffening typically decreases the lateral accelerations and has little effect on the vertical velocities and vertical accelerations. Providing both vertical and lateral stiffening causes modal frequencies to increase, except for the torsional mode. This stiffening also causes all dynamic response data to decrease, especially for a bystander. Overall, stiffening does improve the footbridge's properties and response. The dynamic response improvement is greater in the vertical quantities than in the lateral quantities, but the lateral quantities are closer to the comfort limits. The bracing schemes evaluated increase the lateral modal frequencies to values near the maximum achievable with this type of brace and decrease the vertical velocities and vertical accelerations to values near the minimum achievable with this type of brace; however, vertical modal frequencies can be increased and lateral accelerations can be decreased by adding additional bracing.

Chapter 6

Conclusions

6.1 Summary

Pedestrian suspension bridges are needed in rural communities around the world to provide safe, year-long access to basic needs. However, these bridges have a low mass, stiffness, and damping, so they are susceptible to serviceability failures under pedestrian loading. For this reason, the present study investigated how span length, cable sag, vertical stiffness, and lateral stiffness affect the dynamic response of suspension footbridges. This was accomplished through a parametric study conducted in SAP2000, which was validated through constructing and testing two physical bridge models. A modal analysis was conducted to determine if the modal frequencies of the structures are similar to pedestrian walking frequencies. In addition, a nonlinear, direct-integration, time-history analysis was conducted to compare the displacements, velocities, and accelerations to human comfort limits. Conclusions and future research recommendations are presented in the following sections.

6.2 Conclusions

The modal frequency and time-history results from the parametric study support several conclusions:

1. Shorter span lengths have higher modal frequencies; smaller cable sags have higher vertical modal frequencies
2. Adding vertical stiffening greatly increases the first two vertical modal frequencies; adding lateral stiffening increases the first two lateral modal frequencies and slightly increases the first torsional modal frequency; adding both vertical and lateral stiffening causes the all modal frequencies to increase, except the torsional modal frequency
3. Shorter span lengths typically have higher dynamic responses, but models with a modal frequency close to the pedestrian walking frequency have a higher dynamic response; the vertical dynamic responses increase as the cable sag increases
4. Adding vertical stiffening causes the vertical velocities and vertical accelerations to decrease, so the vertical accelerations felt by a bystander are within the comfort limits; adding lateral stiffening typically causes the lateral accelerations to decrease; adding both vertical and lateral stiffening decreases the response felt by a walker for most bridges and greatly decreases the response felt by a bystander
5. For most span lengths, especially 50 m spans, the second lateral mode is close to 1 Hz, which is the lateral frequency of a normal pedestrian walk, so these modes are anticipated to be most easily excited under normal walking conditions
6. For all span lengths, the lateral displacements resulting from one pedestrian walking are within the limit for human comfort, and the lateral accelerations only slightly exceed the limit for human comfort; however, the vertical velocities and vertical accelerations greatly exceed the human comfort limits, so the vertical vibrations are a greater concern
7. The vertical stiffening evaluated does not increase the vertical modal frequencies enough to meet vertical frequency limits for pedestrian suspension bridges, and the lateral

stiffening evaluated does not increase the lateral modal frequencies enough to meet lateral frequency limits; the frequencies are closer to the limits when stiffening is present, but large vibrations could occur if many pedestrians walk at frequencies similar to the modal frequencies of the structure

8. The vertical and lateral stiffening do not decrease the dynamic response of the bridge to meet human comfort limits; however, the response is improved with stiffening, especially regarding the response felt by a bystander
9. Vertical stiffening has a greater effect on the frequencies and dynamic responses than lateral stiffening, but the models are closer to the lateral comfort limits than the vertical comfort limits

6.3 Recommendations for Further Research

Based on the scope of the present study, the following recommendations are made:

- Further validate the modeling techniques by calibrating the numerical models to full scale bridge data if available
- Investigate other loading scenarios, including a person running, groups of people, animals, and people with animals
- Consider longer span lengths for pedestrian suspension bridges because the span length limits are increasing for standard suspension footbridges
- Explore different back span cable angles and loaded back stays
- Examine wind guys, which are cables used to support the bridge on the sides from independent anchors

- Study additional ways to improve the lateral response because most footbridges have lateral modal frequencies similar to a normal pedestrian lateral walking frequency
- Investigate additional vertical stiffening schemes because many models have a higher vertical modal frequency similar to a normal pedestrian vertical walking frequency
- Explore adding mass in different locations along the bridge to improve the dynamic response

Appendix

Time History Data

Table A.1: Time History Results for 40-5-N-N

		Vertical Velocity (mm/s)						
	Location (m)	0 to 6	6 to 12	12 to 18	18 to 24	24 to 30	30 to 36	36 to 40
Time (sec)	**Moving Person Region**	**1**	**2**	**3**	**4**	**5**	**6**	**7**
0-5	**1**	110	103	138	109	132	144	55
5-10	**2**	167	383	226	235	236	142	119
10-15	**3**	150	251	301	288	240	215	109
	Lateral Acceleration (mm/s^2)							
	Location (m)	0 to 6	6 to 12	12 to 18	18 to 24	24 to 30	30 to 36	36 to 40
Time (sec)	**Moving Person Region**	**1**	**2**	**3**	**4**	**5**	**6**	**7**
0-5	**1**	137	490	451	290	424	382	86
5-10	**2**	220	694	825	460	720	445	104
10-15	**3**	242	422	687	445	667	511	69
	Vertical Acceleration (mm/s^2)							
	Location (m)	0 to 6	6 to 12	12 to 18	18 to 24	24 to 30	30 to 36	36 to 40
Time (sec)	**Moving Person Region**	**1**	**2**	**3**	**4**	**5**	**6**	**7**
0-5	**1**	3480	1878	2143	1802	2367	2095	807
5-10	**2**	2643	7125	4573	3977	3389	2259	1900
10-15	**3**	2288	4941	9683	5167	4560	3878	2376

Table A.2: Time History Results for 40-5-N-L

	Vertical Velocity (mm/s)							
	Location (m)	0 to 6	6 to 12	12 to 18	18 to 24	24 to 30	30 to 36	36 to 40
Time (sec)	**Moving Person Region**	**1**	**2**	**3**	**4**	**5**	**6**	**7**
0-5	**1**	108	95	145	107	143	141	57
5-10	**2**	164	360	216	276	226	343	102
10-15	**3**	208	330	275	272	267	299	116
	Lateral Acceleration (mm/s^2)							
	Location (m)	0 to 6	6 to 12	12 to 18	18 to 24	24 to 30	30 to 36	36 to 40
Time (sec)	**Moving Person Region**	**1**	**2**	**3**	**4**	**5**	**6**	**7**
0-5	**1**	130	262	323	336	335	569	82
5-10	**2**	299	711	434	632	450	662	92
10-15	**3**	245	602	443	382	596	462	61
	Vertical Acceleration (mm/s^2)							
	Location (m)	0 to 6	6 to 12	12 to 18	18 to 24	24 to 30	30 to 36	36 to 40
Time (sec)	**Moving Person Region**	**1**	**2**	**3**	**4**	**5**	**6**	**7**
0-5	**1**	3560	1855	2306	1667	2240	2053	880
5-10	**2**	2892	8321	7234	5559	3854	6161	1725
10-15	**3**	4071	7619	5625	6299	4855	5674	2567

Table A.3: Time History Results for 40-5-V-N

	Vertical Velocity (mm/s)							
	Location (m)	0 to 6	6 to 12	12 to 18	18 to 24	24 to 30	30 to 36	36 to 40
Time (sec)	**Moving Person Region**	**1**	**2**	**3**	**4**	**5**	**6**	**7**
0-5	**1**	59	55	49	40	41	56	28
5-10	**2**	52	202	131	53	50	61	27
10-15	**3**	65	102	181	82	52	43	22
	Lateral Acceleration (mm/s^2)							
	Location (m)	0 to 6	6 to 12	12 to 18	18 to 24	24 to 30	30 to 36	36 to 40
Time (sec)	**Moving Person Region**	**1**	**2**	**3**	**4**	**5**	**6**	**7**
0-5	**1**	121	395	339	273	297	293	22
5-10	**2**	176	514	469	497	524	333	74
10-15	**3**	257	438	496	387	728	328	121
	Vertical Acceleration (mm/s^2)							
	Location (m)	0 to 6	6 to 12	12 to 18	18 to 24	24 to 30	30 to 36	36 to 40
Time (sec)	**Moving Person Region**	**1**	**2**	**3**	**4**	**5**	**6**	**7**
0-5	**1**	1858	787	845	468	557	756	422
5-10	**2**	2012	5198	2846	896	739	836	458
10-15	**3**	1100	2492	4485	1590	792	703	339

Table A.4: Time History Results for 40-5-V-L

	Vertical Velocity (mm/s)							
	Location (m)	0 to 6	6 to 12	12 to 18	18 to 24	24 to 30	30 to 36	36 to 40
Time (sec)	**Moving Person Region**	**1**	**2**	**3**	**4**	**5**	**6**	**7**
0-5	**1**	61	42	49	39	39	58	28
5-10	**2**	50	194	130	62	45	63	30
10-15	**3**	63	138	159	48	43	41	25
	Lateral Acceleration (mm/s^2)							
	Location (m)	0 to 6	6 to 12	12 to 18	18 to 24	24 to 30	30 to 36	36 to 40
Time (sec)	**Moving Person Region**	**1**	**2**	**3**	**4**	**5**	**6**	**7**
0-5	**1**	118	241	380	129	279	310	43
5-10	**2**	192	734	520	350	484	483	68
10-15	**3**	283	662	559	338	628	571	82
	Vertical Acceleration (mm/s^2)							
	Location (m)	0 to 6	6 to 12	12 to 18	18 to 24	24 to 30	30 to 36	36 to 40
Time (sec)	**Moving Person Region**	**1**	**2**	**3**	**4**	**5**	**6**	**7**
0-5	**1**	1642	939	743	457	486	818	419
5-10	**2**	2169	4709	2688	1110	906	828	465
10-15	**3**	1055	3696	4395	1925	889	621	382

Table A.5: Time History Results for 40-7.5-N-N

	Vertical Velocity (mm/s)							
	Location (m)	0 to 6	6 to 12	12 to 18	18 to 24	24 to 30	30 to 36	36 to 40
Time (sec)	**Moving Person Region**	**1**	**2**	**3**	**4**	**5**	**6**	**7**
0-5	**1**	97	166	97	88	102	164	49
5-10	**2**	180	279	325	323	174	358	130
10-15	**3**	194	185	222	237	229	272	116

	Lateral Acceleration (mm/s^2)							
	Location (m)	0 to 6	6 to 12	12 to 18	18 to 24	24 to 30	30 to 36	36 to 40
Time (sec)	**Moving Person Region**	**1**	**2**	**3**	**4**	**5**	**6**	**7**
0-5	**1**	287	655	749	320	535	332	98
5-10	**2**	297	854	869	531	1112	528	130
10-15	**3**	129	431	464	417	505	375	76

	Vertical Acceleration (mm/s^2)							
	Location (m)	0 to 6	6 to 12	12 to 18	18 to 24	24 to 30	30 to 36	36 to 40
Time (sec)	**Moving Person Region**	**1**	**2**	**3**	**4**	**5**	**6**	**7**
0-5	**1**	3150	3465	1906	1430	1546	2531	754
5-10	**2**	3281	9078	5477	4764	3492	5762	1948
10-15	**3**	3004	5158	9237	5765	5537	5500	2072

Table A.6: Time History Results for 40-7.5-N-L

	Vertical Velocity (mm/s)							
	Location (m)	0 to 6	6 to 12	12 to 18	18 to 24	24 to 30	30 to 36	36 to 40
Time (sec)	**Moving Person Region**	**1**	**2**	**3**	**4**	**5**	**6**	**7**
0-5	**1**	84	167	95	94	103	155	45
5-10	**2**	123	248	260	253	159	294	150
10-15	**3**	180	273	317	241	157	238	98

	Lateral Acceleration (mm/s^2)							
	Location (m)	0 to 6	6 to 12	12 to 18	18 to 24	24 to 30	30 to 36	36 to 40
Time (sec)	**Moving Person Region**	**1**	**2**	**3**	**4**	**5**	**6**	**7**
0-5	**1**	162	331	275	173	305	407	51
5-10	**2**	228	596	364	402	454	422	69
10-15	**3**	262	557	465	476	607	565	95

	Vertical Acceleration (mm/s^2)							
	Location (m)	0 to 6	6 to 12	12 to 18	18 to 24	24 to 30	30 to 36	36 to 40
Time (sec)	**Moving Person Region**	**1**	**2**	**3**	**4**	**5**	**6**	**7**
0-5	**1**	2819	3462	1851	1547	1501	2372	756
5-10	**2**	2774	5267	4676	4480	2972	4859	2514
10-15	**3**	3303	4916	7329	5147	2947	5071	2256

Table A.7: Time History Results for 40-7.5-V-N

	Vertical Velocity (mm/s)							
	Location (m)	0 to 6	6 to 12	12 to 18	18 to 24	24 to 30	30 to 36	36 to 40
Time (sec)	**Moving Person Region**	**1**	**2**	**3**	**4**	**5**	**6**	**7**
0-5	**1**	66	52	50	31	54	25	13
5-10	**2**	50	346	413	122	123	43	28
10-15	**3**	46	309	306	173	208	43	32

	Lateral Acceleration (mm/s^2)							
	Location (m)	0 to 6	6 to 12	12 to 18	18 to 24	24 to 30	30 to 36	36 to 40
Time (sec)	**Moving Person Region**	**1**	**2**	**3**	**4**	**5**	**6**	**7**
0-5	**1**	107	340	260	188	218	200	27
5-10	**2**	153	491	437	361	569	335	81
10-15	**3**	187	635	676	362	704	423	94

	Vertical Acceleration (mm/s^2)							
	Location (m)	0 to 6	6 to 12	12 to 18	18 to 24	24 to 30	30 to 36	36 to 40
Time (sec)	**Moving Person Region**	**1**	**2**	**3**	**4**	**5**	**6**	**7**
0-5	**1**	1571	768	725	465	553	343	194
5-10	**2**	1846	9466	8097	2743	2244	735	542
10-15	**3**	867	5431	7087	3211	3605	821	496

Table A.8: Time History Results for 40-7.5-V-L

	Vertical Velocity (mm/s)							
	Location (m)	0 to 6	6 to 12	12 to 18	18 to 24	24 to 30	30 to 36	36 to 40
Time (sec)	**Moving Person Region**	**1**	**2**	**3**	**4**	**5**	**6**	**7**
0-5	**1**	70	53	51	31	55	26	12
5-10	**2**	48	312	292	105	133	47	29
10-15	**3**	51	308	356	162	203	37	35

	Lateral Acceleration (mm/s^2)							
	Location (m)	0 to 6	6 to 12	12 to 18	18 to 24	24 to 30	30 to 36	36 to 40
Time (sec)	**Moving Person Region**	**1**	**2**	**3**	**4**	**5**	**6**	**7**
0-5	**1**	95	225	193	132	311	196	27
5-10	**2**	235	648	412	265	563	339	64
10-15	**3**	266	821	604	302	568	552	70

	Vertical Acceleration (mm/s^2)							
	Location (m)	0 to 6	6 to 12	12 to 18	18 to 24	24 to 30	30 to 36	36 to 40
Time (sec)	**Moving Person Region**	**1**	**2**	**3**	**4**	**5**	**6**	**7**
0-5	**1**	1666	760	724	499	579	361	186
5-10	**2**	1696	8547	6221	1790	2340	703	655
10-15	**3**	794	6874	6800	2557	3099	712	619

Table A.9: Time History Results for 50-5-N-N

	Vertical Velocity (mm/s)								
	Location (m)	0 to 6	6 to 12	12 to 18	18 to 24	24 to 30	30 to 36	36 to 42	42 to 50
Time (sec)	**Moving Person Region**	**1**	**2**	**3**	**4**	**5**	**6**	**7**	**8**
0-5	**1**	134	111	98	81	91	58	94	74
5-10	**2**	215	195	166	120	118	159	146	165
10-15	**3**	159	181	187	159	144	172	136	154
15-20	**4**	160	116	104	138	90	130	98	123

	Lateral Acceleration (mm/s^2)								
	Location (m)	0 to 6	6 to 12	12 to 18	18 to 24	24 to 30	30 to 36	36 to 40	42 to 50
Time (sec)	**Moving Person Region**	**1**	**2**	**3**	**4**	**5**	**6**	**7**	**8**
0-5	**1**	178	410	393	382	396	318	588	225
5-10	**2**	288	798	727	517	810	578	917	397
10-15	**3**	298	877	1025	583	780	612	1012	480
15-20	**4**	324	717	657	547	495	540	662	269

	Vertical Acceleration (mm/s^2)								
	Location (m)	0 to 6	6 to 12	12 to 18	18 to 24	24 to 30	30 to 36	36 to 40	42 to 50
Time (sec)	**Moving Person Region**	**1**	**2**	**3**	**4**	**5**	**6**	**7**	**8**
0-5	**1**	2682	2273	1774	1388	1305	1025	1491	1124
5-10	**2**	5131	4457	3134	2630	1970	2345	2359	2396
10-15	**3**	2861	3513	5191	2496	2651	3105	2046	2451
15-20	**4**	2579	2266	1646	4668	2108	2679	2187	2404

Table A.10: Time History Results for 50-5-N-L

		Vertical Velocity (mm/s)							
	Location (m)	0 to 6	6 to 12	12 to 18	18 to 24	24 to 30	30 to 36	36 to 42	42 to 50
Time (sec)	**Moving Person Region**	**1**	**2**	**3**	**4**	**5**	**6**	**7**	**8**
0-5	**1**	165	102	123	80	124	85	112	85
5-10	**2**	235	181	153	120	120	161	127	136
10-15	**3**	150	154	171	128	112	162	124	141
15-20	**4**	184	141	153	178	110	95	144	118

		Lateral Acceleration (mm/s^2)							
	Location (m)	0 to 6	6 to 12	12 to 18	18 to 24	24 to 30	30 to 36	36 to 40	42 to 50
Time (sec)	**Moving Person Region**	**1**	**2**	**3**	**4**	**5**	**6**	**7**	**8**
0-5	**1**	164	426	282	445	270	183	364	220
5-10	**2**	341	1080	736	623	548	352	643	297
10-15	**3**	265	890	522	456	474	306	784	403
15-20	**4**	234	948	521	549	379	348	566	286

		Vertical Acceleration (mm/s^2)							
	Location (m)	0 to 6	6 to 12	12 to 18	18 to 24	24 to 30	30 to 36	36 to 40	42 to 50
Time (sec)	**Moving Person Region**	**1**	**2**	**3**	**4**	**5**	**6**	**7**	**8**
0-5	**1**	3003	2133	2072	1762	2005	1172	1589	1276
5-10	**2**	5164	3941	3144	2481	1838	2598	2668	1990
10-15	**3**	2951	3318	4611	1837	2398	2299	2046	2558
15-20	**4**	2624	2372	1900	4331	2946	2239	2664	2136

Table A.11: Time History Results for 50-5-V-N

		Vertical Velocity (mm/s)							
	Location (m)	0 to 6	6 to 12	12 to 18	18 to 24	24 to 30	30 to 36	36 to 42	42 to 50
Time (sec)	**Moving Person Region**	**1**	**2**	**3**	**4**	**5**	**6**	**7**	**8**
0-5	**1**	70	76	16	37	25	14	38	25
5-10	**2**	76	214	101	59	65	58	40	29
10-15	**3**	26	63	207	130	84	82	62	39
15-20	**4**	34	46	78	200	106	61	59	16

	Lateral Acceleration (mm/s^2)								
	Location (m)	0 to 6	6 to 12	12 to 18	18 to 24	24 to 30	30 to 36	36 to 40	42 to 50
Time (sec)	**Moving Person Region**	**1**	**2**	**3**	**4**	**5**	**6**	**7**	**8**
0-5	**1**	134	260	318	196	419	173	421	214
5-10	**2**	145	563	463	278	642	301	630	282
10-15	**3**	213	568	577	272	538	287	611	305
15-20	**4**	232	399	324	466	306	176	474	283

	Vertical Acceleration (mm/s^2)								
	Location (m)	0 to 6	6 to 12	12 to 18	18 to 24	24 to 30	30 to 36	36 to 40	42 to 50
Time (sec)	**Moving Person Region**	**1**	**2**	**3**	**4**	**5**	**6**	**7**	**8**
0-5	**1**	1049	2731	324	576	325	153	512	337
5-10	**2**	1495	4821	2003	1442	1153	811	530	393
10-15	**3**	397	2347	5695	2936	1822	1334	1047	506
15-20	**4**	454	1293	1867	4811	2268	1267	1068	241

Table A.12: Time History Results for 50-5-V-L

		Vertical Velocity (mm/s)							
	Location (m)	0 to 6	6 to 12	12 to 18	18 to 24	24 to 30	30 to 36	36 to 42	42 to 50
Time (sec)	**Moving Person Region**	**1**	**2**	**3**	**4**	**5**	**6**	**7**	**8**
0-5	**1**	80	78	16	33	29	16	38	26
5-10	**2**	83	244	101	60	64	61	37	41
10-15	**3**	31	111	170	139	94	85	74	37
15-20	**4**	34	63	84	170	70	75	62	22

	Lateral Acceleration (mm/s^2)								
	Location (m)	0 to 6	6 to 12	12 to 18	18 to 24	24 to 30	30 to 36	36 to 40	42 to 50
Time (sec)	**Moving Person Region**	**1**	**2**	**3**	**4**	**5**	**6**	**7**	**8**
0-5	**1**	141	304	260	195	319	139	405	250
5-10	**2**	181	567	472	274	439	208	520	285
10-15	**3**	207	531	395	327	409	252	519	324
15-20	**4**	163	412	421	397	308	212	463	347

	Vertical Acceleration (mm/s^2)								
	Location (m)	0 to 6	6 to 12	12 to 18	18 to 24	24 to 30	30 to 36	36 to 40	42 to 50
Time (sec)	**Moving Person Region**	**1**	**2**	**3**	**4**	**5**	**6**	**7**	**8**
0-5	**1**	1036	2170	293	484	359	176	510	351
5-10	**2**	1376	5201	2255	1345	972	908	526	489
10-15	**3**	503	3211	3880	2863	1865	1288	1308	532
15-20	**4**	446	1744	2377	4583	1586	1299	1116	319

Table A.13: Time History Results for 50-7.5-N-N

	Vertical Velocity (mm/s)								
	Location (m)	0 to 6	6 to 12	12 to 18	18 to 24	24 to 30	30 to 36	36 to 42	42 to 50
Time (sec)	**Moving Person Region**	**1**	**2**	**3**	**4**	**5**	**6**	**7**	**8**
0-5	**1**	85	114	83	85	110	107	95	73
5-10	**2**	124	254	180	252	208	229	155	226
10-15	**3**	130	233	213	151	174	217	129	153
15-20	**4**	103	143	194	317	189	200	127	153

	Lateral Acceleration (mm/s^2)								
	Location (m)	0 to 6	6 to 12	12 to 18	18 to 24	24 to 30	30 to 36	36 to 40	42 to 50
Time (sec)	**Moving Person Region**	**1**	**2**	**3**	**4**	**5**	**6**	**7**	**8**
0-5	**1**	137	298	249	246	192	282	337	139
5-10	**2**	228	796	807	623	771	742	1073	525
10-15	**3**	190	601	1026	394	679	684	856	355
15-20	**4**	226	395	549	558	389	627	548	337

	Vertical Acceleration (mm/s^2)								
	Location (m)	0 to 6	6 to 12	12 to 18	18 to 24	24 to 30	30 to 36	36 to 40	42 to 50
Time (sec)	**Moving Person Region**	**1**	**2**	**3**	**4**	**5**	**6**	**7**	**8**
0-5	**1**	2393	3017	1723	1658	1537	1350	1399	1045
5-10	**2**	2645	5048	3797	4842	3827	3698	2845	3820
10-15	**3**	2249	6300	5749	3613	2806	4281	2320	2440
15-20	**4**	1864	3286	4554	6427	4788	4037	2123	2624

Table A.14: Time History Results for 50-7.5-N-L

	Vertical Velocity (mm/s)								
	Location (m)	0 to 6	6 to 12	12 to 18	18 to 24	24 to 30	30 to 36	36 to 42	42 to 50
Time (sec)	**Moving Person Region**	**1**	**2**	**3**	**4**	**5**	**6**	**7**	**8**
0-5	**1**	72	118	82	83	105	117	90	73
5-10	**2**	112	248	176	267	198	185	136	242
10-15	**3**	157	267	201	155	163	179	130	176
15-20	**4**	153	120	229	355	227	260	157	107

	Lateral Acceleration (mm/s^2)								
	Location (m)	0 to 6	6 to 12	12 to 18	18 to 24	24 to 30	30 to 36	36 to 40	42 to 50
Time (sec)	**Moving Person Region**	**1**	**2**	**3**	**4**	**5**	**6**	**7**	**8**
0-5	**1**	169	360	331	274	211	163	240	119
5-10	**2**	319	888	877	509	522	290	656	387
10-15	**3**	230	397	548	313	422	249	481	295
15-20	**4**	88	387	395	281	281	211	316	194

	Vertical Acceleration (mm/s^2)								
	Location (m)	0 to 6	6 to 12	12 to 18	18 to 24	24 to 30	30 to 36	36 to 40	42 to 50
Time (sec)	**Moving Person Region**	**1**	**2**	**3**	**4**	**5**	**6**	**7**	**8**
0-5	**1**	2254	2949	1763	1602	1468	1428	1339	1046
5-10	**2**	2633	5379	3707	5033	3593	2729	2463	3866
10-15	**3**	2454	6752	6019	6120	3379	3604	2264	2763
15-20	**4**	2311	5219	3715	7158	7874	4283	3153	2068

Table A.15: Time History Results for 50-7.5-V-N

	Vertical Velocity (mm/s)								
	Location (m)	0 to 6	6 to 12	12 to 18	18 to 24	24 to 30	30 to 36	36 to 42	42 to 50
Time (sec)	**Moving Person Region**	**1**	**2**	**3**	**4**	**5**	**6**	**7**	**8**
0-5	**1**	55	52	53	29	52	24	47	33
5-10	**2**	50	386	118	105	63	64	46	30
10-15	**3**	44	91	150	155	71	92	62	57
15-20	**4**	37	91	115	228	102	77	71	37

	Lateral Acceleration (mm/s^2)								
	Location (m)	0 to 6	6 to 12	12 to 18	18 to 24	24 to 30	30 to 36	36 to 40	42 to 50
Time (sec)	**Moving Person Region**	**1**	**2**	**3**	**4**	**5**	**6**	**7**	**8**
0-5	**1**	146	296	201	221	248	147	308	143
5-10	**2**	168	536	421	274	671	347	661	331
10-15	**3**	187	619	651	329	645	407	690	457
15-20	**4**	256	536	422	595	536	401	592	384

	Vertical Acceleration (mm/s^2)								
	Location (m)	0 to 6	6 to 12	12 to 18	18 to 24	24 to 30	30 to 36	36 to 40	42 to 50
Time (sec)	**Moving Person Region**	**1**	**2**	**3**	**4**	**5**	**6**	**7**	**8**
0-5	**1**	1372	1150	917	582	703	382	695	474
5-10	**2**	1124	7488	2277	2123	969	626	643	437
10-15	**3**	675	3063	4110	2940	1418	1212	998	705
15-20	**4**	503	2119	2452	3906	1700	1336	1127	506

Table A.16: Time History Results for 50-7.5-V-L

	Vertical Velocity (mm/s)								
	Location (m)	0 to 6	6 to 12	12 to 18	18 to 24	24 to 30	30 to 36	36 to 42	42 to 50
Time (sec)	**Moving Person Region**	**1**	**2**	**3**	**4**	**5**	**6**	**7**	**8**
0-5	**1**	53	47	55	30	55	27	49	33
5-10	**2**	50	387	124	107	65	65	47	33
10-15	**3**	40	94	156	146	79	92	67	60
15-20	**4**	40	76	108	191	102	81	67	40

	Lateral Acceleration (mm/s^2)								
	Location (m)	0 to 6	6 to 12	12 to 18	18 to 24	24 to 30	30 to 36	36 to 40	42 to 50
Time (sec)	**Moving Person Region**	**1**	**2**	**3**	**4**	**5**	**6**	**7**	**8**
0-5	**1**	108	270	248	164	260	94	303	185
5-10	**2**	202	617	549	264	417	187	542	282
10-15	**3**	246	778	658	369	475	222	596	382
15-20	**4**	224	746	355	336	213	221	437	213

	Vertical Acceleration (mm/s^2)								
	Location (m)	0 to 6	6 to 12	12 to 18	18 to 24	24 to 30	30 to 36	36 to 40	42 to 50
Time (sec)	**Moving Person Region**	**1**	**2**	**3**	**4**	**5**	**6**	**7**	**8**
0-5	**1**	1236	1234	918	683	792	410	708	467
5-10	**2**	1093	7337	2410	1992	920	830	705	463
10-15	**3**	646	3183	3984	2680	1506	1405	1075	744
15-20	**4**	579	1600	1993	5369	1544	1159	932	512

Table A.17: Time History Results for 60-5-N-N

	Vertical Velocity (mm/s)										
	Location (m)	0 to 6	6 to 12	12 to 18	18 to 24	24 to 30	30 to 36	36 tp 42	42 to 48	48 to 54	54 to 60
Time (sec)	**Moving Person Region**	**1**	**2**	**3**	**4**	**5**	**6**	**7**	**8**	**9**	**10**
0-5	**1**	69	106	112	110	79	98	90	131	130	150
5-10	**2**	184	197	108	76	76	86	98	134	152	163
10-15	**3**	146	139	178	131	106	102	96	93	81	89
15-20	**4**	93	127	114	170	129	132	124	145	141	178
20-25	**5**	144	132	136	126	146	132	80	86	78	95

	Lateral Acceleration (mm/s^2)										
	Location (m)	0 to 6	6 to 12	12 to 18	18 to 24	24 to 30	30 to 36	36 tp 42	42 to 48	48 to 54	54 to 60
Time (sec)	**Moving Person Region**	**1**	**2**	**3**	**4**	**5**	**6**	**7**	**8**	**9**	**10**
0-5	**1**	146	339	263	310	197	205	177	193	152	62
5-10	**2**	189	375	667	442	347	250	404	436	299	138
10-15	**3**	193	489	776	666	454	416	562	588	432	201
15-20	**4**	177	393	452	429	378	543	726	571	448	159
20-25	**5**	121	249	403	248	456	598	581	537	273	146

	Vertical Acceleration (mm/s^2)										
	Location (m)	0 to 6	6 to 12	12 to 18	18 to 24	24 to 30	30 to 36	36 tp 42	42 to 48	48 to 54	54 to 60
Time (sec)	**Moving Person Region**	**1**	**2**	**3**	**4**	**5**	**6**	**7**	**8**	**9**	**10**
0-5	**1**	1784	3066	2322	2386	1494	1709	1500	1838	2021	2042
5-10	**2**	3484	5042	2404	1536	1757	1699	1586	2127	2394	2322
10-15	**3**	3328	4224	5033	3785	3192	1937	2170	2048	1452	1629
15-20	**4**	1430	2466	2350	4414	3271	3008	2441	2647	2337	2769
20-25	**5**	2286	2510	3005	2443	4676	2896	2111	1837	1805	1701

Table A.18: Time History Results for 60-5-N-L

	Vertical Velocity (mm/s)										
	Location (m)	0 to 6	6 to 12	12 to 18	18 to 24	24 to 30	30 to 36	36 to 42	42 to 48	48 to 54	54 to 60
Time (sec)	**Moving Person Region**	**1**	**2**	**3**	**4**	**5**	**6**	**7**	**8**	**9**	**10**
0-5	**1**	68	104	113	107	76	96	83	128	124	142
5-10	**2**	176	212	82	69	71	77	102	133	151	159
10-15	**3**	179	181	192	126	110	92	98	120	101	109
15-20	**4**	84	114	105	170	117	101	114	110	112	125
20-25	**5**	112	126	120	102	175	158	93	89	107	113

	Lateral Acceleration (mm/s^2)										
	Location (m)	0 to 6	6 to 12	12 to 18	18 to 24	24 to 30	30 to 36	36 to 40	42 to 48	48 to 54	54 to 60
Time (sec)	**Moving Person Region**	**1**	**2**	**3**	**4**	**5**	**6**	**7**	**8**	**9**	**10**
0-5	**1**	129	233	157	255	85	167	194	118	212	100
5-10	**2**	205	361	297	334	119	216	223	318	346	152
10-15	**3**	178	393	376	336	189	294	359	334	283	133
15-20	**4**	203	383	317	327	190	259	351	269	295	123
20-25	**5**	157	325	193	195	205	135	208	172	261	138

	Vertical Acceleration (mm/s^2)										
	Location (m)	0 to 6	6 to 12	12 to 18	18 to 24	24 to 30	30 to 36	36 to 40	42 to 48	48 to 54	54 to 60
Time (sec)	**Moving Person Region**	**1**	**2**	**3**	**4**	**5**	**6**	**7**	**8**	**9**	**10**
0-5	**1**	1791	3023	2361	2364	1432	1582	1409	1871	1963	2004
5-10	**2**	4173	4805	3087	1550	1762	1541	1679	2110	2356	2186
10-15	**3**	3483	5271	5643	2670	2360	1728	2182	2076	1853	1643
15-20	**4**	1206	2490	2589	5984	2448	2168	2398	1974	1979	1988
20-25	**5**	1905	2349	2806	2013	5265	3439	2236	2196	2189	1812

Table A.19: Time History Results for 60-5-V-N

	Vertical Velocity (mm/s)										
	Location (m)	0 to 6	6 to 12	12 to 18	18 to 24	24 to 30	30 to 36	36 to 42	42 to 48	48 to 54	54 to 60
Time (sec)	**Moving Person Region**	**1**	**2**	**3**	**4**	**5**	**6**	**7**	**8**	**9**	**10**
0-5	**1**	47	32	29	29	19	7	24	30	7	10
5-10	**2**	39	42	62	56	29	20	25	26	11	8
10-15	**3**	28	44	188	174	69	42	94	93	16	29
15-20	**4**	30	16	149	184	73	27	104	111	14	26
20-25	**5**	30	18	97	120	69	35	78	95	16	21

	Lateral Acceleration (mm/s^2)										
	Location (m)	0 to 6	6 to 12	12 to 18	18 to 24	24 to 30	30 to 36	36 to 40	42 to 48	48 to 54	54 to 60
Time (sec)	**Moving Person Region**	**1**	**2**	**3**	**4**	**5**	**6**	**7**	**8**	**9**	**10**
0-5	**1**	124	177	182	237	119	143	158	163	201	90
5-10	**2**	115	228	313	265	211	134	254	241	204	91
10-15	**3**	135	323	488	369	324	391	433	387	375	182
15-20	**4**	167	307	439	448	335	456	612	496	411	189
20-25	**5**	132	185	379	297	509	591	533	512	226	131

	Vertical Acceleration (mm/s^2)										
	Location (m)	0 to 6	6 to 12	12 to 18	18 to 24	24 to 30	30 to 36	36 to 40	42 to 48	48 to 54	54 to 60
Time (sec)	**Moving Person Region**	**1**	**2**	**3**	**4**	**5**	**6**	**7**	**8**	**9**	**10**
0-5	**1**	1474	546	504	432	291	80	339	412	103	156
5-10	**2**	1093	1676	1456	1455	338	217	300	377	124	93
10-15	**3**	706	2138	7143	3777	1820	1300	1416	1355	277	444
15-20	**4**	540	686	3150	6105	2484	1347	1570	1689	313	365
20-25	**5**	418	415	2434	2725	2938	1201	1491	1712	234	262

Table A.20: Time History Results for 60-5-V-L

	Vertical Velocity (mm/s)										
	Location (m)	0 to 6	6 to 12	12 to 18	18 to 24	24 to 30	30 to 36	36 to 42	42 to 48	48 to 54	54 to 60
Time (sec)	**Moving Person Region**	**1**	**2**	**3**	**4**	**5**	**6**	**7**	**8**	**9**	**10**
0-5	**1**	46	32	28	29	20	7	25	31	7	11
5-10	**2**	40	42	62	54	29	21	26	27	11	8
10-15	**3**	29	45	188	169	68	46	99	98	17	31
15-20	**4**	30	16	146	181	71	25	103	111	14	26
20-25	**5**	30	20	96	113	65	34	82	96	15	21

	Lateral Acceleration (mm/s^2)										
	Location (m)	0 to 6	6 to 12	12 to 18	18 to 24	24 to 30	30 to 36	36 to 40	42 to 48	48 to 54	54 to 60
Time (sec)	**Moving Person Region**	**1**	**2**	**3**	**4**	**5**	**6**	**7**	**8**	**9**	**10**
0-5	**1**	108	154	145	223	80	151	190	122	215	101
5-10	**2**	93	195	270	266	104	186	229	207	231	101
10-15	**3**	109	218	372	371	141	200	301	192	249	128
15-20	**4**	131	251	386	291	163	234	318	190	272	140
20-25	**5**	91	158	219	171	124	156	178	155	216	123

	Vertical Acceleration (mm/s^2)										
	Location (m)	0 to 6	6 to 12	12 to 18	18 to 24	24 to 30	30 to 36	36 to 40	42 to 48	48 to 54	54 to 60
Time (sec)	**Moving Person Region**	**1**	**2**	**3**	**4**	**5**	**6**	**7**	**8**	**9**	**10**
0-5	**1**	1468	542	487	415	299	79	351	428	102	158
5-10	**2**	1088	1681	1463	1426	347	240	310	391	121	95
10-15	**3**	719	2142	7227	3832	1983	1346	1427	1457	336	458
15-20	**4**	560	785	3135	6180	2462	1453	1547	1717	317	365
20-25	**5**	424	450	2467	2760	3140	1183	1407	1777	278	266

Table A.21: Time History Results for 60-7.5-N-N

	Vertical Velocity (mm/s)										
	Location (m)	0 to 6	6 to 12	12 to 18	18 to 24	24 to 30	30 to 36	36 to 42	42 to 48	48 to 54	54 to 60
Time (sec)	**Moving Person Region**	**1**	**2**	**3**	**4**	**5**	**6**	**7**	**8**	**9**	**10**
0-5	**1**	88	137	152	79	103	129	78	151	80	164
5-10	**2**	141	246	172	155	240	256	134	207	236	265
10-15	**3**	323	259	325	119	305	351	184	287	216	324
15-20	**4**	357	318	377	334	338	313	173	332	346	422
20-25	**5**	308	308	270	227	378	386	171	247	254	294

	Lateral Acceleration (mm/s^2)										
	Location (m)	0 to 6	6 to 12	12 to 18	18 to 24	24 to 30	30 to 36	36 to 40	42 to 48	48 to 54	54 to 60
Time (sec)	**Moving Person Region**	**1**	**2**	**3**	**4**	**5**	**6**	**7**	**8**	**9**	**10**
0-5	**1**	107	179	237	258	189	180	219	217	221	86
5-10	**2**	150	383	502	420	288	259	284	388	263	122
10-15	**3**	114	307	533	542	428	495	520	474	350	174
15-20	**4**	141	329	470	614	433	558	647	543	308	133
20-25	**5**	128	336	466	425	708	815	723	562	221	105

	Vertical Acceleration (mm/s^2)										
	Location (m)	0 to 6	6 to 12	12 to 18	18 to 24	24 to 30	30 to 36	36 to 40	42 to 48	48 to 54	54 to 60
Time (sec)	**Moving Person Region**	**1**	**2**	**3**	**4**	**5**	**6**	**7**	**8**	**9**	**10**
0-5	**1**	2218	2724	2087	1378	1365	1958	1117	2020	1136	2214
5-10	**2**	2845	3598	2557	3302	3825	4145	1836	3059	3740	3817
10-15	**3**	4887	4087	6186	2247	5175	5619	3610	3966	3742	4795
15-20	**4**	5865	4786	5633	8243	6140	4800	2759	5179	5501	6320
20-25	**5**	5044	5267	4744	5919	9647	5731	3914	4111	3902	4249

Table A.22: Time History Results for 60-7.5-N-L

	Vertical Velocity (mm/s)										
	Location (m)	0 to 6	6 to 12	12 to 18	18 to 24	24 to 30	30 to 36	36 to 42	42 to 48	48 to 54	54 to 60
Time (sec)	**Moving Person Region**	**1**	**2**	**3**	**4**	**5**	**6**	**7**	**8**	**9**	**10**
0-5	**1**	93	150	161	81	108	126	81	148	81	158
5-10	**2**	161	240	179	158	254	245	153	211	242	271
10-15	**3**	287	269	334	156	278	365	190	301	240	328
15-20	**4**	328	378	345	374	388	302	153	331	366	387
20-25	**5**	232	309	246	236	275	294	166	191	196	126

	Lateral Acceleration (mm/s^2)										
	Location (m)	0 to 6	6 to 12	12 to 18	18 to 24	24 to 30	30 to 36	36 to 40	42 to 48	48 to 54	54 to 60
Time (sec)	**Moving Person Region**	**1**	**2**	**3**	**4**	**5**	**6**	**7**	**8**	**9**	**10**
0-5	**1**	94	155	157	188	99	118	198	116	180	88
5-10	**2**	165	301	406	372	255	215	261	201	247	114
10-15	**3**	198	327	705	485	320	294	265	318	243	157
15-20	**4**	122	228	464	371	277	219	290	318	286	113
20-25	**5**	56	158	239	250	199	213	186	221	228	101

	Vertical Acceleration (mm/s^2)										
	Location (m)	0 to 6	6 to 12	12 to 18	18 to 24	24 to 30	30 to 36	36 to 40	42 to 48	48 to 54	54 to 60
Time (sec)	**Moving Person Region**	**1**	**2**	**3**	**4**	**5**	**6**	**7**	**8**	**9**	**10**
0-5	**1**	2109	2367	2657	1470	1819	1721	1132	1865	1220	2055
5-10	**2**	3067	4348	2581	3494	4129	3783	2152	3064	3571	3908
10-15	**3**	4748	4087	5866	2543	4035	5345	3379	4572	4373	4690
15-20	**4**	5091	5960	4786	9708	9017	4996	2225	5052	6293	6059
20-25	**5**	3346	4879	4157	5749	6898	6386	3849	4191	3201	2002

Table A.23: Time History Results for 60-7.5-V-N

	Vertical Velocity (mm/s)										
	Location (m)	0 to 6	6 to 12	12 to 18	18 to 24	24 to 30	30 to 36	36 to 42	42 to 48	48 to 54	54 to 60
Time (sec)	**Moving Person Region**	**1**	**2**	**3**	**4**	**5**	**6**	**7**	**8**	**9**	**10**
0-5	**1**	66	48	33	40	20	24	23	33	35	38
5-10	**2**	67	78	64	66	25	29	31	40	38	43
10-15	**3**	46	68	231	174	68	32	52	43	39	43
15-20	**4**	33	28	165	240	73	42	51	61	22	27
20-25	**5**	34	25	115	86	142	52	53	48	32	35

	Lateral Acceleration (mm/s^2)										
	Location (m)	0 to 6	6 to 12	12 to 18	18 to 24	24 to 30	30 to 36	36 to 40	42 to 48	48 to 54	54 to 60
Time (sec)	**Moving Person Region**	**1**	**2**	**3**	**4**	**5**	**6**	**7**	**8**	**9**	**10**
0-5	**1**	129	190	154	244	120	132	141	189	117	59
5-10	**2**	126	196	300	268	122	190	185	236	180	88
10-15	**3**	129	276	521	507	370	366	441	471	347	201
15-20	**4**	189	411	697	612	551	819	758	655	364	145
20-25	**5**	136	199	445	578	784	792	704	591	222	148

	Vertical Acceleration (mm/s^2)										
	Location (m)	0 to 6	6 to 12	12 to 18	18 to 24	24 to 30	30 to 36	36 to 40	42 to 48	48 to 54	54 to 60
Time (sec)	**Moving Person Region**	**1**	**2**	**3**	**4**	**5**	**6**	**7**	**8**	**9**	**10**
0-5	**1**	1584	999	581	746	348	336	431	527	450	522
5-10	**2**	1249	1834	1385	1105	401	456	531	726	535	575
10-15	**3**	1006	1743	5633	2741	1773	575	687	593	539	540
15-20	**4**	586	798	3360	3798	3010	1608	1239	934	389	337
20-25	**5**	540	493	2581	1666	3514	1707	1035	1135	641	524

Table A.24: Time History Results for 60-7.5-V-L

	Vertical Velocity (mm/s)										
	Location (m)	0 to 6	6 to 12	12 to 18	18 to 24	24 to 30	30 to 36	36 to 42	42 to 48	48 to 54	54 to 60
Time (sec)	**Moving Person Region**	**1**	**2**	**3**	**4**	**5**	**6**	**7**	**8**	**9**	**10**
0-5	**1**	66	48	35	43	20	23	28	35	37	41
5-10	**2**	70	83	56	69	25	33	33	43	40	45
10-15	**3**	45	72	232	177	70	35	53	40	39	44
15-20	**4**	32	33	176	258	84	54	51	57	25	29
20-25	**5**	37	26	110	120	147	51	51	45	29	35

	Lateral Acceleration (mm/s^2)										
	Location (m)	0 to 6	6 to 12	12 to 18	18 to 24	24 to 30	30 to 36	36 to 40	42 to 48	48 to 54	54 to 60
Time (sec)	**Moving Person Region**	**1**	**2**	**3**	**4**	**5**	**6**	**7**	**8**	**9**	**10**
0-5	**1**	108	143	195	205	90	152	141	125	171	69
5-10	**2**	98	203	273	267	94	176	244	147	226	103
10-15	**3**	167	341	656	617	178	357	262	200	270	147
15-20	**4**	240	443	747	682	255	280	325	239	338	153
20-25	**5**	160	187	312	389	184	220	211	218	196	143

	Vertical Acceleration (mm/s^2)										
	Location (m)	0 to 6	6 to 12	12 to 18	18 to 24	24 to 30	30 to 36	36 to 40	42 to 48	48 to 54	54 to 60
Time (sec)	**Moving Person Region**	**1**	**2**	**3**	**4**	**5**	**6**	**7**	**8**	**9**	**10**
0-5	**1**	1716	1043	658	795	333	388	514	599	486	529
5-10	**2**	1205	1733	1216	1213	408	521	521	789	579	614
10-15	**3**	1072	1831	5963	2677	1700	849	635	609	501	565
15-20	**4**	584	984	3739	4036	2816	1453	1203	967	375	383
20-25	**5**	605	481	2415	2480	3459	1310	755	691	488	509

Table A.25: Time History Results for 70-5-N-N

	Vertical Velocity (mm/s)												
	Location (m)	0 to 6	6 to 12	12 to 18	18 to 24	24 to 30	30 to 36	36 to 42	42 to 48	48 to 54	54 to 60	60 to 66	66 to 70
Time (sec)	**Moving Person Region**	**1**	**2**	**3**	**4**	**5**	**6**	**7**	**8**	**9**	**10**	**11**	**12**
0-5	**1**	63	104	91	93	90	104	127	116	141	74	37	57
5-10	**2**	169	95	96	163	188	206	174	159	178	116	53	66
10-15	**3**	200	133	212	162	192	193	190	244	243	181	57	101
15-20	**4**	189	134	101	173	161	209	171	168	173	121	48	90
20-25	**5**	142	92	67	58	157	79	65	87	89	69	27	39
25-29.1	**6**	129	76	47	87	125	251	155	149	135	106	47	77

	Lateral Acceleration (mm/s^2)												
	Location (m)	0 to 6	6 to 12	12 to 18	18 to 24	24 to 30	30 to 36	36 to 40	42 to 48	48 to 54	54 to 60	60 to 66	66 to 70
Time (sec)	**Moving Person Region**	**1**	**2**	**3**	**4**	**5**	**6**	**7**	**8**	**9**	**10**	**11**	**12**
0-5	**1**	94	206	361	238	225	192	235	289	198	288	227	36
5-10	**2**	137	285	422	313	370	195	259	318	286	435	376	56
10-15	**3**	215	444	510	391	308	438	234	402	327	307	310	54
15-20	**4**	212	483	344	546	373	429	239	379	408	351	307	51
20-25	**5**	238	447	252	412	374	268	375	198	401	331	307	48
25-29.1	**6**	252	507	272	401	356	429	371	208	512	342	317	54

	Vertical Acceleration (mm/s^2)												
	Location (m)	0 to 6	6 to 12	12 to 18	18 to 24	24 to 30	30 to 36	36 to 40	42 to 48	48 to 54	54 to 60	60 to 66	66 to 70
Time (sec)	**Moving Person Region**	**1**	**2**	**3**	**4**	**5**	**6**	**7**	**8**	**9**	**10**	**11**	**12**
0-5	**1**	1896	1839	1550	1384	1459	1725	2085	1741	1726	1096	457	847
5-10	**2**	2776	2323	1637	2301	3019	3044	2341	2497	2500	1900	793	1103
10-15	**3**	2952	3006	6647	3135	2711	3144	2825	3652	3423	2391	843	1412
15-20	**4**	2656	2507	1888	5613	2854	3291	2357	2490	2580	1762	760	1391
20-25	**5**	1945	1592	1253	1469	6349	2084	1031	1432	1453	1046	506	720
25-29.1	**6**	1784	1348	1190	1656	2171	8944	2712	2332	2381	1659	795	1263

Table A.26: Time History Results for 70-5-N-L

	Vertical Velocity (mm/s)												
	Location (m)	0 to 6	6 to 12	12 to 18	18 to 24	24 to 30	30 to 36	36 to 42	42 to 48	48 to 54	54 to 60	60 to 66	66 to 70
Time (sec)	**Moving Person Region**	**1**	**2**	**3**	**4**	**5**	**6**	**7**	**8**	**9**	**10**	**11**	**12**
0-5	**1**	67	105	93	96	87	90	114	125	134	76	35	46
5-10	**2**	180	103	111	153	190	194	181	136	170	129	63	62
10-15	**3**	221	133	238	168	227	225	190	251	255	195	67	103
15-20	**4**	216	146	93	190	184	245	193	223	221	162	59	104
20-25	**5**	166	127	76	55	179	144	122	91	94	76	38	47
25-29.1	**6**	103	64	54	74	107	178	117	126	113	92	46	50

	Lateral Acceleration (mm/s^2)												
	Location (m)	0 to 6	6 to 12	12 to 18	18 to 24	24 to 30	30 to 36	36 to 40	42 to 48	48 to 54	54 to 60	60 to 66	66 to 70
Time (sec)	**Moving Person Region**	**1**	**2**	**3**	**4**	**5**	**6**	**7**	**8**	**9**	**10**	**11**	**12**
0-5	**1**	92	143	201	221	244	100	162	307	269	218	232	35
5-10	**2**	120	214	339	413	299	214	205	487	633	457	481	73
10-15	**3**	153	321	448	806	265	248	207	312	562	311	242	34
15-20	**4**	142	339	698	1091	314	266	222	522	904	341	279	47
20-25	**5**	145	288	424	722	349	202	213	391	815	328	243	37
25-29.1	**6**	110	214	323	509	175	204	202	360	735	277	314	53

	Vertical Acceleration (mm/s^2)												
	Location (m)	0 to 6	6 to 12	12 to 18	18 to 24	24 to 30	30 to 36	36 to 40	42 to 48	48 to 54	54 to 60	60 to 66	66 to 70
Time (sec)	**Moving Person Region**	**1**	**2**	**3**	**4**	**5**	**6**	**7**	**8**	**9**	**10**	**11**	**12**
0-5	**1**	1590	1853	1708	1527	1603	1570	1810	1542	1762	1197	454	713
5-10	**2**	2806	2225	2036	2227	3065	2825	2834	2377	2363	1716	926	1099
10-15	**3**	2799	2883	6325	3116	2997	3246	3005	3798	3393	2583	905	1450
15-20	**4**	2963	2525	1707	5878	3118	3493	2778	3403	2917	2293	953	1423
20-25	**5**	2328	2181	1576	1881	6113	2386	1914	1665	1443	1109	653	809
25-29.1	**6**	1532	1163	1295	1214	2137	7923	1853	1930	1793	1351	752	725

Table A.27: Time History Results for 70-5-V-N

	Vertical Velocity (mm/s)												
	Location (m)	0 to 6	6 to 12	12 to 18	18 to 24	24 to 30	30 to 36	36 to 42	42 to 48	48 to 54	54 to 60	60 to 66	66 to 70
Time (sec)	**Moving Person Region**	**1**	**2**	**3**	**4**	**5**	**6**	**7**	**8**	**9**	**10**	**11**	**12**
0-5	**1**	67	105	93	96	87	90	114	125	134	76	35	46
5-10	**2**	180	103	111	153	190	194	181	136	170	129	63	62
10-15	**3**	221	133	238	168	227	225	190	251	255	195	67	103
15-20	**4**	216	146	93	190	184	245	193	223	221	162	59	104
20-25	**5**	166	127	76	55	179	144	122	91	94	76	38	47
25-29.1	**6**	103	64	54	74	107	178	117	126	113	92	46	50

	Lateral Acceleration (mm/s^2)												
	Location (m)	0 to 6	6 to 12	12 to 18	18 to 24	24 to 30	30 to 36	36 to 40	42 to 48	48 to 54	54 to 60	60 to 66	66 to 70
Time (sec)	**Moving Person Region**	**1**	**2**	**3**	**4**	**5**	**6**	**7**	**8**	**9**	**10**	**11**	**12**
0-5	**1**	85	110	166	210	179	130	132	128	261	205	166	25
5-10	**2**	64	160	178	232	194	143	159	146	297	221	176	26
10-15	**3**	139	247	481	371	325	396	171	450	362	327	203	42
15-20	**4**	122	309	365	493	345	439	219	523	493	364	285	45
20-25	**5**	136	323	313	446	416	338	208	259	457	248	265	43
25-29.1	**6**	112	194	397	435	391	442	258	260	351	243	223	32

	Vertical Acceleration (mm/s^2)												
	Location (m)	0 to 6	6 to 12	12 to 18	18 to 24	24 to 30	30 to 36	36 to 40	42 to 48	48 to 54	54 to 60	60 to 66	66 to 70
Time (sec)	**Moving Person Region**	**1**	**2**	**3**	**4**	**5**	**6**	**7**	**8**	**9**	**10**	**11**	**12**
0-5	**1**	1497	887	390	234	296	233	125	315	224	89	102	41
5-10	**2**	685	1543	758	321	390	256	117	382	269	101	123	54
10-15	**3**	598	1430	4590	2257	1787	1121	676	720	632	256	187	111
15-20	**4**	533	417	1739	5805	1751	1206	804	1127	851	362	220	147
20-25	**5**	344	421	1673	999	5167	1521	926	1304	946	344	307	177
25-29.1	**6**	435	322	1015	730	1573	5998	1875	1144	746	271	196	134

Table A.28: Time History Results for 70-5-V-L

	Vertical Velocity (mm/s)												
	Location (m)	0 to 6	6 to 12	12 to 18	18 to 24	24 to 30	30 to 36	36 to 42	42 to 48	48 to 54	54 to 60	60 to 66	66 to 70
Time (sec)	**Moving Person Region**	**1**	**2**	**3**	**4**	**5**	**6**	**7**	**8**	**9**	**10**	**11**	**12**
0-5	**1**	45	48	24	16	19	17	10	25	17	7	8	3
5-10	**2**	31	48	33	16	22	17	9	29	21	6	10	3
10-15	**3**	28	48	151	86	88	65	44	63	44	20	13	8
15-20	**4**	20	21	67	132	82	71	45	79	61	24	18	9
20-25	**5**	21	19	63	38	164	68	42	80	61	23	21	9
25-29.1	**6**	27	15	40	30	50	147	41	64	42	17	14	7

	Lateral Acceleration (mm/s^2)												
	Location (m)	0 to 6	6 to 12	12 to 18	18 to 24	24 to 30	30 to 36	36 to 40	42 to 48	48 to 54	54 to 60	60 to 66	66 to 70
Time (sec)	**Moving Person Region**	**1**	**2**	**3**	**4**	**5**	**6**	**7**	**8**	**9**	**10**	**11**	**12**
0-5	**1**	95	94	129	221	150	125	95	306	357	222	154	25
5-10	**2**	89	231	266	531	306	160	171	425	590	306	244	36
10-15	**3**	155	310	494	659	315	196	197	403	580	359	277	50
15-20	**4**	213	416	596	854	390	386	277	639	1145	374	438	72
20-25	**5**	226	446	469	669	586	322	261	645	1104	351	412	65
25-29.1	**6**	117	329	328	545	275	379	189	386	670	310	241	43

	Vertical Acceleration (mm/s^2)												
	Location (m)	0 to 6	6 to 12	12 to 18	18 to 24	24 to 30	30 to 36	36 to 40	42 to 48	48 to 54	54 to 60	60 to 66	66 to 70
Time (sec)	**Moving Person Region**	**1**	**2**	**3**	**4**	**5**	**6**	**7**	**8**	**9**	**10**	**11**	**12**
0-5	**1**	1564	870	388	242	298	226	135	348	251	82	107	40
5-10	**2**	709	1548	761	315	392	252	125	398	287	88	129	57
10-15	**3**	612	1448	4521	2267	1771	1201	743	825	633	314	208	119
15-20	**4**	545	416	1697	5777	1886	1162	857	1143	858	393	240	142
20-25	**5**	314	382	1676	976	5204	1452	979	1200	911	345	292	169
25-29.1	**6**	439	287	1081	792	1710	5800	1931	800	710	237	202	151

Table A.29: Time History Results for 70-7.5-N-N

		Vertical Velocity (mm/s)											
	Location (m)	0 to 6	6 to 12	12 to 18	18 to 24	24 to 30	30 to 36	36 to 42	42 to 48	48 to 54	54 to 60	60 to 66	66 to 70
Time (sec)	**Moving Person Region**	**1**	**2**	**3**	**4**	**5**	**6**	**7**	**8**	**9**	**10**	**11**	**12**
0-5	**1**	83	94	119	96	120	108	130	121	149	124	111	59
5-10	**2**	149	158	189	156	120	101	134	161	166	113	106	68
10-15	**3**	206	167	281	260	226	134	159	229	200	178	83	99
15-20	**4**	205	173	218	224	231	97	219	246	243	200	128	107
20-25	**5**	166	147	166	121	187	140	87	130	129	134	79	86
25-29.1	**6**	114	132	138	121	135	249	133	132	191	130	98	58

		Lateral Acceleration (mm/s^2)											
	Location (m)	0 to 6	6 to 12	12 to 18	18 to 24	24 to 30	30 to 36	36 to 40	42 to 48	48 to 54	54 to 60	60 to 66	66 to 70
Time (sec)	**Moving Person Region**	**1**	**2**	**3**	**4**	**5**	**6**	**7**	**8**	**9**	**10**	**11**	**12**
0-5	**1**	109	195	182	226	132	176	82	246	193	200	190	28
5-10	**2**	152	340	282	270	306	170	206	272	274	289	258	39
10-15	**3**	172	331	401	416	344	402	204	356	460	371	248	39
15-20	**4**	187	414	466	575	382	421	241	394	560	396	291	38
20-25	**5**	180	387	467	499	376	348	404	299	548	449	295	47
25-29.1	**6**	168	360	262	425	362	492	396	316	500	291	191	41

		Vertical Acceleration (mm/s^2)											
	Location (m)	0 to 6	6 to 12	12 to 18	18 to 24	24 to 30	30 to 36	36 to 40	42 to 48	48 to 54	54 to 60	60 to 66	66 to 70
Time (sec)	**Moving Person Region**	**1**	**2**	**3**	**4**	**5**	**6**	**7**	**8**	**9**	**10**	**11**	**12**
0-5	**1**	1645	1687	2786	1460	1918	1401	1639	1627	2061	1897	1593	874
5-10	**2**	2286	2937	3818	2544	1654	1704	1961	2287	2525	1664	1546	1068
10-15	**3**	3103	3023	5607	4346	3144	2113	2623	3647	3436	2751	1297	1387
15-20	**4**	2828	2974	3395	4504	3600	1668	3652	3758	3556	2971	1731	1701
20-25	**5**	2569	2551	2603	2217	3694	2092	1558	1982	2373	2166	1360	1362
25-29.1	**6**	1803	2323	2253	2090	2942	5610	2284	1932	3046	1863	1539	1210

Table A.30: Time History Results for 70-7.5-N-L

	Vertical Velocity (mm/s)											
	Location (m)	0 to 6	6 to 12	12 to 18	18 to 24	24 to 30	30 to 36	36 to 42	42 to 48	48 to 54	54 to 60	60 to 66	66 to 70
Time (sec)	**Moving Person Region**	**1**	**2**	**3**	**4**	**5**	**6**	**7**	**8**	**9**	**10**	**11**	**12**
0-5	**1**	107	95	120	112	121	111	137	113	148	98	108	50
5-10	**2**	146	93	181	170	116	131	151	138	148	94	78	59
10-15	**3**	151	126	273	193	139	113	144	247	211	167	94	107
15-20	**4**	181	170	211	252	147	84	181	223	210	181	97	103
20-25	**5**	218	220	278	181	269	111	156	206	222	181	112	100
25-29.1	**6**	165	163	201	147	155	214	172	145	133	112	107	63

	Lateral Acceleration (mm/s^2)											
	Location (m)	0 to 6	6 to 12	12 to 18	18 to 24	24 to 30	30 to 36	36 to 40	42 to 48	48 to 54	54 to 60	60 to 66	66 to 70
Time (sec)	**Moving Person Region**	**1**	**2**	**3**	**4**	**5**	**6**	**7**	**8**	**9**	**10**	**11**	**12**
0-5	**1**	80	104	227	180	231	124	130	253	215	200	222	35
5-10	**2**	112	269	463	634	306	177	157	480	675	394	379	62
10-15	**3**	219	497	502	920	448	299	254	490	700	429	301	46
15-20	**4**	222	539	907	1474	516	374	252	450	720	403	283	45
20-25	**5**	212	436	853	1128	499	315	260	449	657	486	334	52
25-29.1	**6**	152	302	508	710	238	404	180	432	682	335	253	39

	Vertical Acceleration (mm/s^2)											
	Location (m)	0 to 6	6 to 12	12 to 18	18 to 24	24 to 30	30 to 36	36 to 40	42 to 48	48 to 54	54 to 60	60 to 66	66 to 70
Time (sec)	**Moving Person Region**	**1**	**2**	**3**	**4**	**5**	**6**	**7**	**8**	**9**	**10**	**11**	**12**
0-5	**1**	1775	2082	1944	1621	2081	1610	1959	1603	2156	1482	1588	816
5-10	**2**	2434	1904	3871	3114	1739	2120	2367	2166	2042	1504	1111	935
10-15	**3**	2347	2808	4633	3032	2269	1928	2511	3805	3275	2303	1504	1587
15-20	**4**	2979	3050	3888	4587	2611	1381	3061	3461	3169	2787	1492	1633
20-25	**5**	3344	3434	4175	3154	4634	1761	2468	3155	3833	2711	1719	1711
25-29.1	**6**	2484	2570	2962	2619	2552	5126	2916	2093	2141	2143	1639	1433

Table A.31: Time History Results for 70-7.5-V-N

	Vertical Velocity (mm/s)												
	Location (m)	0 to 6	6 to 12	12 to 18	18 to 24	24 to 30	30 to 36	36 to 42	42 to 48	48 to 54	54 to 60	60 to 66	66 to 70
Time (sec)	**Moving Person Region**	**1**	**2**	**3**	**4**	**5**	**6**	**7**	**8**	**9**	**10**	**11**	**12**
0-5	**1**	42	57	28	34	26	25	15	9	11	12	13	2
5-10	**2**	37	69	43	39	36	33	16	15	10	10	13	3
10-15	**3**	31	89	194	147	130	92	26	59	25	16	13	6
15-20	**4**	18	29	152	174	133	109	31	79	33	21	18	9
20-25	**5**	24	35	174	139	208	117	30	65	34	20	20	9
25-29.1	**6**	30	26	110	113	168	215	44	90	43	30	20	10

	Lateral Acceleration (mm/s^2)												
	Location (m)	0 to 6	6 to 12	12 to 18	18 to 24	24 to 30	30 to 36	36 to 40	42 to 48	48 to 54	54 to 60	60 to 66	66 to 70
Time (sec)	**Moving Person Region**	**1**	**2**	**3**	**4**	**5**	**6**	**7**	**8**	**9**	**10**	**11**	**12**
0-5	**1**	82	74	142	186	147	110	105	157	244	135	97	15
5-10	**2**	65	191	257	295	247	120	176	230	367	239	143	19
10-15	**3**	200	406	510	529	369	341	230	516	474	334	258	43
15-20	**4**	181	422	488	624	501	450	245	634	760	416	354	55
20-25	**5**	186	424	476	555	493	332	261	364	719	434	252	43
25-29.1	**6**	192	396	432	601	414	494	478	296	432	328	216	43

	Vertical Acceleration (mm/s^2)												
	Location (m)	0 to 6	6 to 12	12 to 18	18 to 24	24 to 30	30 to 36	36 to 40	42 to 48	48 to 54	54 to 60	60 to 66	66 to 70
Time (sec)	**Moving Person Region**	**1**	**2**	**3**	**4**	**5**	**6**	**7**	**8**	**9**	**10**	**11**	**12**
0-5	**1**	1550	983	465	613	363	360	191	127	160	179	181	49
5-10	**2**	830	1595	688	596	538	606	275	216	191	147	186	62
10-15	**3**	792	2034	4692	2877	2527	1578	520	707	291	218	187	105
15-20	**4**	313	648	3615	4256	2886	2057	781	1085	706	363	260	182
20-25	**5**	405	807	3648	3005	5592	2198	765	1237	631	273	278	165
25-29.1	**6**	517	559	3195	2297	3485	4539	1257	1518	768	519	197	230

Table A.32: Time History Results for 70-7.5-V-L

	Vertical Velocity (mm/s)											
	Location (m)	0 to 6	6 to 12	12 to 18	18 to 24	24 to 30	30 to 36	36 to 42	42 to 48	48 to 54	54 to 60	60 to 66	66 to 70
Time (sec)	**Moving Person Region**	**1**	**2**	**3**	**4**	**5**	**6**	**7**	**8**	**9**	**10**	**11**	**12**
0-5	**1**	40	57	32	39	32	26	13	9	10	11	13	3
5-10	**2**	35	65	50	45	40	27	15	20	9	13	13	2
10-15	**3**	33	84	204	175	159	118	30	53	28	21	13	6
15-20	**4**	24	37	143	222	192	119	31	80	40	28	19	10
20-25	**5**	25	37	170	136	213	122	34	102	37	29	20	10
25-29.1	**6**	30	28	122	106	183	168	37	80	39	27	17	9

	Lateral Acceleration (mm/s^2)											
	Location (m)	0 to 6	6 to 12	12 to 18	18 to 24	24 to 30	30 to 36	36 to 40	42 to 48	48 to 54	54 to 60	60 to 66	66 to 70
Time (sec)	**Moving Person Region**	**1**	**2**	**3**	**4**	**5**	**6**	**7**	**8**	**9**	**10**	**11**	**12**
0-5	**1**	80	78	149	222	155	131	95	285	348	168	142	24
5-10	**2**	79	245	315	502	292	163	179	531	772	315	234	32
10-15	**3**	194	489	676	731	439	250	291	524	755	647	379	57
15-20	**4**	264	663	903	1181	730	545	461	943	1368	759	519	75
20-25	**5**	317	710	846	1074	771	429	398	1020	1249	771	477	69
25-29.1	**6**	198	558	950	912	576	339	353	670	977	751	512	70

	Vertical Acceleration (mm/s^2)											
	Location (m)	0 to 6	6 to 12	12 to 18	18 to 24	24 to 30	30 to 36	36 to 40	42 to 48	48 to 54	54 to 60	60 to 66	66 to 70
Time (sec)	**Moving Person Region**	**1**	**2**	**3**	**4**	**5**	**6**	**7**	**8**	**9**	**10**	**11**	**12**
0-5	**1**	1420	958	510	683	460	337	198	207	153	165	183	41
5-10	**2**	851	1599	829	618	668	425	246	340	152	202	177	51
10-15	**3**	738	2119	4263	3820	2928	2159	977	744	341	277	183	95
15-20	**4**	441	860	3612	4242	4114	2318	783	1468	706	536	282	215
20-25	**5**	500	774	3599	2781	6438	2911	999	1764	801	444	287	136
25-29.1	**6**	536	531	3263	2470	4344	4197	1230	1567	875	548	255	218

Table A.33: Time History Results for 80-5-N-N

	Vertical Velocity (mm/s)													
	Location (m)	0 to 6	6 to 12	12 to 18	18 to 24	24 to 30	30 to 36	36 to 42	42 to 48	48 to 54	54 to 60	60 to 66	66 to 72	72 to 78
Time (sec)	**Moving Person Region**	**1**	**2**	**3**	**4**	**5**	**6**	**7**	**8**	**9**	**10**	**11**	**12**	**13**
0-5	**1**	61	85	77	81	82	60	69	97	91	62	43	92	87
5-10	**2**	123	68	113	168	119	61	102	148	118	67	69	113	131
10-15	**3**	129	90	129	201	165	92	120	165	196	97	77	185	186
15-20	**4**	171	90	96	208	151	56	136	168	180	80	75	158	180
20-25	**5**	160	89	87	199	233	99	116	149	182	79	60	138	155
25-30	**6**	141	76	98	159	150	196	119	128	111	70	61	93	96

	Lateral Acceleration (mm/s^2)													
	Location (m)	0 to 6	6 to 12	12 to 18	18 to 24	24 to 30	30 to 36	36 to 40	42 to 48	48 to 54	54 to 60	60 to 66	66 to 72	72 to 78
Time (sec)	**Moving Person Region**	**1**	**2**	**3**	**4**	**5**	**6**	**7**	**8**	**9**	**10**	**11**	**12**	**13**
0-5	**1**	86	112	148	62	260	135	147	135	200	173	118	126	86
5-10	**2**	107	240	215	180	510	316	413	295	433	279	227	332	203
10-15	**3**	89	213	195	169	431	351	431	277	377	313	217	321	215
15-20	**4**	91	229	223	308	524	282	485	245	410	342	167	270	174
20-25	**5**	126	273	265	230	593	307	478	319	552	280	146	302	209
25-30	**6**	155	324	266	243	477	485	647	397	606	363	176	303	248

	Vertical Acceleration (mm/s^2)													
	Location (m)	0 to 6	6 to 12	12 to 18	18 to 24	24 to 30	30 to 36	36 to 40	42 to 48	48 to 54	54 to 60	60 to 66	66 to 72	72 to 78
Time (sec)	**Moving Person Region**	**1**	**2**	**3**	**4**	**5**	**6**	**7**	**8**	**9**	**10**	**11**	**12**	**13**
0-5	**1**	1407	1814	1055	1634	1434	1265	1083	1452	1510	1008	710	1516	1518
5-10	**2**	2090	1893	2130	3022	2154	1518	1667	2149	2171	1309	960	1579	2136
10-15	**3**	1995	1758	2009	3522	2302	1689	2186	2613	3297	1635	1577	2880	2879
15-20	**4**	2552	1781	2312	6255	3450	1382	2175	2529	2970	1210	1200	2400	2758
20-25	**5**	3023	1918	2018	4898	8642	4315	2786	2335	3029	1303	859	2097	2553
25-30	**6**	2137	1471	2008	2622	5082	8509	4722	3129	2508	1453	1201	1555	1548

Table A.34: Time History Results for 80-5-N-L

	Vertical Velocity (mm/s)													
	Location (m)	0 to 6	6 to 12	12 to 18	18 to 24	24 to 30	30 to 36	36 to 42	42 to 48	48 to 54	54 to 60	60 to 66	66 to 72	72 to 78
Time (sec)	**Moving Person Region**	**1**	**2**	**3**	**4**	**5**	**6**	**7**	**8**	**9**	**10**	**11**	**12**	**13**
0-5	**1**	61	85	78	81	84	60	67	93	91	64	41	86	86
5-10	**2**	104	67	112	154	110	59	99	123	128	77	72	111	132
10-15	**3**	111	81	122	189	155	86	99	150	179	81	69	157	174
15-20	**4**	155	79	93	211	150	49	128	164	168	70	75	155	164
20-25	**5**	146	82	86	185	225	99	115	155	171	81	63	146	157
25-30	**6**	153	75	102	161	156	192	116	147	127	81	67	117	116

	Lateral Acceleration (mm/s^2)													
	Location (m)	0 to 6	6 to 12	12 to 18	18 to 24	24 to 30	30 to 36	36 to 40	42 to 48	48 to 54	54 to 60	60 to 66	66 to 72	72 to 78
Time (sec)	**Moving Person Region**	**1**	**2**	**3**	**4**	**5**	**6**	**7**	**8**	**9**	**10**	**11**	**12**	**13**
0-5	**1**	89	147	115	85	240	100	175	67	97	149	66	131	109
5-10	**2**	117	248	182	159	332	141	244	105	197	188	132	167	111
10-15	**3**	85	209	242	188	266	210	266	137	242	247	177	269	157
15-20	**4**	110	256	258	273	397	205	297	138	237	272	178	220	140
20-25	**5**	96	199	241	228	952	185	253	141	238	331	187	240	222
25-30	**6**	122	242	180	156	811	250	306	217	240	205	112	177	134

	Vertical Acceleration (mm/s^2)													
	Location (m)	0 to 6	6 to 12	12 to 18	18 to 24	24 to 30	30 to 36	36 to 40	42 to 48	48 to 54	54 to 60	60 to 66	66 to 72	72 to 78
Time (sec)	**Moving Person Region**	**1**	**2**	**3**	**4**	**5**	**6**	**7**	**8**	**9**	**10**	**11**	**12**	**13**
0-5	**1**	1391	1814	1048	1647	1449	1226	1034	1370	1498	1030	651	1457	1452
5-10	**2**	1944	1775	2112	2836	1642	1201	1768	1788	1995	1302	1025	1623	1877
10-15	**3**	1715	1694	2017	3421	2273	1426	2002	2365	3093	1288	1146	2234	2897
15-20	**4**	2339	1771	2435	6172	3203	1147	2152	2570	2688	1304	1234	2316	2549
20-25	**5**	2755	1890	2065	4587	8424	3709	2526	2428	2804	1345	1005	2126	2465
25-30	**6**	2212	1346	1983	2768	4580	8378	4285	2541	2129	1471	1228	1830	1664

Table A.35: Time History Results for 80-5-V-N

	Vertical Velocity (mm/s)													
	Location (m)	0 to 6	6 to 12	12 to 18	18 to 24	24 to 30	30 to 36	36 to 42	42 to 48	48 to 54	54 to 60	60 to 66	66 to 72	72 to 78
Time (sec)	**Moving Person Region**	**1**	**2**	**3**	**4**	**5**	**6**	**7**	**8**	**9**	**10**	**11**	**12**	**13**
0-5	**1**	50	31	24	32	37	17	14	11	24	11	7	5	8
5-10	**2**	30	50	21	35	38	18	17	12	30	15	11	6	11
10-15	**3**	21	21	40	81	68	33	26	24	30	14	13	4	8
15-20	**4**	23	19	30	139	142	68	60	48	86	43	43	15	28
20-25	**5**	21	20	21	95	203	107	75	59	92	39	39	15	29
25-30	**6**	16	12	17	87	121	112	73	57	90	40	37	14	29

	Lateral Acceleration (mm/s^2)													
	Location (m)	0 to 6	6 to 12	12 to 18	18 to 24	24 to 30	30 to 36	36 to 40	42 to 48	48 to 54	54 to 60	60 to 66	66 to 72	72 to 78
Time (sec)	**Moving Person Region**	**1**	**2**	**3**	**4**	**5**	**6**	**7**	**8**	**9**	**10**	**11**	**12**	**13**
0-5	**1**	94	124	78	113	225	148	153	85	134	139	81	141	81
5-10	**2**	79	169	78	153	248	183	210	111	192	148	109	168	98
10-15	**3**	69	100	129	98	205	214	216	123	163	150	135	137	97
15-20	**4**	76	188	147	213	335	266	336	288	251	308	130	238	178
20-25	**5**	90	200	211	220	509	312	312	315	299	263	134	205	183
25-30	**6**	98	237	200	225	273	295	443	424	335	216	89	214	191

	Vertical Acceleration (mm/s^2)													
	Location (m)	0 to 6	6 to 12	12 to 18	18 to 24	24 to 30	30 to 36	36 to 40	42 to 48	48 to 54	54 to 60	60 to 66	66 to 72	72 to 78
Time (sec)	**Moving Person Region**	**1**	**2**	**3**	**4**	**5**	**6**	**7**	**8**	**9**	**10**	**11**	**12**	**13**
0-5	**1**	1571	596	339	584	479	236	207	135	307	162	93	68	101
5-10	**2**	873	1462	624	618	583	264	247	154	362	209	182	76	139
10-15	**3**	370	884	1046	1261	1031	615	367	321	399	201	210	47	114
15-20	**4**	674	776	1270	5734	3635	1110	1271	840	1141	665	717	230	411
20-25	**5**	699	849	1207	3654	9577	3172	1912	1321	1670	611	656	250	438
25-30	**6**	308	216	534	1734	4512	7265	2969	1816	1878	765	660	216	409

Table A.36: Time History Results for 80-5-V-L

	Vertical Velocity (mm/s)													
	Location (m)	0 to 6	6 to 12	12 to 18	18 to 24	24 to 30	30 to 36	36 to 42	42 to 48	48 to 54	54 to 60	60 to 66	66 to 72	72 to 78
Time (sec)	**Moving Person Region**	**1**	**2**	**3**	**4**	**5**	**6**	**7**	**8**	**9**	**10**	**11**	**12**	**13**
0-5	**1**	51	31	25	26	31	16	11	11	29	13	9	5	10
5-10	**2**	28	50	22	33	33	17	14	13	31	15	13	6	12
10-15	**3**	21	21	40	77	55	25	23	27	27	16	14	4	9
15-20	**4**	20	17	31	140	115	53	45	49	96	46	42	15	32
20-25	**5**	20	17	25	102	201	83	58	59	95	44	39	16	33
25-30	**6**	19	15	24	98	146	105	71	59	105	44	39	15	32

	Lateral Acceleration (mm/s^2)													
	Location (m)	0 to 6	6 to 12	12 to 18	18 to 24	24 to 30	30 to 36	36 to 40	42 to 48	48 to 54	54 to 60	60 to 66	66 to 72	72 to 78
Time (sec)	**Moving Person Region**	**1**	**2**	**3**	**4**	**5**	**6**	**7**	**8**	**9**	**10**	**11**	**12**	**13**
0-5	**1**	84	92	62	105	151	85	123	61	133	101	69	151	95
5-10	**2**	63	127	58	133	147	112	133	57	142	147	98	146	108
10-15	**3**	74	95	134	122	138	128	143	58	128	148	112	126	99
15-20	**4**	77	152	138	191	378	164	232	119	267	281	117	225	161
20-25	**5**	99	169	186	206	1027	154	221	107	269	236	123	215	191
25-30	**6**	104	155	133	169	662	213	137	113	174	257	90	191	188

	Vertical Acceleration (mm/s^2)													
	Location (m)	0 to 6	6 to 12	12 to 18	18 to 24	24 to 30	30 to 36	36 to 40	42 to 48	48 to 54	54 to 60	60 to 66	66 to 72	72 to 78
Time (sec)	**Moving Person Region**	**1**	**2**	**3**	**4**	**5**	**6**	**7**	**8**	**9**	**10**	**11**	**12**	**13**
0-5	**1**	1620	600	336	533	411	213	174	138	361	187	133	64	118
5-10	**2**	826	1488	628	576	542	251	202	173	420	202	192	71	156
10-15	**3**	372	893	1041	1261	896	506	332	425	413	209	194	47	121
15-20	**4**	770	869	1347	5857	2491	999	685	747	1393	621	676	229	459
20-25	**5**	730	737	1136	3409	10419	2586	1483	1396	1602	644	550	240	471
25-30	**6**	341	319	665	1900	3844	6804	2511	2083	1968	849	700	215	464

Table A.37: Time History Results for 80-7.5-N-N

	Vertical Velocity (mm/s)													
	Location (m)	0 to 6	6 to 12	12 to 18	18 to 24	24 to 30	30 to 36	36 to 42	42 to 48	48 to 54	54 to 60	60 to 66	66 to 72	72 to 78
Time (sec)	**Moving Person Region**	**1**	**2**	**3**	**4**	**5**	**6**	**7**	**8**	**9**	**10**	**11**	**12**	**13**
0-5	**1**	61	85	77	81	82	60	69	97	91	62	43	92	87
5-10	**2**	123	68	113	168	119	61	102	148	118	67	69	113	131
10-15	**3**	129	90	129	201	165	92	120	165	196	97	77	185	186
15-20	**4**	171	90	96	208	151	56	136	168	180	80	75	158	180
20-25	**5**	160	89	87	199	233	99	116	149	182	79	60	138	155
25-30	**6**	141	76	98	159	150	196	119	128	111	70	61	93	96

	Lateral Acceleration (mm/s^2)													
	Location (m)	0 to 6	6 to 12	12 to 18	18 to 24	24 to 30	30 to 36	36 to 40	42 to 48	48 to 54	54 to 60	60 to 66	66 to 72	72 to 78
Time (sec)	**Moving Person Region**	**1**	**2**	**3**	**4**	**5**	**6**	**7**	**8**	**9**	**10**	**11**	**12**	**13**
0-5	**1**	86	112	148	62	260	135	147	135	200	173	118	126	86
5-10	**2**	107	240	215	180	510	316	413	295	433	279	227	332	203
10-15	**3**	89	213	195	169	431	351	431	277	377	313	217	321	215
15-20	**4**	91	229	223	308	524	282	485	245	410	342	167	270	174
20-25	**5**	126	273	265	230	593	307	478	319	552	280	146	302	209
25-30	**6**	155	324	266	243	477	485	647	397	606	363	176	303	248

	Vertical Acceleration (mm/s^2)													
	Location (m)	0 to 6	6 to 12	12 to 18	18 to 24	24 to 30	30 to 36	36 to 40	42 to 48	48 to 54	54 to 60	60 to 66	66 to 72	72 to 78
Time (sec)	**Moving Person Region**	**1**	**2**	**3**	**4**	**5**	**6**	**7**	**8**	**9**	**10**	**11**	**12**	**13**
0-5	**1**	1407	1814	1055	1634	1434	1265	1083	1452	1510	1008	710	1516	1518
5-10	**2**	2090	1893	2130	3022	2154	1518	1667	2149	2171	1309	960	1579	2136
10-15	**3**	1995	1758	2009	3522	2302	1689	2186	2613	3297	1635	1577	2880	2879
15-20	**4**	2552	1781	2312	6255	3450	1382	2175	2529	2970	1210	1200	2400	2758
20-25	**5**	3023	1918	2018	4898	8642	4315	2786	2335	3029	1303	859	2097	2553
25-30	**6**	2137	1471	2008	2622	5082	8509	4722	3129	2508	1453	1201	1555	1548

Table A.38: Time History Results for 80-7.5-N-L

	Vertical Velocity (mm/s)													
	Location (m)	0 to 6	6 to 12	12 to 18	18 to 24	24 to 30	30 to 36	36 to 42	42 to 48	48 to 54	54 to 60	60 to 66	66 to 72	72 to 78
Time (sec)	**Moving Person Region**	**1**	**2**	**3**	**4**	**5**	**6**	**7**	**8**	**9**	**10**	**11**	**12**	**13**
0-5	**1**	61	85	78	81	84	60	67	93	91	64	41	86	86
5-10	**2**	104	67	112	154	110	59	99	123	128	77	72	111	132
10-15	**3**	111	81	122	189	155	86	99	150	179	81	69	157	174
15-20	**4**	155	79	93	211	150	49	128	164	168	70	75	155	164
20-25	**5**	146	82	86	185	225	99	115	155	171	81	63	146	157
25-30	**6**	153	75	102	161	156	192	116	147	127	81	67	117	116

	Lateral Acceleration (mm/s^2)													
	Location (m)	0 to 6	6 to 12	12 to 18	18 to 24	24 to 30	30 to 36	36 to 40	42 to 48	48 to 54	54 to 60	60 to 66	66 to 72	72 to 78
Time (sec)	**Moving Person Region**	**1**	**2**	**3**	**4**	**5**	**6**	**7**	**8**	**9**	**10**	**11**	**12**	**13**
0-5	**1**	89	147	115	85	240	100	175	67	97	149	66	131	109
5-10	**2**	117	248	182	159	332	141	244	105	197	188	132	167	111
10-15	**3**	85	209	242	188	266	210	266	137	242	247	177	269	157
15-20	**4**	110	256	258	273	397	205	297	138	237	272	178	220	140
20-25	**5**	96	199	241	228	952	185	253	141	238	331	187	240	222
25-30	**6**	122	242	180	156	811	250	306	217	240	205	112	177	134

	Vertical Acceleration (mm/s^2)													
	Location (m)	0 to 6	6 to 12	12 to 18	18 to 24	24 to 30	30 to 36	36 to 40	42 to 48	48 to 54	54 to 60	60 to 66	66 to 72	72 to 78
Time (sec)	**Moving Person Region**	**1**	**2**	**3**	**4**	**5**	**6**	**7**	**8**	**9**	**10**	**11**	**12**	**13**
0-5	**1**	1391	1814	1048	1647	1449	1226	1034	1370	1498	1030	651	1457	1452
5-10	**2**	1944	1775	2112	2836	1642	1201	1768	1788	1995	1302	1025	1623	1877
10-15	**3**	1715	1694	2017	3421	2273	1426	2002	2365	3093	1288	1146	2234	2897
15-20	**4**	2339	1771	2435	6172	3203	1147	2152	2570	2688	1304	1234	2316	2549
20-25	**5**	2755	1890	2065	4587	8424	3709	2526	2428	2804	1345	1005	2126	2465
25-30	**6**	2212	1346	1983	2768	4580	8378	4285	2541	2129	1471	1228	1830	1664

Table A.39: Time History Results for 80-7.5-V-N

	Vertical Velocity (mm/s)													
	Location (m)	0 to 6	6 to 12	12 to 18	18 to 24	24 to 30	30 to 36	36 to 42	42 to 48	48 to 54	54 to 60	60 to 66	66 to 72	72 to 78
Time (sec)	**Moving Person Region**	**1**	**2**	**3**	**4**	**5**	**6**	**7**	**8**	**9**	**10**	**11**	**12**	**13**
0-5	**1**	50	31	24	32	37	17	14	11	24	11	7	5	8
5-10	**2**	30	50	21	35	38	18	17	12	30	15	11	6	11
10-15	**3**	21	21	40	81	68	33	26	24	30	14	13	4	8
15-20	**4**	23	19	30	139	142	68	60	48	86	43	43	15	28
20-25	**5**	21	20	21	95	203	107	75	59	92	39	39	15	29
25-30	**6**	16	12	17	87	121	112	73	57	90	40	37	14	29

	Lateral Acceleration (mm/s^2)													
	Location (m)	0 to 6	6 to 12	12 to 18	18 to 24	24 to 30	30 to 36	36 to 40	42 to 48	48 to 54	54 to 60	60 to 66	66 to 72	72 to 78
Time (sec)	**Moving Person Region**	**1**	**2**	**3**	**4**	**5**	**6**	**7**	**8**	**9**	**10**	**11**	**12**	**13**
0-5	**1**	94	124	78	113	225	148	153	85	134	139	81	141	81
5-10	**2**	79	169	78	153	248	183	210	111	192	148	109	168	98
10-15	**3**	69	100	129	98	205	214	216	123	163	150	135	137	97
15-20	**4**	76	188	147	213	335	266	336	288	251	308	130	238	178
20-25	**5**	90	200	211	220	509	312	312	315	299	263	134	205	183
25-30	**6**	98	237	200	225	273	295	443	424	335	216	89	214	191

	Vertical Acceleration (mm/s^2)													
	Location (m)	0 to 6	6 to 12	12 to 18	18 to 24	24 to 30	30 to 36	36 to 40	42 to 48	48 to 54	54 to 60	60 to 66	66 to 72	72 to 78
Time (sec)	**Moving Person Region**	**1**	**2**	**3**	**4**	**5**	**6**	**7**	**8**	**9**	**10**	**11**	**12**	**13**
0-5	**1**	1571	596	339	584	479	236	207	135	307	162	93	68	101
5-10	**2**	873	1462	624	618	583	264	247	154	362	209	182	76	139
10-15	**3**	370	884	1046	1261	1031	615	367	321	399	201	210	47	114
15-20	**4**	674	776	1270	5734	3635	1110	1271	840	1141	665	717	230	411
20-25	**5**	699	849	1207	3654	9577	3172	1912	1321	1670	611	656	250	438
25-30	**6**	308	216	534	1734	4512	7265	2969	1816	1878	765	660	216	409

Table A.40: Time History Results for 80-7.5-V-L

	Vertical Velocity (mm/s)													
	Location (m)	0 to 6	6 to 12	12 to 18	18 to 24	24 to 30	30 to 36	36 to 42	42 to 48	48 to 54	54 to 60	60 to 66	66 to 72	72 to 78
Time (sec)	**Moving Person Region**	**1**	**2**	**3**	**4**	**5**	**6**	**7**	**8**	**9**	**10**	**11**	**12**	**13**
0-5	**1**	51	31	25	26	31	16	11	11	29	13	9	5	10
5-10	**2**	28	50	22	33	33	17	14	13	31	15	13	6	12
10-15	**3**	21	21	40	77	55	25	23	27	27	16	14	4	9
15-20	**4**	20	17	31	140	115	53	45	49	96	46	42	15	32
20-25	**5**	20	17	25	102	201	83	58	59	95	44	39	16	33
25-30	**6**	19	15	24	98	146	105	71	59	105	44	39	15	32

	Lateral Acceleration (mm/s^2)													
	Location (m)	0 to 6	6 to 12	12 to 18	18 to 24	24 to 30	30 to 36	36 to 40	42 to 48	48 to 54	54 to 60	60 to 66	66 to 72	72 to 78
Time (sec)	**Moving Person Region**	**1**	**2**	**3**	**4**	**5**	**6**	**7**	**8**	**9**	**10**	**11**	**12**	**13**
0-5	**1**	84	92	62	105	151	85	123	61	133	101	69	151	95
5-10	**2**	63	127	58	133	147	112	133	57	142	147	98	146	108
10-15	**3**	74	95	134	122	138	128	143	58	128	148	112	126	99
15-20	**4**	77	152	138	191	378	164	232	119	267	281	117	225	161
20-25	**5**	99	169	186	206	1027	154	221	107	269	236	123	215	191
25-30	**6**	104	155	133	169	662	213	137	113	174	257	90	191	188

	Vertical Acceleration (mm/s^2)													
	Location (m)	0 to 6	6 to 12	12 to 18	18 to 24	24 to 30	30 to 36	36 to 40	42 to 48	48 to 54	54 to 60	60 to 66	66 to 72	72 to 78
Time (sec)	**Moving Person Region**	**1**	**2**	**3**	**4**	**5**	**6**	**7**	**8**	**9**	**10**	**11**	**12**	**13**
0-5	**1**	1620	600	336	533	411	213	174	138	361	187	133	64	118
5-10	**2**	826	1488	628	576	542	251	202	173	420	202	192	71	156
10-15	**3**	372	893	1041	1261	896	506	332	425	413	209	194	47	121
15-20	**4**	770	869	1347	5857	2491	999	685	747	1393	621	676	229	459
20-25	**5**	730	737	1136	3409	10419	2586	1483	1396	1602	644	550	240	471
25-30	**6**	341	319	665	1900	3844	6804	2511	2083	1968	849	700	215	464

BIBLIOGRAPHY

A. Noble & Son Ltd. (2013). *Wire Rope and Strand Catalog*. Section 2.

Armstrong – Alar Chain Corporation. (2014). 6x19 IWRC Wire Rope. *Wire Rope*. Prospect Heights, IL.

ARUP. (2014). The Millennium Bridge. *London Millennium Bridge*.

American Association of State Highway and Transportation Officials. (1997). *Guide Specifications for Design of Pedestrian Bridges*. Washington, D.C.

Bridges to Prosperity. (2013). *Bridge Builder Manual*. 3rd ed. Denver, CO.

British Standards Association. (1978). Steel, Concrete and Composite Bridges Part 2: Specification for Loads; Appendix C: Vibration Serviceability Requirements for Foot and Cycle Track Bridges, BS 5400. London, UK.

Brownjohn, J. (1997). Vibration Characteristics Of A Suspension Footbridge. *Journal of Sound and Vibration*(202), 29-46.

Builders Fence Company. (2014). *Chain Link Fabric*. Sacramento, CA.

Chung, P., & Fang, J. (2014) Hanging Over the 10. *Modern Steel Construction*, 56-58.

Computers & Structures Inc. (1995). *CSI Analysis Reference Manual*. Berkeley, CA.

The Crosby Group. (2012). *Wire Rope End Terminations User's Manual*. Tulsa, OK.

European Committee for Standardization. (2002). Basis of Structural Design - Eurocode EN1990. Brussels, Belgium.

Gentile, C., & Gallino, N. (2008). Ambient Vibration Testing and Structural Evaluation of an Historic Suspension Footbridge. *Advances in Engineering Software*(39), 356-366.

Hauksson, F., Sandberg, G., Austrell, P., & Camper, H. (2005). Dynamic Behavior of Footbridges Subjected to Pedestrian-Induced Vibrations. Master's Dissertation. Lund University, Lund, Sweden.

Heinemeyer, C., & Feldmann, M. (2008). European Design Guide for Footbridge Vibration. *Proceedings from the Third International Footbridge Conference* (2008).

Huang, M., Thambiratnam, D., & Perera, N. (2007). Dynamic Performance of Slender Suspension Footbridges Under Eccentric Walking Dynamic Loads. *Journal of Sound and Vibration*(303), 239-254.

International Standardization Organization . (2005). Bases for design of structures - Serviceability of buildings and walkways against vibration, ISO 10137. Geneva, Switzerland.

Kawada, T. (2010). *History of the Modern Suspension Bridge: Solving the Dilemma between Economy and Stiffness*. Reston, Virginia: American Society of Civil Engineers.

Kumar, S., Itoh, Y., Saizuka, K., & Usami, T. (1997). Pseudodynamic Testing of Scaled Models. *Journal of Structural Engineering*(123), 524-526.

Meng, X., Dodson, A., & Roberts, G. (2007). Detecting Bridge Dynamics with GPS and Triaxial Accelerometers. *Engineering Structures*(29.11), 3178-184.

Moschas, F., & Stiros, S.. (2011). Measurement of the Dynamic Displacements and of the Modal Frequencies of a Short-span Pedestrian Bridge Using GPS and an Accelerometer. *Engineering Structures*(33), 10-17.

Murray, T., Allen, D., & Ungar, E. (2012). Floor Vibrations Due to Human Activity. *Steel Design Guide Series*(11).

Obata, T., Hayashikawa, T., & Sato, K. (1995). Experimental and Analytical Study of Human Vibration Sensibility On Pedestrian Bridges. *Proceedings of the Fifth East Asia-Pacific Conference on Structural Engineering and Construction Building for the 21st Century*(2), 1225-1230.

Shi, Z., Su, W., Guo, J., & Pu, Q. (2013). Analysis on Natural Vibration and Dynamic Response of Footbridge. *Applied Mechanics and Materials*(361.363), 1389-1396.

Zivanovic, S., Pavic, A., & Reynolds, P. (2005). Vibration Serviceability of Footbridges Under Human-Induced Excitation: a Literature Review. *Journal of Sound and Vibration*(279), 1-74.

Zivanovic, S., Pavic, A., & Reynolds, P. (2007). Finite Element Modeling and Updating of a Lively Footbridge: the Complete Process. *Journal of Sound and Vibration*(301), 126-145.

ACADEMIC VITA

Jennifer Kearney
312 Simmons Hall, University Park, PA 16802
Jak5580@psu.edu

EDUCATION

Master of Science in Civil Engineering (Structures) anticipated May 2015
The Pennsylvania State University, University Park, PA
Thesis: "Dynamic Analysis of Pedestrian Suspension Bridges"

While strength is a very important design consideration, serviceability is equally important, especially for suspension footbridges. This study determines, through the use of physical and numerical models, how changing cable sag or providing lateral and/or vertical stiffening cables affects the dynamic response of suspension footbridges.

Bachelor of Science in Civil Engineering (Structures) anticipated May 2015
Minor in Engineering Leadership Development
The Pennsylvania State University**,** University Park, PA
Schreyer Honors College

ENGINEERING EXPERIENCE

Project Manager Aug 2013 - June 2014
Penn State Bridges to Prosperity

- Lead a team of three students on a survey assessment trip to Panama in August 2013
- Supervised and directed bridge design and construction planning, including obtaining local
  materials and working with the community in Panama
- Managed a team of ten students to construct 250 foot pedestrian suspended bridge in Panama

Structural Intern May - August 2013
Johnson, Mirmiran, and Thompson

- Designed single span and two span concrete bridges, sound walls, and sign structures
- Inspected three overhead highway signs to evaluate their structural stability
- Utilized PennDOT design programs to design bearing pads and pre-stressed bridge girders

Structural Intern May - August 2012
Carney Engineering Group

- Designed ten projects including schools, offices, renovation projects, and warehouses
- Calculated design loads, sized members, and modeled structures in RISA
- Effectively communicated with design team members including architects and contractors

WORK EXPERIENCE

Math and Science Academic Tutor Feb 2009 - Jan 2013
Dallastown Area High School

- Tutored Calculus, Geometry, Physics, and Chemistry (including Advanced Placement courses) for middle and high school students
- Notable achievement: 10 student participants achieved 1-2 level grade point improvement

SOFTWARE	AutoCAD, MicroStation, COGO, Revit, Enercalc, Tedds, RISA, SolidWorks, Excel, SAP2000	
PROFESSIONAL DEVELOPMENT	Bridge Builder Conference, Winter Park, CO	September 2014
	Bridge Builder Conference, Sevierville, TN	September 2013
	American Society of Civil Engineers [ASCE] Conference, Montreal, Canada	October 2012
	Society of Women Engineers Conference, Houston, TX	November 2012
TECHNICAL PRESENTATIONS	**Project Management**, Bridge Builder Conference [BBC]	September 2014
	Dynamic Response of Suspension Footbridges Technical Poster, BBC	September 2014
	Pedestrian Suspension Bridges, PSU Leonard Center Engr. Contest	September 2014
	Penn State Bridges to Prosperity, ASCE Region 2 Assembly	November 2013
ACTIVITIES	Tau Beta Pi - Engineering Honor Society	2014 - present
	Chi Epsilon - The Civil Engineering Honor Society	2012 - present
	American Society of Civil Engineers	2011 - present
	American Institute of Steel Construction	2012 - present
	American Concrete Institute	2013 - present
	Society of Women Engineers	2011 - present
	Engineers Without Borders	2011 - present
	Penn State Campus Crusade for Christ	2011 - 2014
	Engineering Orientation Network	2011 - 2014

LEADERSHIP

Founder — Jan 2013 - present

Bridges to Prosperity [B2P] Penn State Chapter

- Created official Penn State organization and received status as B2P university chapter
- Recruited and organized members, officers, and faculty advisors to generate organization
- Secured approval for B2P Program Project in Panama for 2013 - 2014 academic year

President — Jan 2013 - Aug 2014

Bridges to Prosperity [B2P] Penn State Chapter

- Coordinated Program Project completion in collaboration with national organization
- Lead officer team to steer all aspects of pedestrian bridge project in Panama to completion including fundraising, bridge design, construction planning, and managing cultural relations
- Planned and organized a 5 week trip to Panama for a team of 10 engineering students to oversee and assist with bridge construction
- Notable achievement: chapter received the Bridge Builder Team of the Year award out of 15+ Bridges to Prosperity university chapters

Overall Lead / Leadership Team Member — May 2012 - present

Penn State Women in Engineering Program Orientation [WEPO]

- Managed a team of 7 Leads to facilitate all aspects of three-day orientation in 2014
- Directed and coordinated logistics for three-day orientation for 240 undergraduates from 5 Penn State campuses
- Managed 52 leadership team members and 185 first-year students
- Mentored team of first-year women throughout 2013-14 academic year to optimize engineering retention
- Instructed hands-on SolidWorks tutorial for 180+ first-year engineering students in 2012
- Facilitated behind-the-scenes logistics in 2012

Logistics and Funding Officer — Aug 2012 - May 2014

Penn State Steel Bridge Team

- Planned regional competition trip for 24 students including all travel coordination
- Completed and formalized all documentation to acquire university funding

ACHIEVEMENTS	**Student Marshal**, PSU Department of Civil and Environmental Engineering	May 2015
	Class Award in Structural Engineering, Penn State Civil Engineering	April 2015
	New Faces of Engineering College Edition, DiscoverE	April 2015
	Achieving Women Award, Penn State Commission for Women	March 2015
	New Faces of Civil Engineering Collegiate Edition, ASCE	January 2015
	Bridge Builder Team of the Year, Bridges to Prosperity	September 2014
	People's Choice Award, PSU Leonhard Center Engr. Speaking Contest	September 2014
	Research Award, Bridge Builder Conference Poster Session	September 2014
	Joelle Award for Engineering Leadership, PSU Women in Engr. Program	April 2014
	Honorable Mention, Nadine Barrie Smith Mentor Award, PSU WEP	April 2014
	Aspire Award, Penn State Society of Women Engineers	April 2012